RESEARCH REPORT

HEALTH EFFECTS INSTITUTE

Number 199
March 2019

Real-World Vehicle Emissions Characterization for the Shing Mun Tunnel in Hong Kong and Fort McHenry Tunnel in the United States

Xiaoliang Wang, Andrey Khlystov, Kin-Fai Ho, Dave Campbell, Judith C. Chow, Steven D. Kohl, John G. Watson, Shun-cheng Frank Lee, Lung-Wen Antony Chen, Minggen Lu, and Steven Sai Hang Ho

Real-World Vehicle Emissions Characterization for the Shing Mun Tunnel in Hong Kong and Fort McHenry Tunnel in the United States

Xiaoliang Wang, Andrey Khlystov, Kin-Fai Ho, Dave Campbell,
Judith C. Chow, Steven D. Kohl, John G. Watson, Shun-cheng Frank Lee,
Lung-Wen Antony Chen, Minggen Lu, and Steven Sai Hang Ho

---

with a Critique by the HEI Review Committee

Research Report 199
Health Effects Institute
Boston, Massachusetts

Trusted Science • Cleaner Air • Better Health

Publishing history: This document was posted at *www.healtheffects.org* in March 2019.

Citation for document:

Wang XL, Khlystov A, Ho KF, Campbell D, Chow JC, Kohl SD, et al. 2019. Real-World Vehicle Emissions Characterization for the Shing Mun Tunnel in Hong Kong and Fort McHenry Tunnel in the United States. Research Report 199. Boston, MA:Health Effects Institute.

 Cameographics, Union, Me., Compositor. Printed by Recycled Paper Printing, Boston, Mass. Library of Congress Catalog Number for the HEI Report Series: WA 754 R432.

Cover paper: made with at least 55% recycled content, of which at least 30% is post-consumer waste; free of acid and elemental chlorine. Text paper: made with 100% post-consumer waste recycled content; acid free; no chlorine used in processing. The book is of permanent archival quality.

CONTENTS

ABOUT HEI

The Health Effects Institute is a nonprofit corporation chartered in 1980 as an independent research organization to provide high-quality, impartial, and relevant science on the effects of air pollution on health. To accomplish its mission, the institute

- Identifies the highest-priority areas for health effects research;
- Competitively funds and oversees research projects;
- Provides intensive independent review of HEI-supported studies and related research;
- Integrates HEI's research results with those of other institutions into broader evaluations; and
- Communicates the results of HEI's research and analyses to public and private decision makers.

HEI typically receives balanced funding from the U.S. Environmental Protection Agency and the worldwide motor vehicle industry. Frequently, other public and private organizations in the United States and around the world also support major projects or research programs. HEI has funded more than 340 research projects in North America, Europe, Asia, and Latin America, the results of which have informed decisions regarding carbon monoxide, air toxics, nitrogen oxides, diesel exhaust, ozone, particulate matter, and other pollutants. These results have appeared in more than 260 comprehensive reports published by HEI, as well as in more than 1,000 articles in the peer-reviewed literature.

HEI's independent Board of Directors consists of leaders in science and policy who are committed to fostering the public–private partnership that is central to the organization. The Research Committee solicits input from HEI sponsors and other stakeholders and works with scientific staff to develop a Five-Year Strategic Plan, select research projects for funding, and oversee their conduct. The Review Committee, which has no role in selecting or overseeing studies, works with staff to evaluate and interpret the results of funded studies and related research.

All project results and accompanying comments by the Review Committee are widely disseminated through HEI's website (*www.healtheffects.org*), printed reports, newsletters and other publications, annual conferences, and presentations to legislative bodies and public agencies.

ABOUT THIS REPORT

Research Report 199, *Real-World Vehicle Emissions Characterization for the Shing Mun Tunnel in Hong Kong and Fort McHenry Tunnel in the United States,* presents a research project funded by the Health Effects Institute and conducted by Dr. Xiaoliang Wang of the Desert Research Institute, Reno, Nevada, and his colleagues. The report contains three main sections.

The HEI Statement, prepared by staff at HEI, is a brief, nontechnical summary of the study and its findings; it also briefly describes the Review Committee's comments on the study.

The Investigators' Report, prepared by Wang and colleagues, describes the scientific background, aims, methods, results, and conclusions of the study.

The Critique, prepared by members of the Review Committee with the assistance of HEI staff, places the study in a broader scientific context, points out its strengths and limitations, and discusses remaining uncertainties and implications of the study's findings for public health and future research.

This report has gone through HEI's rigorous review process. When an HEI-funded study is completed, the investigators submit a draft final report presenting the background and results of the study. This draft report is first examined by outside technical reviewers and a biostatistician. The report and the reviewers' comments are then evaluated by members of the Review Committee, an independent panel of distinguished scientists who have no involvement in selecting or overseeing HEI studies. During the review process, the investigators have an opportunity to exchange comments with the Review Committee and, as necessary, to revise their report. The Critique reflects the information provided in the final version of the report.

HEI STATEMENT

Synopsis of Research Report 199

Vehicle Emissions Characterization in Tunnels in Hong Kong and Baltimore, Maryland

INTRODUCTION

Traffic emissions are an important source of urban air pollution, and exposure to traffic-related air pollution is known to be associated with various adverse health effects. Emissions from motor vehicles have changed substantially over the last few decades because of new fuels, changes in engine designs and operation, and improved emission control technology. Tunnel studies allow for characterization of real-world emissions from a large fleet of in-use motor vehicles, and a series of studies in the same traffic tunnels can be used to characterize changes in the emissions of the motor vehicle fleet over time.

In this study, Dr. Xiaoliang Wang and colleagues from the Desert Research Institute sought to evaluate how mobile-source emissions have changed through real-world emissions characterization in two traffic tunnels that had been studied in the past: the Shing Mun Tunnel in Hong Kong and the Fort McHenry Tunnel in Baltimore, Maryland. They measured a large suite of more than 300 pollutants and used the data to derive fleet-average, pollutant-specific emission factors; they then compared their results with previous studies in the same tunnels and elsewhere. In addition, they established VOC and $PM_{2.5}$ source profiles and differentiated between tailpipe and non-tailpipe $PM_{2.5}$. Lastly, they evaluated the performance of mobile-source emission models used in the regulatory process by comparing the modeled emission factors to the emission factors measured in the tunnels.

APPROACH

This study evaluated changes in mobile-source emission factors since 2003–2004 in the Hong Kong Tunnel and since 1992 in the Baltimore Tunnel. The tunnels represent two locations with very different fleet compositions, emission controls, fuels, and near-road air pollutant concentrations (Statement Table). These tunnels were selected for the current study because they had been intensively studied previously. The earlier studies were conducted prior to recent changes in regulations, technologies, and fleet composition that were expected to reduce the emissions of air pollutants from motor vehicles. Therefore comparison of the new data obtained by this project with historical data allows for assessment of changes in emissions over time.

What This Study Adds

- This study measured emissions of more than 300 pollutants in 2015 from motor vehicles in two tunnels — the Shing Mun Tunnel in Hong Kong and the Fort McHenry Tunnel in Baltimore, Maryland.
- The measured emission factors for light- and heavy-duty vehicles for most pollutants were markedly lower compared with earlier studies in the same tunnels although increased use of liquefied petroleum gas in Hong Kong appeared to result in increases in emissions of certain pollutants.
- The Hong Kong regulatory emissions model generally agreed with measured emissions. However, the United States regulatory emissions model used in Baltimore estimated emissions that were substantially higher than measured emissions for most pollutants, suggesting that the model is significantly overestimating actual on-road emissions.
- All of the data collected in the current study are available online (see Additional Materials 1 on the HEI website). They will be very useful in tracking past as well as future changes in motor vehicle emissions and in updating and evaluating emissions models used in the regulatory process.

This Statement, prepared by the Health Effects Institute, summarizes a research project funded by HEI and conducted by Dr. Xiaoliang Wang, Desert Research Institute, Reno, Nevada, and colleagues. Research Report 199 contains both the detailed Investigators' Report and a Critique of the study prepared by the Institute's Review Committee.

Statement Table. Sampling Conditions and Descriptive Characteristics of the Shing Mun Tunnel and Fort McHenry Tunnel

Parameters	Shing Mun Tunnel	Fort McHenry Tunnel
Location	Hong Kong, China	Baltimore, Maryland, United States
Earlier sampling periods	August 2003 and January–February 2004	June 1992
Current sampling periods	January–March 2015	February 2015 and July–August 2015
Description of tunnels	One bore in each direction, with 2 lanes per bore	Two bores in each direction, with two lanes per bore and trucks directed to the right-most bores
Fleet composition	2003–2004: 9% liquefied petroleum gas, 41% gasoline vehicles, 50% diesel vehicles 2015: 13% liquefied petroleum gas, 45% gasoline vehicles, and 42% diesel vehicles	1992 and 2015: Left bore: <3% heavy-duty (mostly diesel) vehicles and >97% light-duty (mostly gasoline) vehicles Right bore: 55% to 92% light-duty vehicles and 8% to 45% heavy-duty vehicles
Traffic volume	~53,000 vehicles/day in both 2003–2004 and 2015	~55,000 vehicles/day in both 1992 and 2015
Pollutants measured	*Continuous:* CO, CO_2, NO, NO_x, VOCs, $PM_{2.5}$, SO_2, BC, PNC *Integrated*: NH_3, VOCs (C2–C12), carbonyls, PAHs, $PM_{2.5}$, road dust	*Continuous*: CO, CO_2, NO, NO_x, VOCs, $PM_{2.5}$, UFP size distribution *Integrated*: NH_3, VOCs (C2–C12), carbonyls, PAHs, $PM_{2.5}$, road dust, CO, CO_2

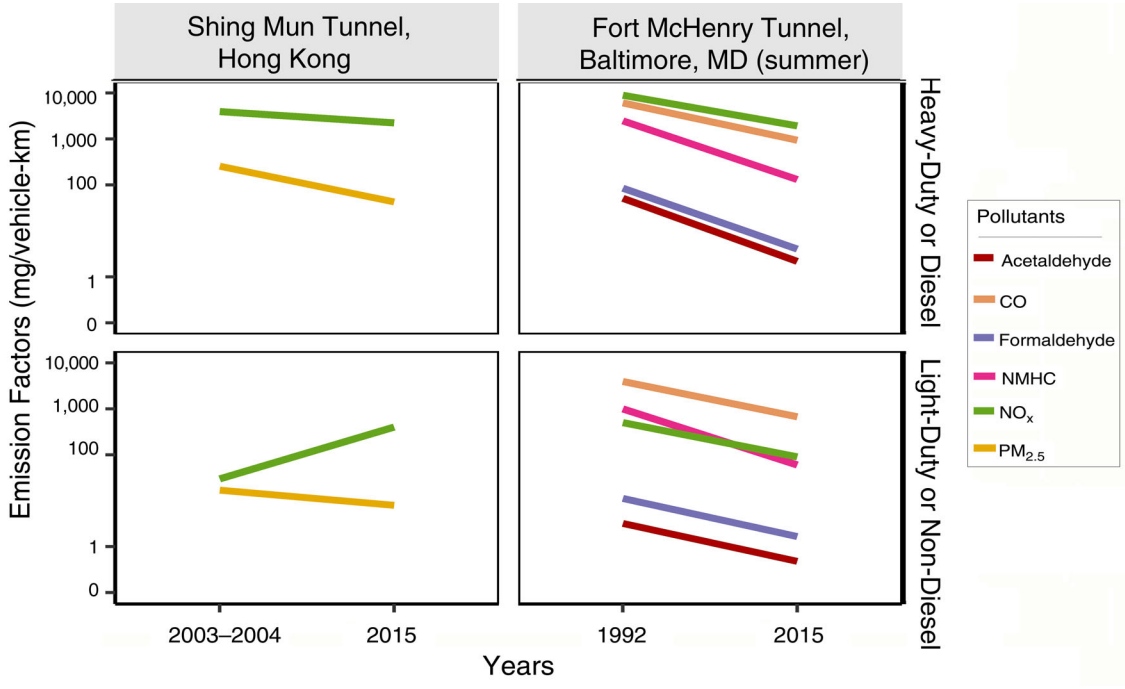

Statement Figure 1. Emission factors in the Shing Mun Tunnel in Hong Kong and the Fort McHenry Tunnel in Baltimore, Maryland, over time. Not all pollutants were measured in each study.

The investigators measured concentrations of a large suite of pollutants at the entrance (or air inlet) and exit of each tunnel in the winter (both tunnels) and summer (Baltimore tunnel only) of 2015. They counted and classified vehicles passing through the tunnels; vehicles in the Hong Kong tunnel were classified as fueled by diesel, gasoline, or liquefied petroleum gas, and vehicles in the Baltimore tunnel were classified as light-duty or heavy-duty. The investigators assumed that the difference in pollutant concentration measured between the inlet and exit of the tunnels was emitted by vehicles in the tunnel. They used this assumption to calculate the fleet-average, pollutant-specific emission factors. They also attributed the emissions of the various pollutants to vehicles in the different categories used for classification.

Finally, the investigators put their results in context by comparing them to previously published emissions data. They compared their results with previous studies in the same tunnels and other tunnels in Hong Kong and the United States to explore how vehicular emissions have changed over time. In addition, they evaluated performance of two mobile-source emission models (EMFAC-HK and MOVES) by comparing the modeled emission factors to the emission factors measured in the tunnels.

REVIEW OF THE REPORT

In its independent review of the report, the HEI Review Committee thought that Wang and colleagues had successfully collected a comprehensive set of emissions measurements in two tunnel locations that have been studied before and then used those data to estimate emission factors for the fleet average and for specific vehicle classes. Major contributions of this study were the assessment of emission trends over time, comparisons of measured and modeled emission estimates, and synthesization of results from these multiple data sources. The Committee found that even though the analyses identified uncertainties in some of the results, the major conclusions of the study were sound.

SUMMARY OF RESULTS

An important finding of the study is that the emission factors of most of the pollutants measured in the two tunnels were lower in 2015 than they were in earlier studies in the same tunnels (Statement Figure 1). In the Hong Kong tunnel, the greatest declines in emission factors between 2003–2004 and 2015 were for $PM_{2.5}$, which decreased by about 80% for fleet average and diesel vehicles and was halved for non-diesel vehicles, and for SO_2, which dropped about 80% for fleet average (Statement Figure 2). However,

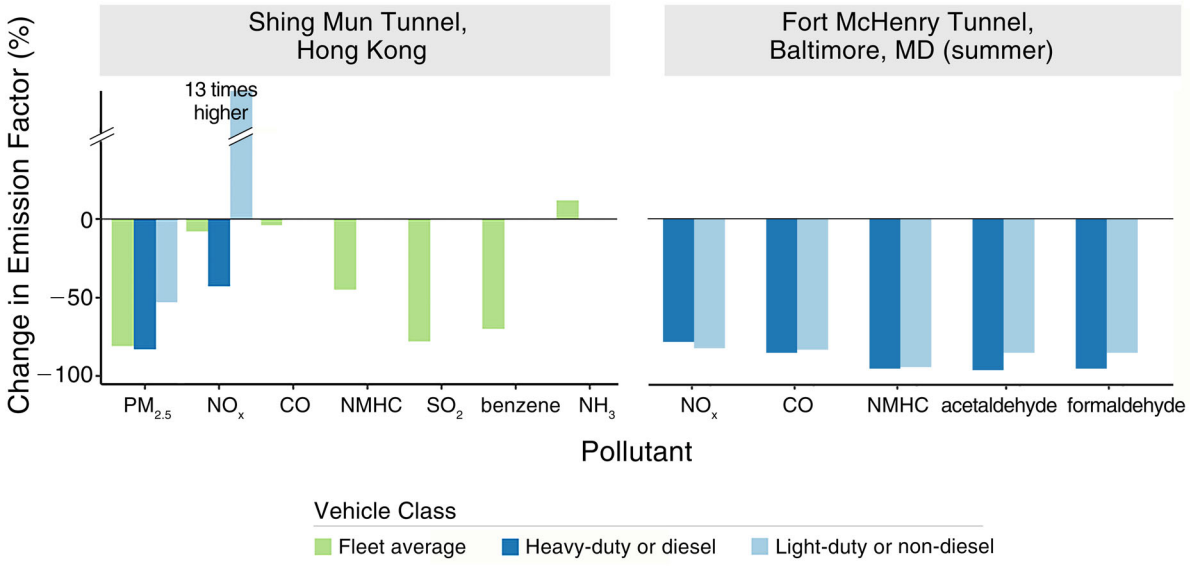

Statement Figure 2. Percent change in emission factors between 2003–2004 and 2015 in the Shing Mun Tunnel in Hong Kong and between 1992 and 2015 in the Fort McHenry Tunnel in Baltimore, Maryland. Not all pollutants were measured in each study.

the increased proportion of vehicles fueled by liquefied petroleum gas in Hong Kong resulted in increased emissions of certain pollutants associated with that fuel: increased NO_x emissions from non-diesel vehicles were likely related to both the increase in liquefied petroleum gas vehicles and different methods of separating the fleet-average emissions between diesel and non-diesel vehicles in this versus the earlier study.

In the Baltimore tunnel, emission factors of NO_x, CO, NMHCs, acetaldehyde, and formaldehyde from both light-duty and heavy-duty vehicles decreased by 78% to 96% between 1992 and 2015. ($PM_{2.5}$ was not measured in the earlier study.) Much of this difference was related to reductions in emissions from light-duty vehicles. Determination of the relative effectiveness of the regulations for light-duty versus heavy-duty vehicles needs further investigation.

The investigators compared their results to earlier studies in the same tunnels, to other tunnel studies in the same countries, and to models used in the regulatory process in order to confirm their main findings and highlight sources of uncertainty to be explored in future research. Despite the different tunnel configurations and fleet characteristics in the two tunnels, measured changes in pollutant emission factors over time were generally consistent between the two tunnels or explainable by well-understood properties of the vehicle fleets. The model used for the regulatory process in Hong Kong also produced results consistent with the measurements. A notable exception to consistency between measurements and models was that the regulatory emissions model for the United States substantially overestimated the real-world emissions in the Baltimore tunnel. Therefore, future work will be important to understand the reasons for that overestimation in order to develop accurate inventories of actual on-road vehicle emissions.

CONCLUSIONS

Quantifying the contribution of vehicle emissions to ambient concentrations of major pollutants — including $PM_{2.5}$ (and its major constituents), NO_x, and NMHCs — is a topic of interest for scientists and policymakers; therefore, having vehicle source profiles that represent emissions from the current fleet is important. The data collected in the current study (available online) are useful in tracking past as well as future changes in motor vehicle emissions and updating emissions models used in the regulatory process. Quantifying emissions from motor vehicles will continue to be important. As populations grow, urbanization continues, and the density of vehicle traffic in major cities increases, large numbers of people continue to be exposed to traffic-related emissions that affect population health even as emissions from individual vehicles go down, underscoring the role of studies such as this to quantify emissions from motor vehicles.

INVESTIGATORS' REPORT

Real-World Vehicle Emissions Characterization for the Shing Mun Tunnel in Hong Kong and Fort McHenry Tunnel in the United States

Xiaoliang Wang[1], Andrey Khlystov[1], Kin-Fai Ho[2], Dave Campbell[1], Judith C. Chow[1], Steven D. Kohl[1], John G. Watson[1], Shun-cheng Frank Lee[3], Lung-Wen Antony Chen[4], Minggen Lu[5], and Steven Sai Hang Ho[6]

[1]*Desert Research Institute, Reno, Nevada, United States;* [2]*The Chinese University of Hong Kong, China;* [3]*The Hong Kong Polytechnic University, Hong Kong, China;* [4]*University of Nevada, Las Vegas, United States;* [5]*University of Nevada, Reno, United States;* [6]*Hong Kong Premium Services and Research Laboratory, Hong Kong, China*

ABSTRACT

INTRODUCTION

Motor vehicle exhaust is an important source of air pollutants and greenhouse gases. Concerns over the health and climate effects of mobile-source emissions have prompted worldwide efforts to reduce vehicle emissions. Implementation of more stringent emission standards have driven advances in vehicle, engine, and exhaust after-treatment technologies as well as fuel formulations. On the other hand, vehicle numbers and travel distances have been increasing because of population and economic growth and changes in land use. These factors have resulted in changes to the amount and chemical composition of vehicle emissions.

Roadway tunnel studies are a practical way to characterize real-world emissions from the on-road vehicle fleet in an environment isolated from other combustion pollution sources. Measurements in the same tunnel over time allow evaluation of vehicle emission changes and the effectiveness of emission reduction measures. Tunnel studies estimate the impacts of vehicle emissions on air quality and traffic-related exposures, generate source profile inputs for receptor-oriented source apportionment models, provide data to evaluate emission models, and serve as a baseline for future comparisons.

The present study characterized motor vehicle emission factors and compositions in two roadway tunnels that were first studied over a decade ago. The specific aims were to (1) quantify current fleet air pollutant emission factors, (2) evaluate emission change over time, (3) establish source profiles for volatile organic compounds (VOCs*) and particulate matter ≤2.5 µm in aerodynamic diameter ($PM_{2.5}$), (4) estimate contributions of fleet components and non-tailpipe emissions to VOCs and $PM_{2.5}$, and (5) evaluate the performance of the latest versions of mobile-source emission models (i.e., the EMission FACtors vehicle emission model used in Hong Kong [EMFAC-HK] and the MOtor Vehicle Emission Simulator used in the United States [MOVES]).

METHODS

Measurements were conducted in the Shing Mun Tunnel (SMT) in Hong Kong and the Fort McHenry Tunnel (FMT) in Baltimore, Maryland, in the United States, representing the different fleet compositions, emission controls, fuels, and near-road exposure levels found in Hong Kong and the United States. These tunnels have extensive databases acquired in 2003–2004 for the SMT and 1992 for the FMT. The SMT sampling was conducted during the period from 1/19/2015 to 3/31/2015, and the FMT sampling occurred during the periods from 2/8/2015 to 2/15/2015 (winter) and 7/31/2015 to 8/7/2015 (summer). Concentrations of criteria pollutants (e.g., carbon monoxide [CO], nitrogen oxides [NO_x],

This Investigators' Report is one part of Health Effects Institute Research Report 199, which also includes a Critique by the Review Committee and an HEI Statement about the research project. Correspondence concerning the Investigators' Report may be addressed to Dr. Xiaoliang Wang, Desert Research Institute, 2215 Raggio Pkwy., Reno, NV 89512; e-mail: *xiaoliang.wang@dri.edu*.

Although this document was produced with partial funding by the United States Environmental Protection Agency under Assistance Award CR–83467701 to the Health Effects Institute, it has not been subjected to the Agency's peer and administrative review and therefore may not necessarily reflect the views of the Agency, and no official endorsement by it should be inferred. The contents of this document also have not been reviewed by private party institutions, including those that support the Health Effects Institute; therefore, it may not reflect the views or policies of these parties, and no endorsement by them should be inferred.

* A list of abbreviations and other terms appears at the end of this volume.

and particulate matter [PM]) were measured in real time, and integrated samples of VOCs, carbonyls, polycyclic aromatic hydrocarbons (PAHs), and $PM_{2.5}$ were collected in canisters and sampling media for off-line analyses. Emission factors were calculated from the tunnel measurements and compared with previous studies to evaluate emission changes over time. Emission contributions by different vehicle types were assessed by source apportionment modeling or linear regression. Vehicle emissions were modeled by EMFAC-HK version 3.3 and MOVES version 2014a for the SMT and the FMT, respectively, and compared with measured values. The influences of vehicle fleet composition and environmental parameters (i.e., temperature and relative humidity) on emissions were evaluated.

RESULTS

In the SMT, emissions of $PM_{2.5}$, sulfur dioxide (SO_2), and total non-methane hydrocarbons (NMHCs) markedly decreased from 2003–2004 to 2015: SO_2 and $PM_{2.5}$ were reduced by ~80%, and total NMHCs was reduced by ~44%. Emission factors of ethene and propene, key tracers for diesel vehicle (DV) emissions, decreased by ~65%. These reductions demonstrate the effectiveness of control measures, such as the implementation of low-sulfur fuel regulations and the phasing out of older DVs. However, the emission factors of isobutane and *n*-butane, markers for liquefied petroleum gas (LPG), increased by 32% and 17% between 2003–2004 and 2015, respectively, because the number of LPG vehicles increased. Nitrogen dioxide (NO_2) to NO_x volume ratios increased between 2003–2004 and 2015, indicating an increased NO_2 fraction in primary exhaust emissions. Although geological mineral concentrations were similar between the 2003–2004 and 2015 studies, the contribution of geological materials to $PM_{2.5}$ increased from 2% in 2003–2004 to 5% in 2015, signifying the continuing importance of non-tailpipe PM emissions as tailpipe emissions decrease. Emissions of CO, ammonia (NH_3), nitric oxide (NO), NO_2, and NO_x, as well as carbonyls and PAHs in the SMT did not show statistically significant (at $P < 0.05$ based on Student's *t*-test) decreases from 2003–2004 to 2015. The reason for this is not clear and requires further investigation.

A steady decrease in emissions of all measured pollutants during the past 23 years has been observed from tunnel studies in the United States, reflecting the effect of emission standards and new technologies that were introduced during this period. Emission reductions were more pronounced for the light-duty (LD) fleet than for the heavy-duty (HD) fleet. In comparison with the 1992 FMT study, the 2015 FMT study demonstrated marked reductions in LD emissions for all pollutants: emission factors for naphthalene were reduced the most, by 98%; benzene, toluene, ethylbenzene, and xylene (BTEX), by 94%; CO, NMHCs, and NO_x, by 87%; and aldehydes by about 71%. Smaller reductions were observed for HD emission factors: naphthalene emissions were reduced by 95%, carbonyl emissions decreased by about 75%, BTEX by 60%, and NO_x 58%.

The 2015 fleet-average emission factors were higher in the SMT for CO, NO_x, and summer $PM_{2.5}$ than those in the FMT. The higher CO emissions in the SMT were possibly attributable to a larger fraction of motorcycles and LPG vehicles in the Hong Kong fleet. DVs in Hong Kong and the United States had similar emission factors for NO_x. However, the non-diesel vehicles (NDVs), particularly LPG vehicles, had higher emission factors than those of gasoline cars, contributing to higher NO_x emissions in the SMT. The higher $PM_{2.5}$ emission factors in the SMT were probably attributable to there being more double-deck buses in Hong Kong.

In both tunnels, PAHs were predominantly in the gas phase, with larger (four and more aromatic rings) PAHs mostly in the particulate phase. Formaldehyde, acetaldehyde, crotonaldehyde, and acetone were the most abundant carbonyl compounds in the SMT. In the FMT, the most abundant carbonyls were formaldehyde, acetone, acetaldehyde, and propionaldehyde. HD vehicles emitted about threefold more carbonyl compounds than LD vehicles did. In the SMT, the NMHC species were enriched with marker species for LPG (e.g., *n*-butane, isobutane, and propane) and gasoline fuel vapor (e.g., toluene, isopentane, and *m/p*-xylene), indicating evaporative losses. Source contributions to SMT $PM_{2.5}$ mass were diesel exhaust (51.5 ± 1.8%), gasoline exhaust (10.0 ± 0.8%), LPG exhaust (5.0 ± 0.5%), secondary sulfate (19.9 ± 1.0%), secondary nitrate (6.3 ± 0.9%), and road dust (7.3 ± 1.3%). In the FMT, total NMHC emissions were 14% and 8% higher in winter than in summer for LD and HD vehicles, respectively. Elemental carbon (EC) and organic carbon (OC) were the major constituents of tunnel $PM_{2.5}$. De-icing salt contributions to $PM_{2.5}$ were observed in the FMT in winter.

Emission estimates by the EMFAC-HK agreed with SMT measurements for CO_2; the modeled emission factors for CO, NO_x, and NMHCs were 1.5, 1.6, and 2.2 times the measurements, respectively; and the modeled emission factor for $PM_{2.5}$ was 61% of the measured value in 2003. The EMFAC-HK estimates and SMT measurements for 2015 differed by less than 35%. The MOVES2014a model generally overestimated emissions of most of the pollutants measured in the FMT. No pollutants were significantly underestimated. The largest overestimation was observed for emissions measured during HD-rich driving conditions in winter.

CONCLUSIONS

Significant reductions in SO_2 and $PM_{2.5}$ emissions between 2003 and 2015 were observed in the SMT,

indicating the effectiveness of control measures on these two pollutants. The total NMHC emissions in the SMT were reduced by 44%, although isobutane and *n*-butane emissions increased because of the increase in the size of the LPG fleet. No significant reductions were observed for CO and NO_x, results that differed from those for roadside ambient concentrations, emission inventory estimates, and EMFAC-HK estimates. In contrast, there was a steady decrease in emissions of most pollutants in the tunnels in the United States.

INTRODUCTION

Motor vehicles are a principal source of urban air pollution, directly emitting large amounts of CO, VOCs, NO_x, PM, and mobile-source air toxics (Parrish 2006; Sawyer et al. 2000). Some of these pollutants react in the atmosphere to form secondary pollutants such as ozone (O_3) and PM with inorganic and organic constituents (Bahreini et al. 2012; May et al. 2014). Epidemiological and toxicological studies have found that vehicle emissions possibly contribute to a broad range of adverse health effects, such as allergies, asthma, other respiratory ailments, and cardiovascular disease (HEI Panel on the Health Effects of Traffic-Related Air Pollution 2010; Krzyzanowski et al. 2005). With growth in populations and the vehicle fleet as well as with changes in land use, more people are living and working close to busy highways and roads. HEI Panel on the Health Effects of Traffic-Related Air Pollution (2010) estimated that 30%–45% of people in large North American cities live or work within an exposure zone of 300–500 m from busy roads. Asian cities have higher human exposures to vehicle emissions owing to enclosed street canyons, near-road residences, and a high presence of people on sidewalks and roadways. Vehicles are also major contributors to greenhouse gas emissions. On-road vehicles contributed to 24.1% and 21% of total greenhouse gases emitted in the United States and in the European Union, respectively (European Environment Agency [EEA] 2016; U.S. Environmental Protection Agency [U.S. EPA] 2016).

Concerns over health and climate effects have prompted worldwide efforts to reduce vehicle emissions, including advances in vehicle, engine, and after-treatment technologies, fuel improvements, traffic management optimization, and implementation of more stringent emission standards (HEI Special Committee on Emerging Technologies 2011; Shindell et al. 2011). On the other hand, because of population growth, increasing suburban populations, and increasing goods shipment, vehicle-miles traveled (VMT; or vehicle-kilometers traveled [VKT]) have been steadily increasing in the past several decades. There was a VMT decrease around the recession in 2008, but VMT continued to increase soon thereafter (U.S. DOT 2016, 2017). Between 2003 and 2015, the daily VMT in Hong Kong increased by 19% (HKTD 2016). VMT increases are even larger in developing nations with rapidly increasing urbanization and motorization (Huo et al. 2012; Zhang et al. 2014), partially offsetting emission reductions from vehicles. Real-world characterizations of on-road vehicle fleet emissions over time (e.g., a decade) are needed to evaluate emission changes, assess the effectiveness of emission control actions, and improve assessment of human exposure to vehicle emissions. Such measurements would update current emission levels and serve as a baseline for future comparisons.

In addition to the amounts of pollutants emitted by vehicles, the chemical compositions of vehicle emissions have also changed over time. Although certain pollutant emissions (e.g., PM from DVs) may have been reduced, others may have increased. For example, blending diesel with biodiesel and/or ethanol may reduce PM but may increase NO_x and carbonyl emissions (Shahir et al. 2015); gasoline direct-injection engines have better fuel economy but emit more ultrafine particles (UFPs) (Xue et al. 2016; Zhao et al. 1999); and diesel engines with catalytic converters or particulate filters may increase tailpipe NO_2 emissions (Carslaw et al. 2011; Tian et al. 2011; Wild et al. 2017). Enhanced emissions from gasoline vehicles (GVs) and LPG vehicles in Hong Kong were found to increase the total NMHC and O_3 concentrations from 2005 to 2013 (Lyu et al. 2017). As new technologies lead to reductions in tailpipe emissions, non-tailpipe emissions, such as fuel evaporation, tire and brake wear, and road dust become relatively more important (Amato et al. 2014; Denier van der Gon et al. 2013). Detailed characterization of the vehicle emission profiles is needed for speciated emission inventories, source apportionment, and heath assessments.

Several methods have been used to characterize vehicle emissions, including chassis and engine dynamometer testing, remote sensing, on-road chasing, on-board measurements by portable emission measurement systems, and tunnel studies (Franco et al. 2013; HEI Panel on the Health Effects of Traffic-Related Air Pollution 2010). Among these methods, tunnel studies have several advantages: (1) the wind condition is well defined; (2) pollutant concentrations are dominated by vehicle-related tailpipe and non-tailpipe emissions and are isolated from other pollution sources; and (3) driving conditions represent the local real-world fuel, fleet, and operating conditions. Many tunnel studies have been conducted to characterize vehicle emissions under real-world in-use conditions. They have been successfully used to evaluate the efficacy of control strategies and assess emission models (El-Fadel

and Hashisho 2001; HEI Panel on the Health Effects of Traffic-Related Air Pollution 2010; Kuykendall et al. 2009).

The current study examined vehicle emission changes over the past two decades through real-world emission characterization in the SMT in Hong Kong and the FMT in Baltimore, Maryland. These two tunnels represent the different fleet compositions, emission controls, fuels, and near-road exposure levels in Hong Kong and the United States. Extensive emission data were acquired in 2003–2004 for the SMT (Cheng et al. 2006, 2010; Ho et al. 2007, 2009a, 2009b; Wang et al. 2006) and in 1992 and later for the FMT (Gertler et al. 1998; Landis et al. 2007; Pierson et al. 1996; Zielinska and Sagebiel 2001). The past study data can be compared with the current study to assess emission changes.

SPECIFIC AIMS

The primary objective of the current study was to characterize motor vehicle emissions through tunnel studies in the SMT and FMT. These two tunnels represent real-world traffic in Southeastern Asia and the eastern United States with different, region-specific vehicle fleets and fuels that are subject to different controls and regulations. Both tunnels were studied more than a decade ago, and a comparison between the previous and current studies allows an evaluation of changes in emissions over time owing to new technologies and fuels. Study hypotheses and specific aims are listed below.

The four hypotheses were:

1. Changes in engine design, emission controls, and fuel formulations over the past two decades have caused major changes in motor vehicle emission factors and compositions.

2. Vehicle source profiles need to be updated to better distinguish contributions to gases and particles by different types of engines, fuels, and operating conditions.

3. The fraction of non-tailpipe (e.g., evaporation and road dust) emissions to total emissions has increased over the past years owing to lower tailpipe emissions.

4. Mobile-source emission models, such as the EMFAC-HK by the Hong Kong Environmental Protection Department (HKEPD) and the MOVES by the U.S. EPA, reasonably estimate traffic emissions.

The five specific aims were to:

1. Measure fleet-average emission factors (EFs) for criteria and non-criteria pollutants, including CO, carbon dioxide (CO_2), VOCs, gas- and particle-phase PAHs, carbonyls, NH_3, NO_x, UFP, and $PM_{2.5}$ mass and its constituents;

2. Compare results from current and previous tunnel studies to evaluate the influences of fleet composition, emission controls, and fuel improvements on EFs and pollutant mixtures;

3. Establish VOC and $PM_{2.5}$ source profiles and compare them with historical and recent profiles to identify markers for different vehicle categories;

4. Estimate the contributions of tailpipe and non-tailpipe emissions to VOC and $PM_{2.5}$; and

5. Evaluate the performance of the latest versions of mobile-source emission models (i.e., EMFAC-HK for the SMT and MOVES for the FMT).

METHOD AND STUDY DESIGN

TUNNEL MEASUREMENTS

Measurements in the SMT

The SMT is a two-bore (north and south) tunnel on the HK Route 9 expressway connecting Sha Tin and Tsuen Wan urban areas in the New Territories of Hong Kong (Appendix Figure A.1 [panel A] in Appendix A, available on the HEI website). The tunnel is 2.6-km long and divided into two sections, 1.6 km east and 1.0 km west. Each bore has two traffic lanes with 70-m^2 cross-sectional areas. There are 80 jet fans and four exhaust fans positioned along the tunnel ceiling, which were not activated during the current study. Ventilation is achieved by the piston effect of traffic movement. Daily vehicle flows were ~53,000 in both 2003 and 2015 (HKTD 2016), with 2003/2015 average fleet mixes of ~41%/45% GVs, ~9%/13% LPG, and ~50%/42% DVs, varying throughout the day. The SMT was previously studied in August 2003 and January–February 2004 (Cheng et al. 2006, 2010; Ho et al. 2007, 2009a, 2009b; Wang et al. 2006).

As in the 2003–2004 study, the 2015 SMT measurements were acquired in the south bore of the east section (closer to Sha Tin), which has a rising slope of 1.054% from the entrance to exit. Because of space and electricity constraints, the inlet and outlet sampling sites were placed 600 m apart, being 686 m from the entrance and 350 m from the exit, respectively, as shown in Figure 1 (top). The setback from the entrance minimized disturbances from outside air and allowed pollutant concentrations to be homogenized across the tunnel cross-section (El-Fadel and

Hashisho, 2001). The posted speed limit is 80 km/hr, and the closest highway ramp is ~2.5 km from the SMT entrance. Therefore, most vehicles were likely operating at hot-stabilized conditions. Traffic video shows that the traffic flowed smoothly through the tunnel, and there was no stop-and-go during the study periods.

Figure 1 (bottom) shows the 2015 sampling setup at the outlet site of the SMT. Instrument specifications are listed in Appendix Table A.1, and pictures of the sampling setup are shown in Appendix Figure A.2. A similar setup was used at the inlet site. Gas samples were drawn from inlets located 1.5 m above ground level adjacent to the right traffic lane, followed by transfer lines to the gas analyzers through Teflon tubing. Teflon-membrane filters in the inlet tubing removed particles that might interfere with the gas analyzers. CO, CO_2, NO, NO_2, and SO_2 were measured with near-real-time gas analyzers. A stream of 27.3 mL/min gas sample was collected in a 2-L canister using a canister sampler for NMHC (C2–C12) analysis (Zielinska and Fujita 1994). Another stream of 0.5 L/min gas sample passed through silica cartridges impregnated with 2,4-dinitrophenylhydrazine (DNPH; Sep-Pak DNPH-Silica Cartridge) for carbonyl sampling. To accommodate equipment accessibility constraints, eight canisters and DNPH cartridges were turned on and off sequentially at the designated sampling periods by solenoid valves activated by preset timers. A Desert Research Institute (DRI) medium-volume gas/particle sampling system sampled through a $PM_{2.5}$ cyclone (Bendix Model 240) at a flow rate of 113 L/min onto a quartz-fiber filter and a downstream XAD-4 adsorbent resin to collect particulate and gaseous PAHs. A DustTrak DRX, a micro-aethalometer, and a condensation particle counter acquired continuous PM mass, black carbon (BC) and UFP concentrations, respectively. The condensation particle counter and micro-aethalometer suffered from concentration saturation and overloading; therefore, the UFP and BC emission factors are not reported here. Two collocated DRI 13-channel medium-volume multichannel sampling system (Chow et al. 1993a) collected filter samples for laboratory analyses. Three parallel channels were activated during each sampling period, including (1) a Teflon-membrane filter backed by a citric acid–impregnated cellulous-fiber filter, (2) a quartz-fiber filter, and (3) a quartz-fiber filter backed by a quartz-fiber filter. Each sampler automatically sequenced through the 12 channels (with one passive channel for the field blank) and acquired eight sets of samples without operator intervention. Two video cameras recorded the traffic flow at the tunnel entrance and the outlet sampling site. Wind speed, wind direction, barometric pressure, temperature, and relative humidity were monitored by a weather station at both inlet and outlet sites. Gas analyzers with different manufacturers or model numbers were used in the 2003 study, but they were calibrated with the same standard gases of known concentrations (Cheng et al. 2006).

The SMT sampling started on 1/19/2015. Most instruments, except real-time CO_2, VOCs, PM, weather station, and the traffic camera were stopped from 2/16/2015 to 3/1/2015 for the Chinese New Year break. The sampling resumed on 3/2/2015, and basic sampling was completed on 3/15/2015. Additional measurements of CO_2, PM, and several canister samplings continued for several periods until the end of March 2015. Detailed sampling periods are listed in Appendix Table A.2, available on HEI's website.

The SMT south bore was closed during ~00:00–05:00 local daylight time (LDT) every Monday and Wednesday for maintenance, and the north bore was closed during ~00:00–05:00 LDT every Tuesday and Thursday. During these periods, tunnel illumination was repaired, and the tunnel pavement was occasionally swept. Traffic in both directions was directed to the open bore. Because the sampling sites could only be accessed for sample changing on Mondays and Wednesdays when the tunnel was closed, integrated samples were taken on Mondays, Tuesdays, and two other days of the week to cover variations between weekdays and weekends. For each sampling day, four 2-hour sampling periods were chosen to cover a range of traffic mixes. These sampling periods include morning and evening rush hours (08:00–10:00 LDT and 17:00–19:00 LDT) when DV proportions were the lowest, and midday hours (11:00–13:00 LDT and 14:00–16:00 LDT) when DV proportions were the highest. Near real-time instruments were operated continuously during most of the sampling periods, as shown in Appendix Table A.2. Data acquired during the tunnel maintenance periods (i.e., 00:00–05:00 LDT from Monday through Thursday) were excluded from analysis.

The Hong Kong Transport Department's SMT tollbooths recorded hourly counts of vehicles in light-, medium-, and heavy-duty (LD, MD, and HD, respectively) categories, but these data did not separate taxis (fueled by LPG) from other gasoline-powered LD vehicles. Manual traffic counting from traffic videos taken at the SMT entrance separated the fleet into nine categories, that is, motorcycle, private car (PC), taxi, light-goods vehicle (LGV), medium-goods vehicle (MGV), heavy-goods vehicle (HGV), light bus, single-deck bus, and double-deck bus, with a time resolution of 15 minutes for each 2-hour sampling period. Total vehicle numbers differed by <4% between manual counting and tollbooth records. The nine vehicle categories were further grouped into LPG vehicles, GVs, and DVs based on the fuel distributions in EMFAC-HK (HKEPD 2017c). LPG vehicles and GVs were further grouped as NDVs.

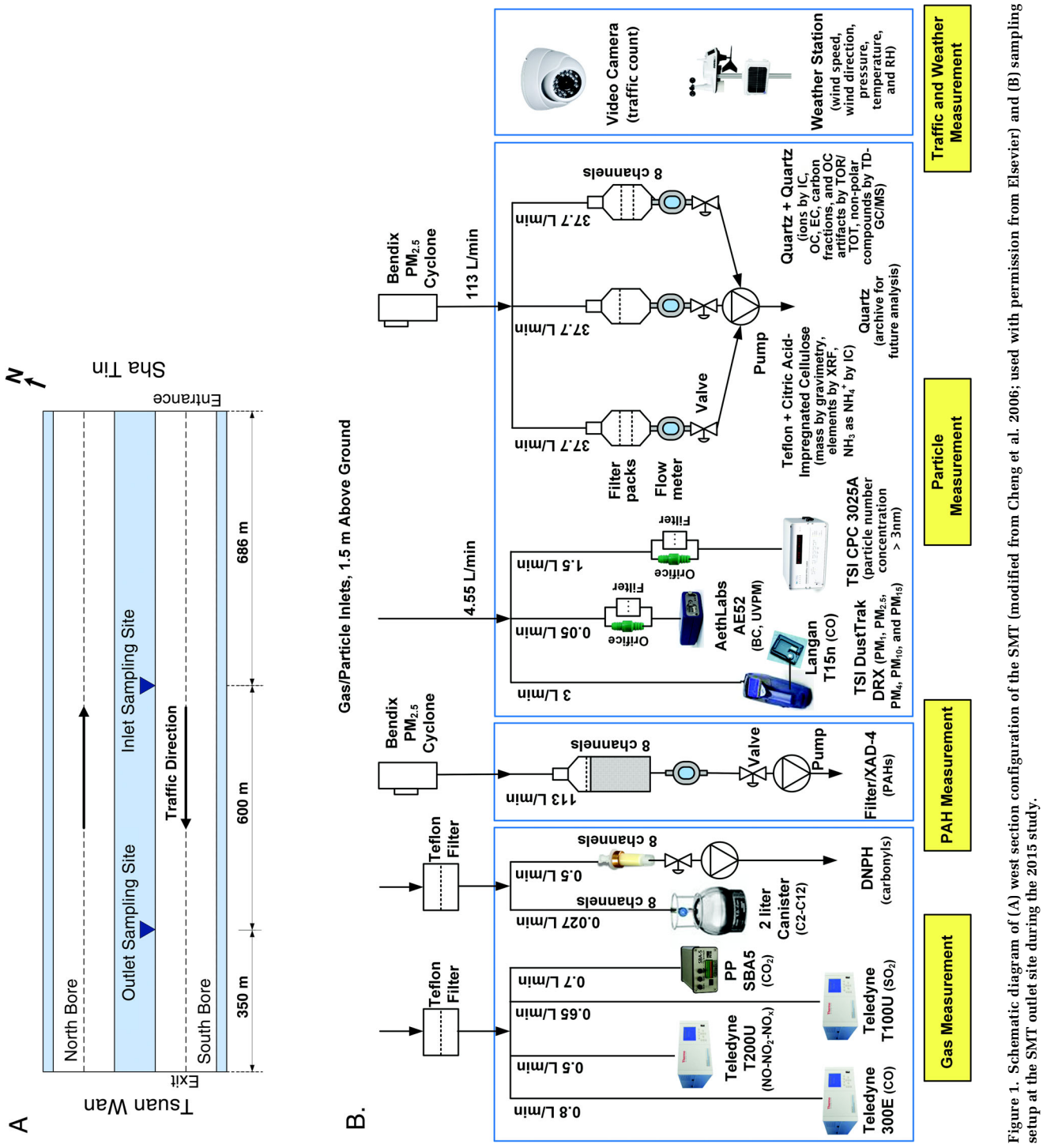

Figure 1. Schematic diagram of (A) west section configuration of the SMT (modified from Cheng et al. 2006; used with permission from Elsevier) and (B) sampling setup at the SMT outlet site during the 2015 study.

The standard operating procedures, including quality insurance and quality control, are listed in Appendix B, available on HEI's website. The total valid numbers of sample pairs (inlet and outlet) collected were 63 filter packs, 70 XAD cartridges, 46 canisters, and 59 DNPH cartridges. A total of six road-dust samples were collected by sweeping the tunnel floor. These were aerosolized in a resuspension chamber and collected on filters for chemical analysis to establish the road-dust source profiles (Chow et al. 1994).

Measurements in the FMT

The FMT is described in detail by Pierson and colleagues (1996) and was studied by multiple groups over the past decades (Gertler et al. 1998; Landis et al. 2007; Zielinska and Sagebiel 2001). The FMT passes under the Baltimore Harbor and carries traffic for Interstate 95, the main highway on the East Coast of the United States (Appendix Figure A.1 [panel B], available on HEI's website). It is a four-bore 2.2-km tunnel, with two lanes per bore. The tunnel downgrade reaches −3.76%, and the upgrade reaches +3.76%, with no significant level portion (Figure 2 [A]). Average grade from west portal to bottom is −1.8% and from bottom to east portal is +3.3%. LD vehicles are allowed in all bores. Trucks (HD vehicles) are directed into the right-hand bores. The posted speed limit is 55 miles/hr (89 km/hr). The daily traffic volume during the current study was ~55,000 vehicles per day. HD vehicles comprised 8%–45% of the total count in the right bore (Bore 4) and less than 3% in the left bore (Bore 3). The nearest eastbound entrance ramps with significant amounts of traffic are more than 2 km west of the entrance portal, and these ramps connect to arteries, not local streets. Therefore, it can be assumed that all vehicles entering the FMT were in hot-stabilized operation (Pierson et al. 1996). The FMT ventilation system supplied air from a duct beneath the roadway. Measurements of the air velocity in the upper ventilation duct during the current study showed that there was practically no air flow there, implying that all tunnel air was removed through the exit of the traffic bores. Appendix Table A.3 summarizes the key traffic and tunnel differences between the SMT and the FMT.

Because there were access restrictions at the west entrance of the tunnel in the 2015 measurements, FMT inlet concentrations were measured in the east ventilation room at the point where ambient air was taken by fans into the tunnel. The ventilation room had eight large fans that drew air from the room. The room was positioned on the third and fourth floors of the five-story building, three sides of which opened to the outside through louvered walls. The instruments were placed away from the fans and close to the middle of the eastern louvered wall to avoid any contamination from fan motors. Because the fans constantly supplied air to both bores, a single sampling point served as the background site for both bores. Exit sampling was conducted simultaneously at the exit of both eastbound bores (Bores 3 and 4). Sampling lines were lowered 20 cm into each bore from the upper ventilation duct. The inlets were positioned between the driving lanes, that is, in the middle of each bore. The sampling equipment was placed in the upper ventilation duct of each bore. Inlet lines were 2 to 3 m in length. Teflon tubing was used to sample gases, and copper tubing was used to sample PM.

The FMT measurement setup is shown in Figure 2 (B), and equipment specifications are listed in Appendix Table A.4. Appendix Figures A.3 and A.4 (available on HEI's website) show pictures of the sampling setup in the east ventilation building (background) and Bores 3 and 4, respectively. Real-time measurements included CO, CO_2, NO_x, and aerosol size distributions (using a scanning mobility particle sizer [SMPS]). Time-integrated measurements included dual-channel $PM_{2.5}$ filter measurements for gravimetric, elemental, ions, and carbon analyses; $PM_{2.5}$ filter-XAD samples for chemical composition measurements of PM and semivolatile organic compounds (SVOCs); DNPH cartridges for aldehyde measurements; and 3-L canisters for CO, CO_2, and NMHC measurements. In addition, temperature and relative humidity data were collected at each measurement location. Hourly traffic counts were obtained from the tollbooths at the exit of the tunnel. In addition, a traffic camera (Miovision Scout) was used to record traffic in each lane. The collected data were processed to obtain vehicle counts per lane grouped into six vehicle types with 5-minute resolution.

Winter measurements in the FMT were carried out during 2/8/2015–2/15/2015, and summer measurements in the FMT were carried out during 7/31/2015–8/6/2015 (Appendix Table A.2). The sampling was carried out during 09:00–15:00 LDT and 15:00–18:30 LDT. On Sundays, one 5.5-hour mid-day sample was collected to account for lighter traffic volumes. Night samples were also collected to extend the sampled range of traffic composition and volume.

LABORATORY ANALYSIS

Canister samples were analyzed for speciated NMHCs (C2–C12) using gas chromatography/mass spectrometry (GC/MS) following U.S. EPA Method TO-15 (U.S. EPA 1999c; Zielinska and Fung 1994). Methane (CH_4), CO, and CO_2 were also analyzed for the FMT samples using a gas chromatography/flame ionization detector equipped with a methanator. DNPH cartridges were analyzed for 14 C1–C8

carbonyl compounds (including acrolein) by high-performance liquid chromatography (Waters Alliance HPLC System with Photodiode Array Detector) (Fujita et al. 2011), according to EPA Method TO-11A (U.S. EPA 1999a). The quartz-fiber filter and XAD-4 resin samples from the SMT were analyzed for gas- and particle-phase PAHs separately using GC/MS following U.S. EPA Method TO-13A (U.S. EPA 1999b). SVOCs and PM-associated species on each filter-XAD sampling train collected from the FMT were extracted separately and analyzed by electron impact GC/MS for PAHs, oxy-PAHs, alkanes, and cycloalkanes (in the range of C12–C40), and hopanes/steranes (Zielinska et al. 2004; 2008). Additionally, extracts from samples collected in FMT Bore 4 were analyzed for nitro-PAH, using GC/MS with the negative-ion chemical ionization method (Samy et al. 2011).

$PM_{2.5}$ filter samples were analyzed for mass, elements, ions, carbon fractions, and organic compounds (Chow and Watson 2013). Teflon-membrane filters were analyzed for mass by gravimetry (Watson et al. 2017) and 51 elements (sodium through uranium) by X-ray fluorescence (Watson et al. 1999). Half of the quartz-fiber filters were extracted in distilled deionized water and analyzed for six water-soluble ions, including chloride (Cl^+), nitrate (NO_3^-), sulfate (SO_4^{2-}), ammonium (NH_4^+), sodium (Na^+), and potassium (K^+), by ion chromatography (Chow and Watson 2017). OC, EC, and eight thermal fractions (OC1–OC4, pyrolyzed carbon, and EC1–EC3) were quantified by the Interagency Monitoring of Protected Visual Environments Alternative thermal/optical protocol (IMPROVE_A; Chow et al. 1993b, 2007a, 2011) from a punch of the quartz-fiber filter. For SMT samples, another two to three punches of the quartz-fiber filter were analyzed for 113 nonpolar speciated organic compounds, including alkanes, alkenes, hopanes, steranes, and PAHs by thermal desorption GC/MS (Chow et al. 2007c; Ho and Yu 2004; Ho et al. 2008). The backup citric acid–impregnated cellulose-fiber filter was analyzed for NH_3 as NH_4^+ by automated colorimetry, and the backup quartz-fiber filter was analyzed by the IMPROVE_A protocol to estimate the organic vapors adsorbed onto the front quartz-fiber filter (Chow et al. 2010; Watson et al. 2009).

Quality control and quality assurance procedures for both field measurements and laboratory analyses are described in Appendix B (available on the HEI website).

STATISTICAL METHODS AND DATA ANALYSIS

Data Preprocessing

As described in Appendix B, (available on the HEI website), real-time instruments used in the SMT were calibrated before, during, and/or after the field campaign.

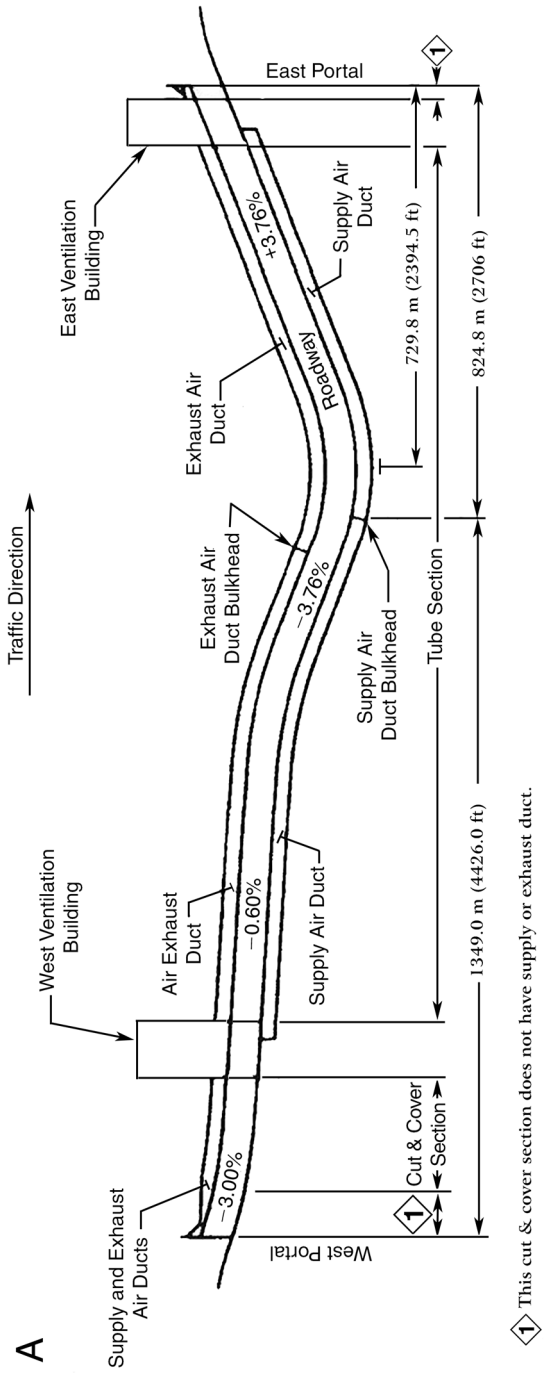

Figure 2. Schematic diagram of (A) eastbound bores of the FMT (modified from Pierson et al. 1996; used with permission from Elsevier) and (B) sampling setup at the FMT outlet site during the 2015 study. (*Figure continues next page.*)

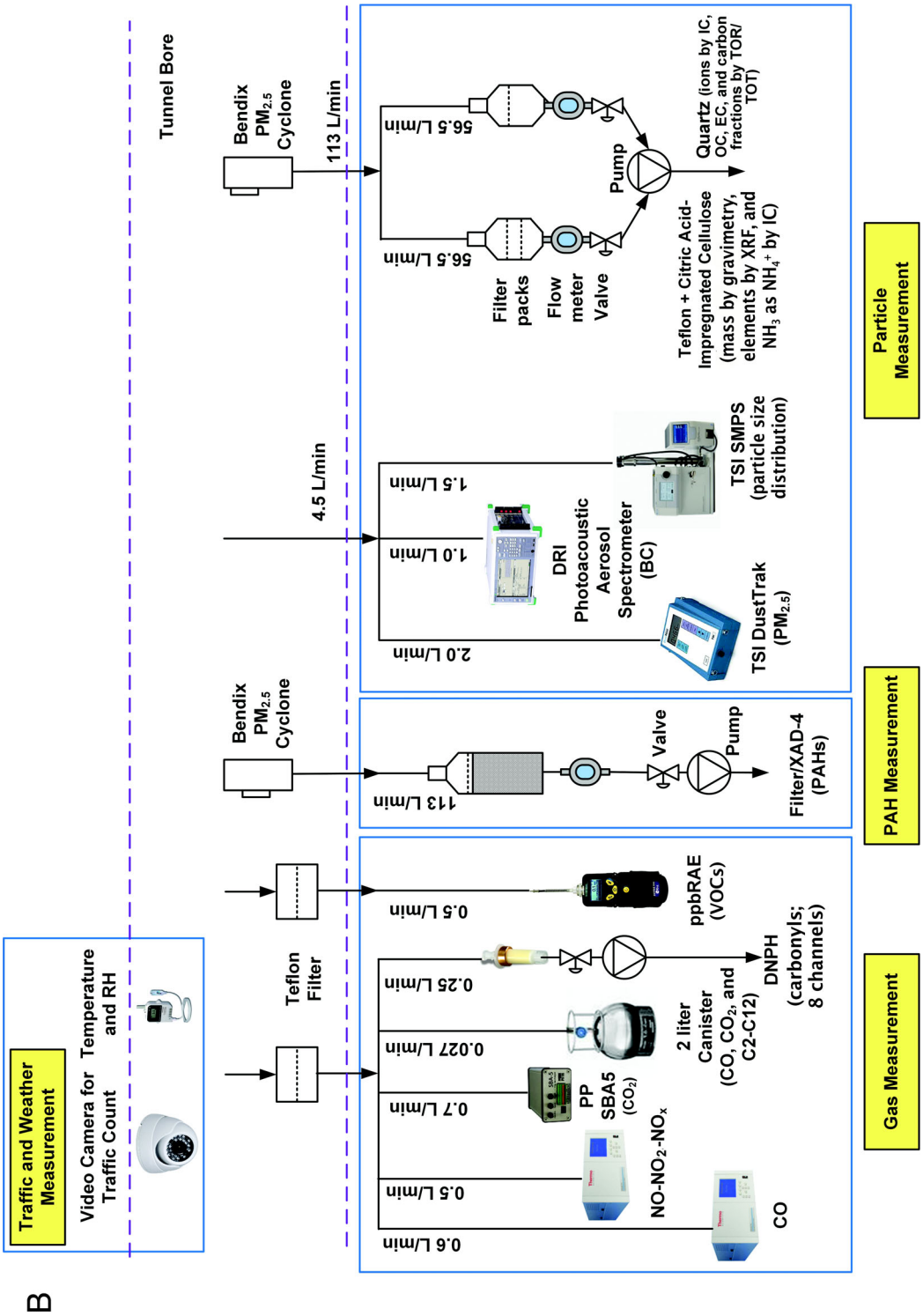

Figure 2. (*Continued*)

Linear regressions were performed between the instrument readings and calibration standards, and the regression equations were used to adjust the raw instrument readings. All data were transformed to 1-minute averages, and time series were inspected to identify outliers or instrument malfunction. The 1-minute data were further averaged over the 2-hour sampling periods of integrated samples.

During the FMT field campaigns, every 1 to 2 days the continuous monitors were challenged with known concentrations of gases until a stable reading was obtained. Baseline readings were also taken by sampling from a Tedlar bag of clean air or span gases. The periodic zero and span checks were reviewed to determine the daily baseline and span value for each monitor, and the results were tabulated, plotted as a function of time for the duration of the measurement period, and reviewed for outliers or suspect data points. A least-squares linear-regression equation was calculated for each monitor (separately for summer and winter campaigns). If the correlation of the baseline and span factor (i.e., $C_{actual}/(C_{indicated} - Z_{indicated})$, in which C_{actual} is the concentration of the gas standard (span gas), $C_{indicated}$ is the monitor reading of the span gas, and $Z_{indicated}$ is the monitor reading when zero air is introduced), variation to time was statistically significant, the continuous data were adjusted using the resulting regression equation. If the correlation of the baseline and span factor was not statistically significant, the median value of the span factor was applied as the correction factor. The continuous measurement data were time-averaged to coincide with the sample collection periods and combined with results from gas and aerosol analyses. Uncertainties for the time-averaged data were estimated from the variance of the calibration results as

$$\sqrt{\left(\sigma^2_{\text{baseline}} + \sigma^2_{\text{residual}}\right)}. \quad (1)$$

The combined data for each parameter and sampling location were screened for outliers (Hubert and Vandervieren 2008). Any points identified as outliers by this method were examined. If these outliers were more than twice the next highest point and five times the analytical uncertainty, they were excluded from subsequent calculations unless the discrepancy could be explained or corrected by review of the raw analytical data. The data returns for SMT and FMT are summarized in Appendix Tables B.4 and B.5, respectively (available on HEI's website).

Emission Factor Calculation

Three types of EFs were calculated from the tunnel measurement data: distance-based EFs (EF_D; in g/veh/km), fuel carbon-based EFs (EF_C; in g/kg-C in the fuel), and fuel-based EFs (EF_F; in g/kg fuel). The distance-based EFs are usually reported for on-road vehicles and are comparable with vehicle emission standards and mobile-source emission models. The fuel carbon- and fuel-based EFs have the advantage of reducing uncertainties caused by changing tunnel air flows, dilutions, gradients, and vehicle operating conditions such as engine load (El-Fadel and Hashisho 2001; Pierson et al. 1996).

The EF_D calculation is based on the mass balance principle (El-Fadel and Hashisho 2001; Gertler et al. 2002; Pierson et al. 1996). Considering a tunnel section bounded by the inlet and outlet sampling sites, the mass of the pollutant i ($Mass_i$; in grams) produced by vehicles within the tunnel section during a sampling period Δt (in seconds) can be calculated as:

$$Mass_i = \sum_j \left(C_{i,out} V_{out}\right)_j - \sum_k \left(C_{i,in} V_{in}\right)_k , \quad (2)$$

where $C_{i,out,j}$ and $V_{out,j}$ are the measured average concentration (g/m^3) of pollutant i and volume of air (m^3) leaving exit j during time Δt, respectively, and $C_{i,in,k}$ and $V_{in,k}$ are measured average pollutant i concentration (g/m^3) and volume of air (m^3) entering entrance k during time Δt, respectively. Equation 2 assumes that (1) pollutants do not deposit or react in the tunnel, (2) wind speeds are uniform at the tunnel inlet and outlet cross-sections, and (3) pollutant concentrations are uniform in tunnel cross-sections (El-Fadel and Hashisho 2001). Because the tunnels are enclosed by walls, gases are likely in dynamic equilibrium between deposition and evaporation. Furthermore, the air mass residence time in the tunnels is short (e.g., ~60 seconds in the SMT), the impacts of pollutant deposition and reaction are expected to be low. For example, at the typical SMT wind speed of 5 m/sec, the turbulent depositional losses within the 600-m SMT measurement section is estimated to be 0.3% and 4.8% for 2.5-µm and 10-µm particles, respectively. Access constraints and safety concerns prevented measurement of wind speed and concentration uniformities in the current study. However, because both the SMT and the FMT are long tunnels with high traffic flow, the wind speed and pollutant concentrations were expected to be relatively uniform. Rogak and colleagues (1998) estimated that in a tunnel with a hydraulic diameter and wind speeds comparable to those of the SMT, the wind speed at 105 cm from the tunnel wall (similar to the wind sensor location in SMT) was close to the average value, and only decreased to 90% of the average speed at 30 cm from the wall. Tracer gas measurements show that, at a wind speed of 5 m/sec, the concentrations can be assumed to be uniform at tunnel cross-sections (Rogak et al. 1998).

When there is only one entrance and one exit in the tunnel section and if the tunnel cross-section areas (A; in m^2) are the same at the inlet and outlet sites, which is the case for the SMT, equation 2 can be simplified to:

$$Mass_i = \left(C_{i,out}\, U_{out} - C_{i,in} U_{in}\right) A\Delta t, \quad (3)$$

where U_{out} and U_{in} are the wind speed (m/sec) at the outlet and inlet sampling sites. The $EF_{D,i}$ for species i is then:

$$EF_{D,i} = Mass_i / NL, \quad (4)$$

where N is the number of vehicles through the tunnel section during the sampling period and L (in km) is the length of the tunnel section between the inlet and outlet sampling sites.

The $EF_{C,i}$ calculation is based on carbon mass balance (Dreher and Harley 1998; Kean et al. 2000b; Moosmüller et al. 2003; Singer and Harley 1996; Wang et al. 2016; Watson et al. 2012).

$$EF_{C,i} = \frac{\Delta C_i}{\Delta C_{CO_2}\left(\frac{M_C}{M_{CO_2}}\right) + \Delta C_{CO}\left(\frac{M_C}{M_{CO}}\right)} \times 1{,}000, \quad (5)$$

where ΔC_i, ΔC_{CO_2} and ΔC_{CO} are the concentration differences for pollutant i, CO_2 and CO (in g/m^3) between outlet and inlet sampling sites, respectively. M_C, M_{CO_2}, and M_{CO} are the atomic or molecular weight of carbon (C), CO_2, and CO in grams/mole, respectively. The factor 1,000 converts units from kilograms to grams. Equation 5 assumes that the carbon that originated from fuel is negligible in CH_4, VOCs, and PM as compared with CO and CO_2 (e.g., >99.5% of fuel carbon was emitted as CO and CO_2 in SMT). When the carbon mass fraction of the fuel (w_c, in kg-C/kg fuel) is estimated, EF_C can be converted to fuel-based EF_F by:

$$EF_{F,i} = EF_{C,i} \times w_c = \frac{\Delta C_i}{\Delta C_{CO_2}\left(\frac{M_C}{M_{CO_2}}\right) + \Delta C_{CO}\left(\frac{M_C}{M_{CO}}\right)} w_c \ . \quad (6)$$

The w_c values depend on local fuel composition and are approximately 0.85 for gasoline, 0.87 for diesel (Kirchstetter et al. 1999), and 0.825 for LPG (typical 30% propane and 70% butane blend in Hong Kong) (Tsai et al. 2006). The fleet-average can be estimated based on the fleet mix, fuel consumption rates, and fuel properties (Dallmann et al. 2013). EF_F or EF_C can be converted to EF_D with fuel economy (FE; in km/kg fuel):

$$EF_{D,i} = EF_{F,i} / FE = \left(EF_{C,i} \times w_c\right) / FE \, . \quad (7)$$

Note that both w_c and FE vary with fuel, and FE is further dependent on vehicle fleet composition, and their values need be known or assumed when using equations 6 and 7.

The SMT measurements allowed direct calculations of EF_D and EF_C, whereas the fleet-average EF_F was calculated with an assumption of fleet-average w_c of 0.85. In the FMT, fresh air was constantly supplied to the tunnel, and the tunnel inlet concentrations were not measured because access was restricted. Therefore, FMT EF_C was directly calculated from measurements of background and tunnel outlet concentrations, whereas EF_F was calculated using equation 6, assuming w_c values of 0.85 for LD and 0.87 for HD, and EF_D was calculated using equation 7 by estimating the fleet-average fuel economy* for the vehicle type distribution observed during each sampling period.

Summary statistics such as counts, means, standard deviations, and standard errors were used to describe the data. Two-sample independent t-tests were applied to compare the population means of EFs between earlier and current tunnel studies. Data management and analysis were performed by R statistical software in the FMT and Microsoft Excel in the SMT. Statistical significance was set at $P < 0.05$.

Linear regressions have been used in tunnel studies to apportion emissions to different components of the fleet (Gertler et al. 2002; Pierson et al. 1996):

$$EF_i = \sum_m \left(EF_{i,m} \times f_m\right) + \varepsilon_i \, , \quad (8)$$

where $EF_{i,m}$ is the EF of the mth fleet component, f_m is the number percentage of the mth vehicle fleet component, weighed by the respective fuel carbon efficiency, and ε_i is the error term. Most previous tunnel studies separate the fleet into two components (i.e., $m = 2$): LD and HD or gasoline and diesel, where equation 8 represents a straight line and $EF_{i,m}$ can be estimated from a linear regression. The previous SMT study apportioned EF_D to NDVs (including gasoline and LPG vehicles) and DVs (Cheng et al. 2006, 2010; Ho et al. 2007, 2009a, 2009b; Wang et al. 2006), whereas the previous FMT study apportioned EF_D

* The 2015 fleet-average fuel economy estimates for vehicle categories and fuel types were taken from various sources compiled by the U.S. Department of Energy Alternative Fuels Data Center *www.afdc.energy.gov/data/*. See Appendix Table A.5, available on HEI's website, for details.

to LD and HD. The fractional uncertainty can be determined from regressions by dividing the standard error in the EFs estimate by the mean and multiplying the regressed values (Gertler et al. 2002).

The linear regression method assumes that emissions from different vehicle categories are linearly dependent on the vehicle number fraction of each category. Because vehicles under the same category may have very different emission factors (e.g., gasoline-fueled motorcycles and passenger cars), vehicle number fraction may not be a good indicator for emissions. A more appropriate method for apportioning emissions to different fleet components could be receptor-based source apportionment, as will be discussed later.

Several recent studies used roadside in-plume sampling and fast-response (≤1 second) instruments to determine carbon-based emission factors from individual vehicles, particularly from high emitters (Dallmann et al. 2012; Wang et al. 2015). This method requires a stable background so that the short-duration (5–20 seconds) concentration peaks by individual vehicles are clearly discernible. It was found that the concentrations inside the busy SMT were too variable to establish a stable baseline to calculate individual vehicle emission factors. Therefore, fleet-average EFs are reported here.

Evaluation of Emission Factor Trend

Vehicle emission measurements through tunnel studies have been conducted in many countries over the past several decades. Some of these studies have been summarized and reviewed in earlier publications (El-Fadel and Hashisho 2001; HEI Panel on the Health Effects of Traffic-Related Air Pollution 2010; Kuykendall et al. 2009). With a specific goal of evaluating the impact of vehicle technologies and emission control measures on emission trends, EFs measured from several tunnels with repeated measurements over a long period were compared with EFs from the current study. These tunnels include the SMT (Cheng et al. 2006, 2010), the FMT (Pierson et al. 1996), the Tuscarora Tunnel in Pennsylvania (Gertler et al. 2002; Pierson et al. 1996), and the Caldecott Tunnel in California (Ban-Weiss et al. 2008a, 2008b; Dallmann et al. 2013; Kean et al. 2000a, 2002, 2009; Kirchstetter et al. 1999). The Zhujiang Tunnel in Guangzhou, China (Liu et al. 2014; Zhang et al. 2015), and three other tunnels in Hong Kong (Brimblecombe et al. 2015) are close to the SMT with similar fuel and vehicle composition and were included in the comparison. Because the directly measured EFs were based on distance, carbon, or fuel, the EFs were converted to the same unit using equation 7 if fuel economy or carbon content was known.

To gain a better understanding of the EF changes in the SMT, the historical trends of criteria pollutant emissions by the road transport sector, VKT, and ambient pollutant concentrations in Hong Kong over the 2003–2015 period were examined.

Emission Models Evaluation

Emission models such as MOVES and EMFAC-HK calculate emissions as the sum of products of vehicle activities, base emission rates, and a series of adjustment factors (Fujita et al. 2012). These models differ in how the vehicle activities are quantified and stratified and how emission factors corresponding to the stratified activities are determined and adjusted. Emission models are useful tools for national-, regional-, and project-level assessments of mobile-source emissions. They allow users to specify vehicle types, operating characteristics, environmental conditions, and road types. By specifying different model scenarios, emission models can be used to generate emission inventory, evaluate emission control effectiveness, analyze project conformity, and predict long-term emission trends. However, emission models usually estimate base emission factors and their adjustment factors based on limited testing data, which may deviate from real-world emissions. Comparison between model prediction and field observation (e.g., tunnel study, remote sensing, or plume-chasing) will provide validation to the model outputs (Fujita et al. 2012; NRC 2000). For such comparisons, the model inputs need to match the conditions under which the experiments are carried out. In the current study, the EMFAC-HK was evaluated using the SMT data, and the MOVES was evaluated using the FMT data.

Vehicle emissions in the SMT were modeled with EMFAC-HK V3.3. Vehicle activities, that is, VKT, were stratified into 16 vehicle classes (motorcycles, cars, trucks, and buses of various weights; see Appendix Table A.6) and three fuel types (gasoline, diesel, and LPG), to each of which base EFs (g/VKT) for CO, CO_2, NMHCs, NO_x, $PM_{2.5}$, and PM ≤ 10 μm in aerodynamic diameter (PM_{10}) were assigned (HKEPD 2017b). The EMFAC-HK does not directly output NMHC values. Instead, NMHCs were calculated as the difference between total hydrocarbons and CH_4. The major adjustment factors are technology group (control and maintenance) and vehicle age (model year); minor factors include vehicle speed, ambient temperature, and relative humidity. EMFAC-HK does not distinguish roadway links (e.g., highways and local streets) or vehicle running modes (e.g., acceleration and deceleration) except for emissions from vehicle start-up, which can be estimated separately by the duration of vehicle idling.

EMFAC-HK also calculates total hydrocarbon evaporative losses in addition to running exhaust from tailpipes.

Total vehicle emissions from the SMT were estimated using the "EMFAC" mode (area fleet-average emissions). The class-specific VKT was the number of vehicles in each class times the 600-m transit distance between the inlet and outlet sampling sites. Because of the difficulties in classifying vehicles into all 16 EMFAC-HK vehicle classes from the traffic videos, manual traffic counting classified vehicles into seven categories (i.e., motorcycle, PC, taxi, LGV, HGV, light bus, and big bus) in 2003 and nine categories (i.e., motorcycle, PC, taxi, LGV, MGV, HGV, light bus, single-deck bus, and double-deck bus) in 2015. Some counted categories covered several EMFAC-HK vehicle classes. For example, LGVs from manual counting in both 2003 and 2015 included EMFAC-HK classes LGV3 (≤2.5 metric tons), LGV4 (2.5–3.5 metric tons), and LGV6 (3.5–5.5 metric tons). The counted LGV numbers were assigned to these categories based on their relative VKT proportions (Appendix Table A.7, available on the HEI website) for both 2003 and 2015. Similarly, the counted light buses in both 2003 and 2015 were assigned to public light buses, private light buses ≤3.5 metric tons, and private light buses >3.5 metric tons. Single-deck buses counted in 2015 were assigned to nonfranchised buses <6.4 metric tons, nonfranchised buses from 6.4 to 15 metric tons, nonfranchised buses >15 metric tons, and single-deck franchised buses based on relative VKT proportions. The 2015 counted MGV-to-HGV ratio was 4.7, which was higher than the EMFAC-HK default ratio of 2.7. The 2003 ratio — assumed to be the same as the 2015 ratio — was used to assign the counted HGV numbers in 2003 to MGV and HGV. Similarly, in 2015 the ratio of counted double-deck buses to single-deck buses was 4.5, which was higher than the EMFAC-HK default ratio of 1.3. The counted ratio was used to assign the counted big buses in 2003 to double-deck and single-deck buses; the single-deck buses were further assigned to subcategories (described above) based on their EMFAC-HK default relative proportions. The correspondence of the manually counted vehicle categories to EMFAC-HK vehicle classes is summarized in Appendix Table A.6.

Because information on model years, fuel types, and technology groups for individual vehicles was not available from the tunnel measurement, the EMFAC-HK default breakdowns for each vehicle class for calendar years 2003 and 2015 were assumed, along with measured ambient temperature and relative humidity, to calculate emissions in the tunnel. Appendix Table A.8 shows the default breakdown of vehicle classes by fuel types. The vehicle speed was assumed to be 80 km/hr (i.e., the posted speed limit). In addition to running exhaust emissions, evaporative running losses of NMHCs were also calculated for each vehicle class assuming a transit time of 27 seconds between the inlet and outlet sampling sites. The fleet-average EF_Ds were calculated using equation 4.

The MOVES model is the U.S. EPA's regulatory tool for on-road mobile-source emissions (U.S. EPA 2015). It is capable of estimating not only emissions from average driving on a regional scale, but also specific driving patterns at the project level. The MOVES model was run at the project level using FMT-specific vehicle driving modes to compare modeled and measured emission factors from the FMT. Before running MOVES, the high-resolution vehicle speed traces measured in the tunnel were reviewed to exclude samples with atypical speed or acceleration patterns. All of the accepted trip samples were parsed into specific MOVES "operating mode" bins according to vehicle-specific power and speed to design profiles representative of the typical range of driving patterns in the tunnel. The speed profile, road grade, and seasonal mean ambient temperature and relative humidity were input into the model. The resulting MOVES emission estimates for a range of vehicle types, fuels, and ages were used to estimate average EF_Cs for the observed mix of vehicle types and ages in each tunnel bore, which were then compared with the in-tunnel measurements. Additional MOVES modeling details are provided in Appendix A.

Source Profile Development and Source Apportionment

Chemical source profiles are used in the effective variance-chemical mass balance receptor model to assess the impact of mobile-source emissions on ambient pollutant concentrations (Chen et al. 2010; Watson et al. 2008, 2016). Comparing the key species in source profiles from current and previous studies can provide insights into the effects of changes in fleet and fuel on emission compositions; comparing source profiles between different sources can yield markers for specific sources. Using the source profiles for the present vehicle fleet is important for accurate source apportionment because the mobile emission composition could have changed over time. The chemical abundances in inlet and outlet samples were similar. Therefore, source profiles for the mobile fleet exhaust were averages of the inlet and outlet samples, and the source profiles for road dust were derived from resuspended road dust samples.

The 2015 SMT study resulted in 126 ambient $PM_{2.5}$ samples (from both the inlet and outlet of the tunnel) characterized for more than 200 inorganic and organic species. Among these, 61 samples also contained concurrent NMHC measurement. The major sources contributing to SMT samples included exhaust from vehicles (fueled by

diesel, gasoline, or LPG), road dust, and background air. Although EMFAC-HK assumes that LPG vehicles do not emit PM, this assumption may not be valid because some particle emissions originate from lubrication oil, and several earlier studies identified LPG contributions to PM (Cao et al. 2006; HKPolyU 2005). The background air in Hong Kong was dominated by motor vehicle exhaust and secondary sulfate and/or nitrate (Cheng et al. 2006). Therefore, six sources of $PM_{2.5}$ and NMHCs were assumed in the SMT source apportionment: diesel exhaust, gasoline exhaust, LPG exhaust, road dust, secondary ammonium sulfate ($[NH_4]_2SO_4$), and secondary ammonium nitrate (NH_4NO_3). The secondary $(NH_4)_2SO_4$ and NH_4NO_3 source profiles contained only secondary species, because it is believed that primary species would be incorporated into primary source profiles (Watson et al. 1994). Road dust samples in the tunnel were collected and analyzed for the same species as the ambient $PM_{2.5}$ samples to construct a "dust" source profile, which contained only PM species. Source profiles for diesel, gasoline, and LPG exhausts specific to Hong Kong with all the markers acquired in the current study were not available. Therefore, the positive matrix factorization (PMF) solution to the chemical mass balance receptor model (CMB) equations (Chen et al. 2007, 2010, 2011; Watson et al. 2008, 2016) was used for constructing a six-factor solution from the speciated $PM_{2.5}$, with three factors constrained to the secondary $(NH_4)_2SO_4$ secondary NH_4NO_3, and dust source profiles. This approach reduced the degree of freedom in the model and helped achieve a unique solution.

The PMF solution links source profiles and ambient concentrations by the CMB equations:

$$C_{i,t} = \sum_j F_{i,j} S_{j,t} + \varepsilon_{i,t}, \quad (9)$$

where $C_{i,t}$ is the concentration of constituent i in $PM_{2.5}$ at time t, $F_{i,j}$ is the fraction of species i in $PM_{2.5}$ source profile j, and $S_{j,t}$ is the source contribution estimate (SCE) of source j at time t. $\varepsilon_{i,t}$ is the deviation between theoretical and measured concentrations attributable to random variability and is minimized in the PMF calculation. PMF solves $F_{i,j}$ and $S_{j,t}$ simultaneously by minimizing the objective function Q value:

$$Q = \sum_t \sum_i q_{i,t}^2 = \sum_t \sum_i \frac{\left(C_{i,t} - \sum_j F_{i,j} S_{j,t}\right)^2}{\Delta C_{i,t}^2}, \quad (10)$$

where $\Delta C_{i,t}$ is the weighting factor for $C_{i,t}$, which mainly corresponds to the measurement uncertainties (random and/or systematic). This PMF calculation is completed using the Multilinear Engine basic two-way model (Paatero 1999) for an easier implementation of the constraints. ΔQ_m, calculated from the fractional change of Q value from the m to $m + 1$ factor solutions, shows little decrease after $m = 6$ (Appendix Figure A.7, available on HEI's website). This supports the assumption that a six-factor solution is appropriate for the dataset and that minor sources, which do not contribute substantially, may not be quantified by PMF. The source profile constraints were then implemented by fixing the corresponding $F_{i,j}$ to constant values.

All $PM_{2.5}$ and NMHC species as well as CO, NO, NO_2, NO_x, and SO_2, were included in the model. Because fewer NMHC samples ($n = 61$) were available than $PM_{2.5}$ samples ($n = 132$), missing data were replaced with average concentrations throughout the monitoring period, with uncertainties 100 times the respective concentrations. This treatment ensured that all measured values are considered in the model while the missing species were heavily downweighted in the fitting process (Reff et al. 2007). In a sensitivity test, it was found that varying the uncertainties from 10 times to 100 times of the average values did not change the SCEs and profiles appreciably, confirming that the model outcomes only depend on those actual measurements.

The PMF results can be evaluated through the performance of fitting, particularly the correlation between measured $C_{i,t}$ and fitted $\sum_j F_{i,j} S_{j,t}$ and the distribution of scaled residuals (i.e., $q_{i,t}$ in equation 10). High correlation coefficients and/or low residuals generally indicate a good fit. As shown in Appendix Figure A.8, the six-factor solution well explained major $PM_{2.5}$ inorganic components, including OC, EC, sulfur (S), NO_3^-, NH_4^+, and most crustal elements, measured in the tunnel (correlation coefficient $r > 0.9$, except for OC [$r = 0.78$]). Some of these species showed average scaled residuals much greater than 1, and thus they dominated the Q value (and PMF fitting process) because of higher measurement precisions (i.e., lower $\Delta C_{i,t}$). Organic markers do not fit well with r generally between 0.3 and 0.5, though their scaled residuals were generally low (0.001–1). This is consistent with the lower signal-to-noise ratio for these organic markers. Species such as vanadium (V), nickel (Ni), Na^+, and acenaphthylene that showed poor fits (low correlation and larger scaled residues) imply the potential impact from additional sources (e.g., crude oil or coal combustion and sea salt) (Stout et al. 2007). However, contributions from these sources to tunnel $PM_{2.5}$ were too small to be quantified by PMF even if the number of factors was increased to seven or eight and/or rotated in any way. On the other hand, they

are not expected to substantially bias the SCEs for major sources (i.e., mobile exhausts and road dust).

The PMF fitting performance for NMHCs and gases is shown in Appendix Figure A.9. Most of the species showed average scaled residuals between 0.1 and 10, suggesting that the *Q* values were more evenly distributed among all species, possibly because of a more uniform estimate of measurement uncertainty. Species that were reproduced well by the PMF solution include isobutane (r = 0.99), propane (r = 0.89), and *n*-butane (r = 0.89), markers for LPG exhausts, as well as propene (r = 0.89), which is a marker for diesel exhaust (Ho et al. 2009b). Isoprene and α-pinene that are of biogenic origins were fitted poorly by the PMF solution, although they contribute very little to total NMHCs in the tunnel. It should be noted that ethylbenzene, *m/p*-xylene, and *o*-xylene had high scaled residuals, mainly because a few outliers occurred at the outlet sampling site on 1/26/2015 and 1/27/2015. The extreme concentrations (>10 times the average) of these outliers may result from unknown contaminations, because they only appeared at the outlet sampling site. These outliers were already weighted much less in the PMF because of the robust fitting algorithm (Paatero 1997).

The differences between outlet and inlet concentrations for each pollutant were used to calculate the fleet-average EF, EF_{fleet}, for each of the valid 2-hour integrated samples. DV-specific EFs by:

$$EF_{DV} = \left(FSC_{DV} \times EF_{fleet}\right) / f_{DV}, \quad (11)$$

where FSC_{DV} is the fractional DV contribution to the pollutant (e.g., $PM_{2.5}$), determined from the PMF source apportionment, and f_{DV} is the fraction of DVs in the fleet. Secondary $(NH_4)_2SO_4$, secondary NH_4NO_3, and road dust did not contribute to EFs substantially, as evidenced by similar concentrations between the outlet and inlet sampling sites. Therefore, FSC_{DV} is defined as:

$$FSC_{DV} = \frac{SCE_{DV}}{\left(SCE_{DV} + SCE_{GV} + SCE_{LPG}\right)}. \quad (12)$$

Equations 11 and 12 were also applied to GV and LPG vehicles as well as NDVs (sum of gasoline and LPG) to determine EF_{GV}, EF_{LPG}, and EF_{NDV}. Because the EFs were determined for each 2-hour sample, average EF and standard error were then reported as the final EF and uncertainty for the DVs, GVs, or LPG vehicles in the SMT study.

Fleet-average EF_Cs for vehicles in the FMT were calculated using equation 5, which were further decomposed into EF_Cs for LD and HD using linear regression, as shown in equation 8. An example of the procedure to derive LD and HD EF_Cs and uncertainties is illustrated in Appendix Figure A.10, where fleet-average EF_Cs for several species for the combined fleet were plotted as a function of the fuel-efficiency-weighted fraction of HD vehicles. The intercept of the linear regression line with the *y*-axis (i.e., when the fleet was solely LD vehicles) was the central estimate of the EF_C for LD vehicles. The EF_C for HD vehicles was calculated by extrapolating the regression line to 100% fraction of HD vehicles. The uncertainties in the linear regression parameters were then used to calculate uncertainties in the EF_Cs for LD and HD. One of the advantages of measurements in the FMT was the restriction of HD vehicles entering Bore 3, which provided three clear traffic mixes: (1) mostly LD traffic (HD fraction <3%) in Bore 3 during the day; (2) mixed LD–HD traffic (8%–15% HD fraction) in Bore 3 during the night and in Bore 4 during afternoons and weekends; and (3) HD-dominated traffic (30%–45% HD fraction) in Bore 4 during weekday mornings. The EF_Cs for all three traffic-mix groups fell onto the linear regression line within the experimental uncertainty for most pollutants, as shown in Appendix Figure A.10. This provides high confidence in the regression parameters.

To assess the trend of NMHCs and $PM_{2.5}$ over time, the SMT profiles for NMHCs and $PM_{2.5}$ from the 2015 study were compared with those from the 2003–2004 study (Cheng et al. 2010; Ho et al. 2007, 2009a, 2009b). This comparison could not be made for the FMT because detailed NMHC and $PM_{2.5}$ composition was not reported in the previous studies.

RESULTS

VEHICLE EMISSIONS IN THE SMT

Temporal Patterns of Traffic, Gases, and Particles

Figure 3 illustrates the diurnal variations of traffic counts (i.e., LD, MD, and HD), and gaseous (i.e., CO, SO_2, NO, NO_2) and PM (i.e., $PM_{2.5}$ and PM_{10}) concentrations measured at the outlet site of the SMT during the periods of 1/19/2015–2/15/2015 and 3/2/2015–3/31/2015 (excluding invalidated data). Additional diurnal patterns of tunnel ambient temperature, relative humidity, wind speed, and CO_2 concentration are shown in the Appendix C (available on the HEI website) in Appendix Figure C.1. Because the traffic patterns were different, data are presented in groups of weekdays (Monday–Friday) and weekends (Saturday–Sunday). Appendix Figure C.2 depicts an example of continuous data measured on 1/26/2015.

Figure 3 (panel A) shows two traffic peaks around 08:00 and 18:00 LDT on weekdays for LD vehicles (including motorcycles, private cars, and taxis), corresponding to morning and afternoon rush hours, respectively. Traffic flows for MD vehicles (including light- and medium-duty trucks and light buses) and HD vehicles (including HD trucks and single- and double-deck buses) were relatively uniform during the daytime (~08:00–18:00 LDT) and lower during early mornings and evenings. Traffic counts from videos show an average of 50% GVs, 14% LPG vehicles, and 36% DVs during morning (08:00–10:00 LDT) and afternoon (17:00–19:00 LDT) rush hours on weekdays. The vehicle fleet contained 37% GVs, 12% LPG vehicles, and 51% DVs during midday sampling periods (11:00–13:00 and 14:00–16:00 LDT).

Traffic patterns were different on weekends (Figure 3 [panel B]). LD vehicle counts gradually increased in the daytime and peaked around 18:00 LDT, with a second peak around 21:00–22:00 LDT, indicating increased late-night activities during weekends. Although the total LD vehicle counts were similar between weekdays and weekends, MD and HD vehicles were 30%–40% lower on weekends. The GV fraction increased from 46% during 08:00–10:00 to 61% during 17:00–19:00, the LPG fraction remained at 15%–20% throughout the day, whereas the DV fractions were 30%–35% during the day and ~24% during 17:00–19:00 LDT on weekends.

Pearson correlation coefficients (r) among pollutants and vehicle categories in Appendix Table C.1 show that CO_2, NO, NO_2, SO_2, $PM_{2.5}$, and PM_{10} were highly correlated ($r > 0.96$), and that CO and other pollutants had lower correlations ($r = 0.57$–0.71). Diurnal patterns of CO concentrations (Figure 3 [panels C and D]) were similar to the LD vehicle counts (Figure 3 [panels A and B]), with $r = 0.91$ for LD vehicles as compared with $r = 0.53$ for MD and HD vehicles. CO is expected to be better correlated with LD vehicles because spark-ignition LD engines emit higher CO (Kean et al. 2003) than compression-ignition MD and HD diesel engines (Wang et al. 2016). On the other hand, NO, NO_2, SO_2, and PM concentrations had higher correlations with MD and HD vehicles ($r > 0.94$) than with LD vehicles ($r \leq 0.90$), which is consistent with MD and HD vehicles being larger emitters of NO_x, SO_2, and PM. As illustrated in Appendix Figure C.2, BC also showed diurnal patterns similar to MD and HD traffic counts. CO_2 concentrations (Appendix Figure C.1 [panels E and F]) may be influenced by both the larger number of LD vehicles with lower EF_Ds as well as the lower number of MD and HD vehicles with higher EF_Ds. Therefore, CO_2 diurnal variations had mixed contributions from all vehicle categories, and the r values (0.92–0.94) were similar among vehicle categories.

Emission Factors of Gases and Particles

Table 1 lists fleet-average EF_Ds (in g/veh/km) for the SMT and the FMT. The 2015 SMT EF_Ds and EF_Cs (average ± standard error) were 1.80 ± 0.13 g/veh/km for CO, 1.58 ± 0.14 g/veh/km and 20.5 ± 0.9 g/kg-C for NO_x (expressed as NO_2), 0.047 ± 0.002 g/veh/km for SO_2, and 0.025 ± 0.003 g/veh/km for $PM_{2.5}$. The measured EF_D for CO_2 was 302 ± 6 g/veh/km (not shown). CO, CO_2, NO, NO_2, NO_x, and SO_2 were averaged from real-time data, whereas NH_3 and $PM_{2.5}$ were calculated from the 2-hour integrated samples. The EF_Ds and EF_Cs measured in the SMT during 2003–2004 are also listed in Table 1 for comparison (Cheng et al. 2006; HKPolyU 2005). EF_Ds, EF_Cs, and EF_Fs from past and current studies are compared in Appendix Tables C.2 through C.4. The most significant decreases were found for SO_2 and $PM_{2.5}$, with ~80% reduction in EF_Ds from 2003–2004 to 2015. These reductions are likely attributable to emission controls, such as reducing the fuel sulfur content (50 to 10 ppm by weight [ppmw] for diesel and 150 to 10 ppmw for gasoline), retrofitting diesel particulate filters or diesel oxidation catalysts, and changing a large fraction of public light buses from diesel to LPG fuels. EF_Ds for CO, NO, and NO_x in 2015 were 5%, 11%, and 8% lower than those in 2003–2004, respectively. However, the differences were not statistically significant at $P < 0.05$ based on Student's t-test. EF_Ds for NO_2 and NH_3 were somewhat higher in 2015 than in 2003–2004, but not statistically significant.

Despite the 20%–30% decrease of average NO and NO_x concentrations in the SMT between 2003–2004 and 2015, NO_2 concentrations increased by 1.4 times at the SMT inlet and 2.2 times at the outlet over this period, consistent with the non-decreasing trend of ambient NO_2 concentrations in Hong Kong (HKEPD 2017d). The 2015 NO_2/NO_x volume ratios at the SMT inlet and outlet were 16.6 ± 2.2% and 16.3 ± 1.6%, respectively, whereas in 2003–2004 these ratios were 5.8 ± 2.7% and 9.5 ± 2.0%, respectively, indicating an increased NO_2 fraction in primary exhaust emissions. These increases are probably related to a higher number of vehicles with diesel oxidation catalysts, which catalytically convert NO to NO_2 for oxidizing CO, hydrocarbons, and PM (Millstein and Harley 2010; Tian et al. 2011). Similar trends have been observed in other cities (Carslaw et al. 2011).

Earlier tunnel studies used linear regression to separate fleet-average emissions to different fleet components (e.g., DVs and NDVs) (Cheng et al. 2006; Pierson et al. 1996). The 2-hour fleet-average EF_Ds versus DV fractions observed in the SMT in 2015 are plotted in Appendix Figure C.3, and the plots do not show linear relationships. Therefore, it appears that a univariate linear regression cannot reliably apportion fleet-average emissions to different fleet

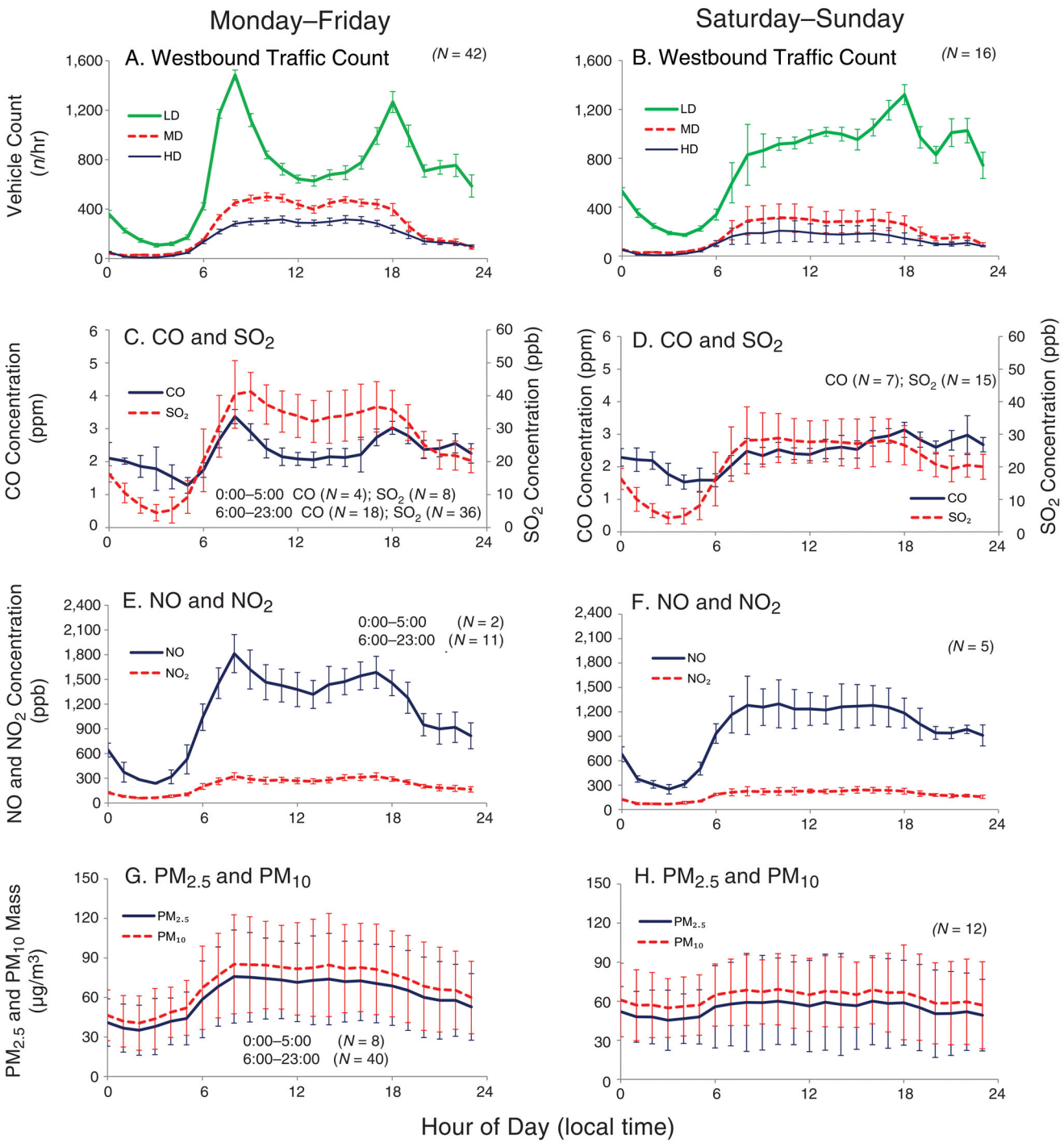

Figure 3. Hourly average diurnal variations in 2015 SMT outlet measurements. (**A** and **B**) westbound traffic counts for light-duty (LD), medium-duty (MD), and heavy-duty (HD) vehicles; (**C** and **D**) CO and SO_2 concentrations; (**E** and **F**) NO and NO_2 concentrations; and (**G** and **H**) $PM_{2.5}$ and PM_{10} mass concentrations during weekdays (left panels) and weekends (right panels). Error bars represent the standard deviation of the hourly average data, and *N* represents the number of days when the indicated measurement was available. Because one of the bores was closed for cleaning and maintenance during 00:00–05:00 Local Daylight Time Monday–Thursday and as a result all traffic was redirected to the other bore, only Friday data were averaged for 00:00–05:00 Local Daylight Time on weekdays. (From Wang et al. 2008. Reprinted by permission of Taylor & Francis Ltd. and the American Association for Aerosol Research.)

Table 1. Comparison of EF_D and EF_C for Gases and $PM_{2.5}$ for 2015 and Past Studies in the SMT and FMT

Tunnel	Year	Vehicle Type	CO	NH_3	NO	NO_2	NO_x (as NO_2)	SO_2	$PM_{2.5}$
EF_D (g/veh/km)[a]									
SMT	2015	Fleet	1.80 ± 0.13	0.019 ± 0.001	0.87 ± 0.08	0.24 ± 0.02	1.58 ± 0.14	0.047 ± 0.002	0.025 ± 0.003
	2003–2004	Fleet	1.88 ± 0.11	0.017 ± 0.003[b]	0.98 ± 0.08	0.22 ± 0.03	1.72 ± 0.13	0.21 ± 0.02	0.131 ± 0.037
FMT[c]	2015 Winter	Fleet	0.69 ± 0.05	0.014 ± 0.001	NA[d]	NA[d]	0.56 ± 0.11	NA[d]	0.024 ± 0.023
		LD	0.69 ± 0.05	0.015 ± 0.002			0.24 ± 0.11		0.016 ± 0.024
		HD	0.66 ± 0.17	0.013 ± 0.005			3.45 ± 0.36		0.093 ± 0.076
	2015 Summer	Fleet	0.70 ± 0.07	0.022 ± 0.002	NA[d]	NA[d]	0.27 ± 0.05	NA[d]	0.007 ± 0.003
		LD	0.67 ± 0.07	0.024 ± 0.002			0.09 ± 0.06		0.001 ± 0.003
		HD	0.94 ± 0.25	0.009 ± 0.006			1.94 ± 0.19		0.065 ± 0.010
	1992 Summer[e]	LD	3.94 ± 0.34	NA[d]	0.29 ± 0.04	0.056 ± 0.042	0.50 ± 0.06	NA[d]	NA[d]
		HD	6.11 ± 18.6		5.26 ± 0.20	0.90 ± 0.20	8.97 ± 0.28		
EF_C (g/kg-C)[a]									
SMT	2015	Fleet	22.5 ± 0.6	0.24 ± 0.01	11.3 ± 0.5	3.2 ± 0.2	20.5 ± 0.9	0.57 ± 0.03	0.30 ± 0.03
	2003—2004	Fleet	26.1 ± 8.3	NA[d]	10.5 ± 2.8	3.1 ± 0.6	19.2 ± 4.8	3.43 ± 0.76	1.75 ± 0.50
FMT[c]	2015 Winter	Fleet	9.5 ± 0.7	0.20 ± 0.02	NA[d]	NA[d]	7.7 ± 1.7	NA[d]	0.33 ± 0.31
		LD	10.0 ± 0.8	0.21 ± 0.02			4.8 ± 1.7		0.26 ± 0.32
		HD	5.2 ± 2.4	0.10 ± 0.07			34.0 ± 5.4		0.93 ± 1.0
	2015 Summer	Fleet	9.6 ± 0.8	0.31 ± 0.02	NA[d]	NA[d]	3.8 ± 0.5	NA[d]	0.10 ± 0.03
		LD	9.7 ± 0.9	0.34 ± 0.02			1.9 ± 0.5		0.03 ± 0.04
		HD	8.7 ± 3.0	0.03 ± 0.08			20.6 ± 3.0		0.70 ± 0.12
	1992 Summer[e]	LD	72.6 ± 6.6	NA[d]	NA[d]	NA[d]	14.7 ± 2.0	NA[d]	NA[d]
		HD	7.7 ± 23.5				50.2 ± 7.2		

[a] SMT data are reported as average ± standard error; and FMT data are reported as central estimate ± 95% confidence interval.

[b] The 2003 SMT NH_3 data are listed for information only because the inlet concentration was not measured and data from a nearby ambient monitoring station were used.

[c] FMT fleet-average EFs were calculated using EFs for LD and HD weighted by their vehicle numbers.

[d] NA = not available.

[e] Emission factors were recalculated from Pierson and colleagues (1996) using the same approach as used in the current FMT study.

components for the 2015 SMT data. The PMF solution was used to separate emissions from different fleet components. Appendix Table C.5 lists the apportioned EF_Ds for LPG vehicles, GVs, DVs, and NDVs. The DV and NDV EF_Ds for NO_x in 2015 obtained by PMF were 2.26 ± 0.39 and 0.40 ± 0.09 g/veh/km, respectively; the corresponding EF_Ds for 2003–2004 obtained from linear regression were 3.97 ± 0.58 and 0.03 ± 0.45 g/veh/km, respectively. Assuming that the 2003–2004 linear regression and 2015 PMF results are comparable, the DV EF_D for NO_x in 2015 was only 57% of that in 2003 and the NDV EF_D for NO_x was 13.3 times that in 2003. The DV and NDV EF_Ds for $PM_{2.5}$ were 0.043 ± 0.003 and 0.008 ± 0.001, respectively, in 2015; the corresponding EF_Ds in 2003–2004 were 0.257 ± 0.031 and 0.017 ± 0.029 g/veh/km (Cheng et al. 2010), indicating that the $PM_{2.5}$ EF_Ds in 2015 were 17% and 47% of those in 2003 for DVs and NDVs, respectively.

Brimblecombe and colleagues (2015) characterized vehicle emissions from three tunnels in Hong Kong using a mobile platform that was driven through the tunnels in 2014. Because of the large uncertainties in fleet fuel economy needed to calculate EF_D using equation 7, only

EF_C and EF_F are compared in Appendix Tables C.3 and C.4, respectively. These tunnels have somewhat different fleet mixes from that of the SMT, with DV fraction differing by ≤7%. The EF_C for CO in SMT in 2015 (22.5 ± 0.6 g/kg-C) was within the range of that of the Aberdeen Tunnel (26.2 g/kg-C), the Lion Rock Tunnel (15.8 g/kg-C), and the Tai Lam Tunnel (13.0 g/kg-C). The higher EF_C for CO in the Aberdeen Tunnel was likely attributable to its LPG vehicle fraction (26%) being higher than that of the other tunnels (6%–13%); LPG vehicles have higher EFs for CO than GVs and DVs (Appendix Table C.5). The EF_C for NO_x in SMT in 2015 (20.5 ± 0.9 g/kg-C) was also within the range of that of the Aberdeen Tunnel (19.3 g/kg-C), the Lion Rock Tunnel (26.7 g/kg-C), and the Tai Lam Tunnel (28.5 g/kg-C). The higher EF_C for NO_x in the Tai Lam Tunnel was likely attributable to its DV fraction being higher (46%) than that of other tunnels (33%–42%). The EF_C for $PM_{2.5}$ in the SMT in 2015 was 49%–73% of those reported for the other three tunnels. The $PM_{2.5}$ in the Aberdeen Tunnel, the Lion Rock Tunnel, and the Tai Lam Tunnel were measured by a DustTrak. As shown in Appendix Figure B.4, the DustTrak overestimates gravimetric mass by about a factor of two using default calibration factors (Wang et al. 2009). Therefore, the EF_Cs for $PM_{2.5}$ in the SMT are likely within the range of those of the other three tunnels after accounting for the DustTrak calibration. Among several other tunnels under comparison, the Zhujiang tunnel in Guangzhou, China (~130 km northwest of the SMT) has a fleet composition and geographical location similar to those of the SMT (Liu et al. 2014; Zhang et al. 2015). Ratios of the fleet-average EF_Ds between the SMT (2015) and Zhujiang Tunnel (2014) were 0.58 for CO, 0.08 for NH_3, 0.84 for NO_x, and 0.30 for $PM_{2.5.}$ The exception is for SO_2, where the EF_D for the SMT was 2.2 times that of the Zhujiang Tunnel. The lower EF_D for most species in the SMT is likely attributable to the more aggressive emission controls in Hong Kong compared with those in mainland China. The gasoline and diesel sulfur content was 10 ppmw in Hong Kong during the 2015 measurement campaign, whereas the fuel sulfur content was 50 ppmw in Guangzhou during the 2014 measurement campaign. The reason for higher SO_2 emissions in the SMT is not known.

Among the 17 quantified PAHs, acenaphthene, naphthalene, and acenaphthylene had the highest gas-phase EF_Ds, and pyrene, fluoranthene, and chrysene had the highest particle-bound EF_Ds, both in 2003–2004 and 2015 (Appendix Figure C.4). The EF_Ds for three PAHs in the gas phase (i.e., naphthalene, acenaphthene, and anthracene) increased 13%–46% from 2003–2004 to 2015; the EF_Ds of other gaseous PAHs remained similar or decreased. On the other hand, the EF_Ds of all particle-bound PAHs except for three (i.e., acenaphthylene, acenaphthene, and fluorine) increased by ~10%–90% from 2003–2004 to 2015. The sums of the EF_Ds of the 17 quantified PAHs were 1.72 mg/veh/km for gas-phase PAHs and 0.131 mg/veh/km for particle-bound PAHs in 2015, an increase of 11% and 32% from those in 2003–2004, respectively.

Among the 16 quantified carbonyl compounds (Appendix Figure C.5), formaldehyde and acetaldehyde had the highest EF_Ds in both 2003–2004 and 2015. In 2015, the respective values were 40.7 and 9.6 mg/veh/km, which were 2.2 and 1.7 times those in 2003–2004. Most other carbonyls showed higher EF_Ds in 2015, with the sum of the 16 carbonyls in 2015 being 82% higher than that in 2003–2004.

The EF_D of the sum of measured NMHCs decreased by 44% from 2003–2004 (105.6 ± 1.9 mg/veh/km) to 2015 (58.8 ± 1.8 mg/veh/km). In 2015, *n*-butane, isobutane, toluene, propane, and ethene had the highest EF_Ds of 10.2 ± 0.9, 7.3 ± 0.7, 5.8 ± 0.8, 4.8 ± 0.4, and 4.2 ± 0.3 mg/veh/km, respectively (Appendix Figure C.6, available on HEI's website). In contrast, the five NMHC species with the highest EF_D in 2003, in decreasing order, were ethene (13.0 ± 0.8 mg/veh/km), toluene (12.0 ± 0.8 mg/veh/km), *n*-butane (8.7 ± 0.6 mg/veh/km), propane (5.7 ± 0.5 mg/veh/km), and isopentane (5.6 ± 0.4 mg/veh/km). As shown in Appendix Figure C.6, EF_D decreased from 2003 to 2015 for most measured NMHCs. As key tracers for diesel vehicular emissions (Lyu et al. 2017), ethene and propene EF_Ds decreased by ~65% from 2003 to 2015, indicating effective reduction of diesel emissions. However, the EF_Ds of isobutane and *n*-butane increased by 32% and 17% from 2003 to 2015, respectively. Note that ~93% of public light buses were powered by diesel in 2003 and ~70% were powered by LPG in 2015. Correspondingly, the fraction of LPG vehicles increased from 9% to 13% from 2003 to 2015. The total LPG consumption by the transportation sector increased by 26% from 2003 to 2015 (HKEMSD 2017).

VEHICLE EMISSIONS IN FMT

Temporal Patterns of Traffic, Gases, and Particles

The diurnal traffic patterns at the FMT differed from those observed at the SMT. A detailed breakdown of the traffic composition observed at the eastbound FMT bores during the 2015 sampling periods is shown in Appendix Figure C.7 (available on HEI's website). Figure 4 (panels A and B) summarizes the diurnal traffic pattern in Bores 3 and 4, respectively. The traffic peak occurred in the afternoon, dominated by the outbound Washington, D.C., traffic (for brevity, only workdays are shown). The schedule

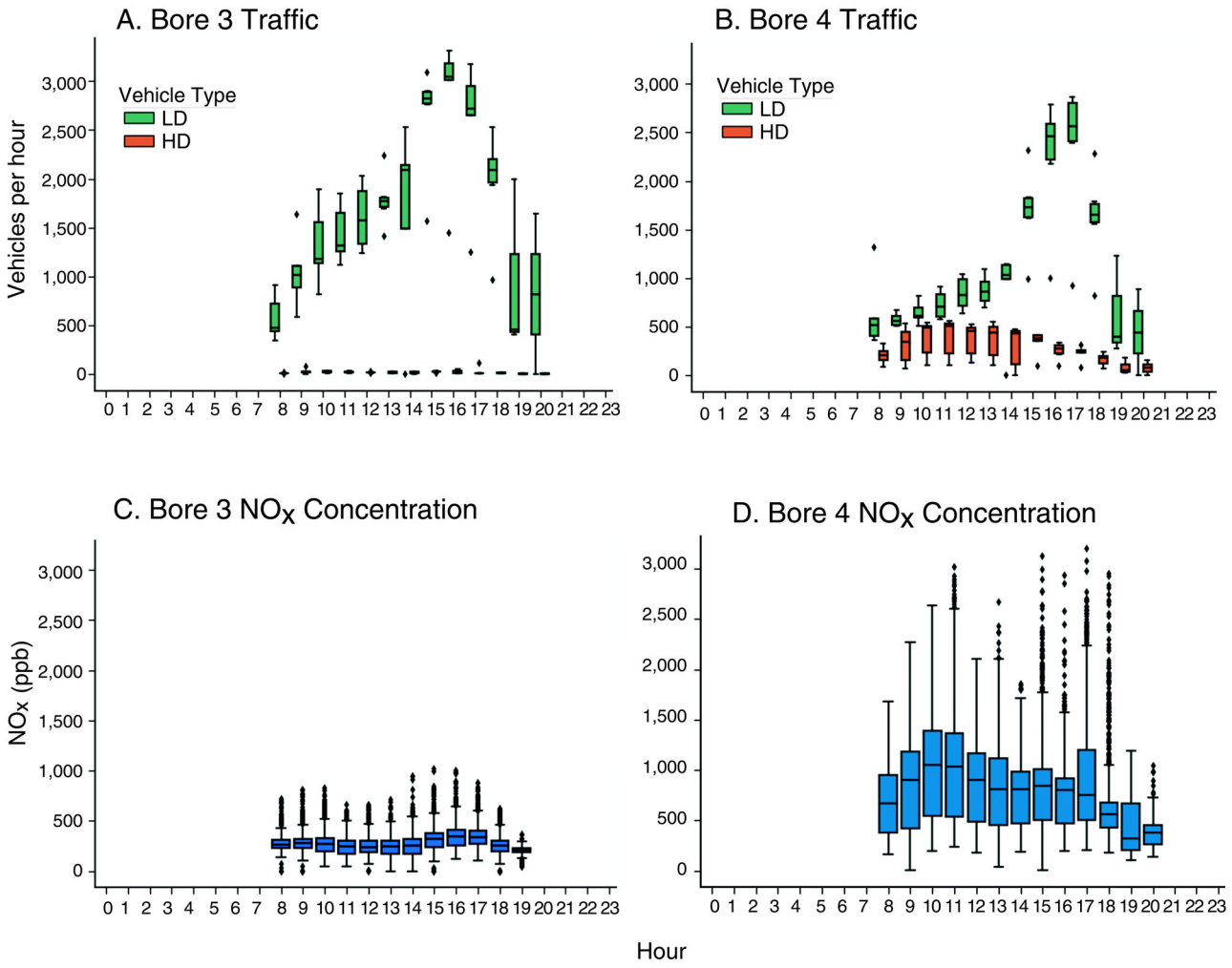

Figure 4. Diurnal variations in the FMT during workdays in the 2015 study. (**A**) LD and HD traffic in Bore 3, (**B**) LD and HD traffic in Bore 4, (**C**) NO_x concentrations in Bore 3, and (**D**) NO_x concentrations in Bore 4. Boxes represent the interquartile range (IQR); horizontal lines denote median values; whiskers extend from the box to show the range of the data extending no more than 1.5 times the IQR from each box edge; flier points are those past the end of the whiskers, that is, potential outliers.

for integrated samples was divided into morning (approximately 09:00–15:00 LDT) and afternoon (15:00–18:30 LDT) periods to capture different traffic compositions. Although LD vehicles dominated traffic counts in Bore 3 (HD fraction <3%), Bore 4 provided different proportions of HD traffic: from ~45% in the morning to ~10% in the afternoon. The fairly wide range of HD fractions was beneficial for derivation of emission factors of LD and HD vehicles. These differences in traffic composition were reflected in the observed pollutant concentrations. NO_x concentrations in Bore 4 were higher in the morning (Figure 4 [panel D]) than in the afternoon owing to the higher proportion of HD vehicles.

Emission Factors of Gases and Particles in FMT

EF_Ds and EF_Cs for criteria pollutants measured in FMT in 2015 were compared with those from the 1992 FMT study (Pierson et al. 1996) (Table 1). EF_Ds, EF_Cs, and EF_Fs from the study of several other tunnels are listed in Appendix Tables C.2 through C.4. As mentioned earlier, EF_Cs were directly calculated from FMT measurements; EF_Ds and EF_Fs were converted from EF_Cs with estimated fuel carbon content and fuel economy and had greater uncertainties. Therefore, only the FMT EF_C results are discussed in this section.

Wintertime EF_Cs for NO_x measured in this study (HD: 34 g/kg-C; LD: 4.8 g/kg-C) were higher than those in summer

(HD: 20.6 g/kg-C; LD: 1.9 g/kg-C). As discussed in Appendix D (available on the HEI website), it is possible that the regression approach of deriving HD emissions of NO_x could bias HD toward high EF_C because of the presence of high-polluting LD vehicles. CO emissions from LD vehicles were about the same in both seasons (10.0 g/kg-C in winter and 9.7 g/kg-C in summer). The mean estimate of CO emissions from HD emissions was about 40% lower in winter (5.2 ± 2.4 g/kg-C) than in summer (8.7 ± 3.0 g/kg-C). However, given the large uncertainties, the two values are not markedly different. HD traffic was found to emit about the same amount of $PM_{2.5}$ in winter (0.93 ± 1.0 g/kg-C) and summer (0.70 ± 0.12 g/kg-C). Although LD vehicle midpoint estimates of EF_C were higher in winter (0.26 ± 0.32 g/kg-C) than in summer (0.03 ± 0.04 g/kg-C), the difference was not statistically significant based on the *t*-test. These observations demonstrate the importance of assessing the effects of temperature, seasonal changes in fuel composition, and other factors on emissions from both HD and LD fleets. Comparison of the measured and MOVES estimate will be discussed in the next section.

Average aerosol size distributions measured during winter and summer in the FMT are shown in Appendix Figure C.8. Significantly higher concentrations, as compared with the background and Bore 3, were observed in Bore 4, which holds the majority of HD traffic at the FMT. The size distributions measured in Bore 4 were characterized by the dominance of UFPs, especially at particle diameters smaller than 50 nm. The UFP number was significantly higher in winter than in summer, suggesting that the difference was driven by homogeneous nucleation attributable to cooling of emitted gases. The EF_Cs for the total number concentration (for particles larger than 15 nm in diameter) in winter were $(1.47 \pm 1.03) \times 10^{15}$ particles/kg-C and $(8.36 \pm 2.29) \times 10^{15}$ particles/kg-C for LD and HD vehicles, respectively. In summer, particle number emissions were significantly lower: the LD EF_C was $(1.42 \pm 3.16) \times 10^{14}$ particles/kg-C, and HD EF_C was $(2.32 \pm 0.79) \times 10^{15}$ particles/kg-C. This compares well with the fleet-average EF_Cs reported elsewhere: $(2.8–4.6) \times 10^{14}$ particles/kg-C for LD vehicles and $(3.3–7.1) \times 10^{15}$ particles/kg-C for HD vehicles (Geller et al. 2005; Kirchstetter et al. 1999; Perkins et al. 2013).

During the FMT study, 117 PAH compounds were measured in both gas and particle phases. The EF_Cs for individual PAH compounds, grouped by the number of aromatic rings, are shown in Appendix Figure C.9. Table 2 provides an overview of EF_Cs for PAHs grouped by the number of aromatic rings. PAHs with two or three rings were found mostly in the gas phase; PAHs with five or more rings were found predominantly in the particle phase. Gas-phase PAH emissions dominated in both seasons. In winter, LD vehicles emitted 9.6 mg/kg-C gas-phase PAHs versus 1.9 mg/kg-C particle-bound PAHs, whereas HD vehicles emitted 16.5 mg/kg-C gas-phase PAHs and 0.9 mg/kg-C particle-bound PAHs. In summer, LD vehicles emitted 9.2 mg/kg-C gas-phase PAHs and 1.0 mg/kg-C particle-bound PAHs; HD vehicles emitted 27.0 mg/kg-C gas–phase PAHs and 3.3 mg/kg-C particle-bound PAHs.

Twenty-eight nitro-PAH compounds were measured in the FMT. Nitro-PAHs are highly mutagenic and carcinogenic and are more toxic than their parent PAHs (Perrini et al. 2005). EF_Cs of individual nitro-PAH compounds are shown in Appendix Figure C.10. Most of these compounds were in the gas phase during both seasons. Nitronaphthalenes were the most abundant compounds among this group. The total EF_C of nitro-PAHs for LD vehicles was 27.25 and 1.25 µg/kg-C in winter and summer, respectively. HD vehicles emitted 13.7 µg/kg-C in winter and 77 µg/kg-C in summer. It should be noted that because the concentrations of these compounds were very low, the split between LD and HD emissions is very uncertain.

Twenty-two hopanes and steranes were measured in the FMT, and their EF_Cs are plotted in Appendix Figure C.11. Most of these compounds were found in the particle phase. These compounds, which are highly stable compounds found in petroleum fuel and oil feedstocks, were used to construct source profiles for HD and LD emissions.

EF_C measurements for 14 carbonyl compounds are shown in Appendix Figure C.12, available on HEI's website. Formaldehyde, acetone, acetaldehyde, and propionaldehyde were the most abundant carbonyls. In winter, LD EF_C was 0.075 µg/kg-C, and HD EF_C was 0.022 µg/kg-C; in summer, these EF_Cs were 0.051 µg/kg-C and 0.12 µg/kg-C, respectively.

EF_C measurements for 46 semi-volatile alkane compounds (with 12 or more carbons) are shown in Appendix Figure C.13. In winter, LD vehicles emitted 13.2 mg/kg-C of these compounds in the gas phase and 1.6 mg/kg-C in the particle phase; HD vehicles emitted 54.6 mg/kg-C and 7.9 mg/kg-C, respectively. In summer, LD vehicles emitted 13.2 mg/kg-C and 0.06 mg/kg-C in the gas- and particle-phases, respectively; HD vehicles emitted 77.4 mg/kg-C and 3.1 mg/kg-C in the gas- and particle-phases, respectively. The EF_Cs generally declined with increasing molecular weight, whereas partitioning progressively shifted to the particle phase. A breakdown of EFs per individual NMHC groups (i.e., alkanes, alkenes, alkynes, and aromatic compounds, cycloalkanes and cycloalkenes) is shown in Appendix Figures C.14 through C.17.

Figure 5 and Appendix Table C.3 provide a comparison of EF_Cs measured during the current study in the FMT

with those reported from past studies. It should be noted that the past measurements in the United States listed in Appendix Table C.3 were all made in summer months. The average temperature in the FMT traffic bores in winter was 7.1°C, ranging from 4.2°C to 8.8°C during the measurement periods. In contrast, average summer temperature in the FMT was 29.7°C, ranging from 25.6°C to 32.7°C. Therefore, the current summer FMT campaign should provide a more meaningful comparison with the previous studies than the winter campaign. Summertime FMT emissions measured in the current study were lower than those in most of the past studies in the United States (Table A.16). LD vehicle EF_C measurements for NO_x and $PM_{2.5}$ in summer 2015 were slightly higher than those from the Caldecott Tunnel in California in 2010 (Dallmann et al. 2013), probably because of differences in fleet composition between the East Coast of the United States and California. Overall, there has been a steady decrease over time in emissions of most pollutants from both LD and HD vehicles.

To compare the 2015 FMT results with those from the 1992 FMT study and the 1992 study of the Tuscarora Tunnel in Pennsylvania, data from the appendix in the study by Pierson and colleagues (1996) were re-evaluated using the same regression approach that was used in the current study. The study by Pierson and colleagues used a weighted regression with weighting done by the total number of vehicles. Because LD vehicles dominated the total vehicle counts, this approach was heavily influenced by the observations with low HD counts, potentially making the derived HD EFs less certain. When processing the 2015 FMT data, weighting was not used in order to give a more balanced representation to all observations, especially those with higher HD vehicle counts. Indeed, the unweighted approach provided somewhat higher HD EFs for the 1992 studies than those reported by Pierson and colleagues (1996). For example, HD EF_C for NO_x increased from the reported 40.3 ± 1.3 g/kg-C to 50.2 ± 7.2 g/kg-C. EF_Cs obtained from the unweighted regression were used to compare with the current study.

Comparison of Criteria Pollutants Emission Factors Between SMT and FMT in 2015

As shown in Table 1, the 2015 fleet-average EF_Ds and EF_Cs in the SMT were higher than those in the FMT for CO (~2.5 times) and NO_x (~2.8 times higher than FMT winter and ~5.6 times higher in summer). The SMT $PM_{2.5}$ EFs were similar to the winter $PM_{2.5}$ EFs in the FMT and were 3.0–3.6 times higher than the summer $PM_{2.5}$ EFs in the FMT. The higher FMT EFs in winter could be attributable to more road dust (deicing materials). The NH_3 EFs were

Table 2. EF_C (µg/kg-C) for Total (Gas and Particles) and Particle-Phase (PM) PAHs by Number of Aromatic Rings, Measured in the FMT in 2015[a]

PAH Ring Number	Vehicle Type	EF_C (µg/kg-C)			
		Winter		Summer	
		Total	PM	Total	PM
2	LD	10,242	1,535	9,101	886
	HD	16,153	69	27,033	1,428
3	LD	733	97	679	4.4
	HD	1,040	615	2,456	1,087
4	LD	506	207	444	93
	HD	161	161	729	729
5	LD	13	13	37	33
	HD	37	37	19	19
6	LD	5.9	5.9	5.6	5.6
	HD	14	14	1.6	1.6
7	LD	1.5	1.5	1.3	1.3
	HD	2.7	2.7	0.0	0.0

[a] Values are central estimates from linear regression.

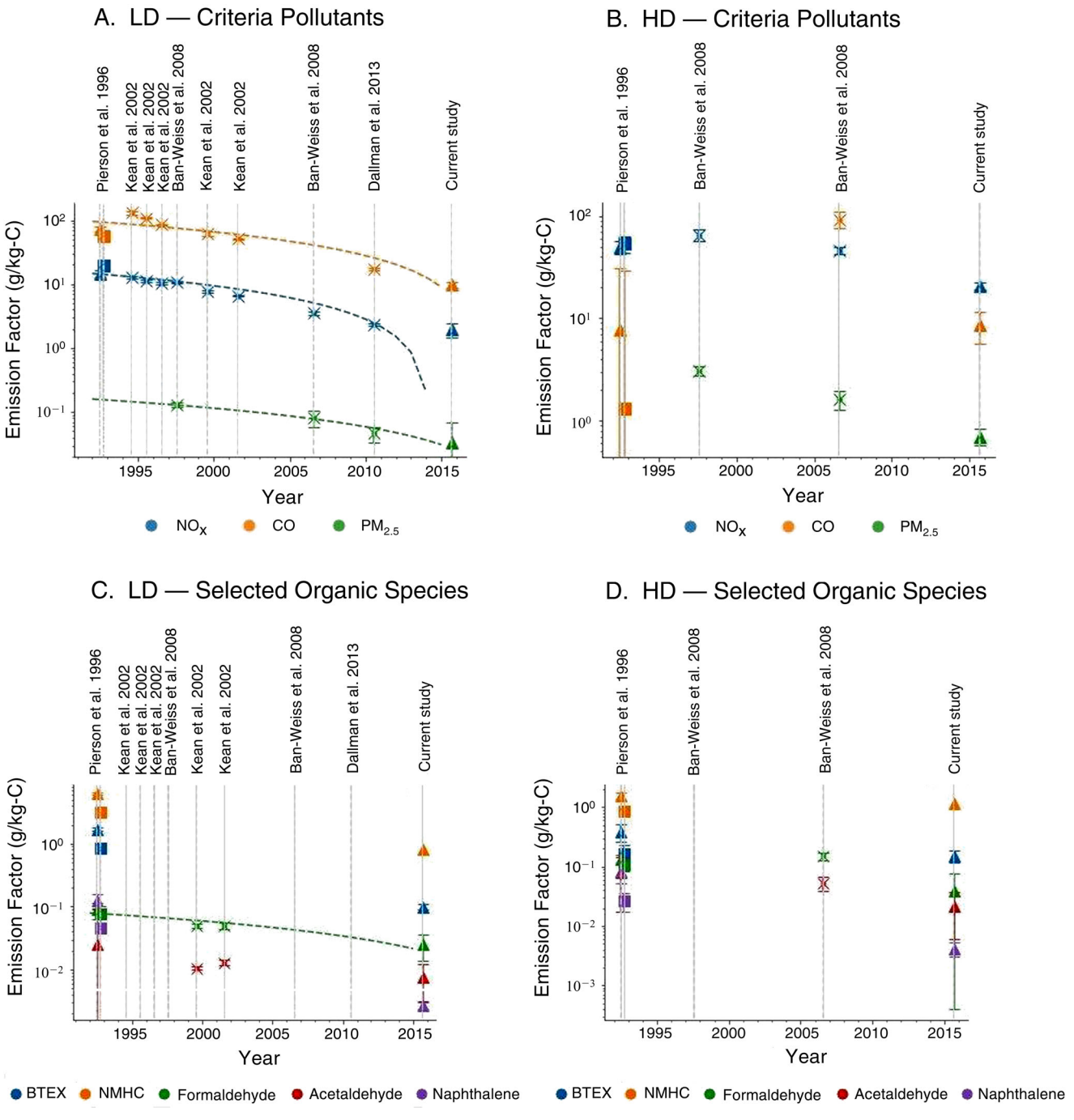

Figure 5. Carbon-based emission factor (EF_C) trends over time for (A) LD emissions of criteria pollutants, (B) HD emissions of criteria pollutants, (C) LD emissions of selected organic species, and (D) HD emissions of selected organic species. ▲= Fort McHenry Tunnel, ■ = Tuscarora Mountain Tunnel, and ✕ = Caldecott Tunnel. Linear regression lines are shown where the temporal correlation was statistically significant (P = 0.05). References for data sources are shown on the upper axis. Winter results from the current study are not included because all other measurements were made during warm weather periods.

similar between the two tunnels. As listed in Appendix Table A.3, the differences between the SMT and the FMT in fleet composition, road gradient, and temperature and relative humidity could contribute to the emission differences. To further explore the potential causes of these differences, Appendix Table C.6 lists average EFs for vehicles with speeds of 80 km/hr for major 2015 fleet categories in Hong Kong and in California as estimated by EMFAC-HK and EMFAC (CARB 2018a), respectively. The EMFAC was used in this comparison because the modeling approach was similar to that of the EMFAC-HK, making the comparison straightforward. The California fleet was used to represent the U.S. fleet for qualitative illustration purposes.

As will be discussed later (Figure 6), EMFAC-HK modeling shows that the principal contributors to SMT CO in 2015 were private cars (26%), taxis (24%), light buses (16%), and motorcycles (15%). Appendix Table C.6 shows that, although the EF_D for CO was 0.12 g/veh/km lower for

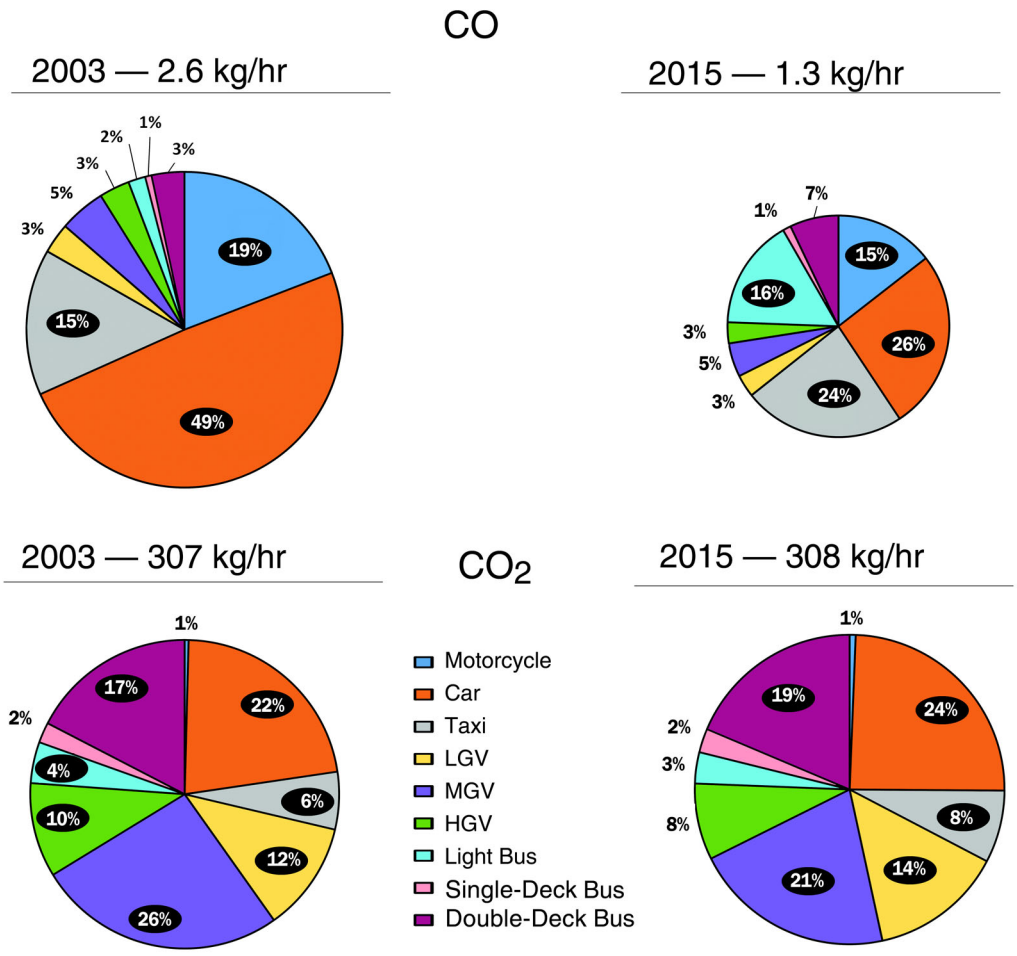

Figure 6. Estimated hourly average emissions of CO, CO_2, evaporative NMHCs, tailpipe NMHCs, total NMHCs, NO_x, $PM_{2.5}$, and PM_{10} in the SMT in 2003 (left) and 2015 (right). EMFAC-HK model estimates included nine vehicle classes determined from manual traffic video counts. The 2015 pie-chart areas are normalized to those of 2003 based on the fleet-average hourly emission rates. (*Figure 6 continues on next 3 pages.*)

gasoline private cars in Hong Kong than those in California, the Hong Kong motorcycle EF_D for CO was 7.46 g/veh/km higher than that in California. Furthermore, the Hong Kong fleet has a higher percentage of motorcycles than that in the United States: motorcycles comprised 2.2% of the fleet during the 2015 SMT study periods and only 0.02% and 0.21% in winter and summer study periods in the FMT, respectively (Appendix Figure C.7). LPG-powered taxis and public light buses had CO EF_Ds of 2.67 g/veh/km and 13.37 g/veh/km and were 11.6% and 1.4% of the SMT fleet, respectively. The higher CO EF_D for motorcycles as well as the high CO EF_D for LPG vehicles were likely the cause of higher fleet-average EF_D for CO in the SMT.

DVs were major contributors to NO_x emissions. Appendix Table C.6 shows that the EF_Ds for DVs differed <40% between the Hong Kong and California fleets. Therefore, the annual aggregated fleet-average DV emission

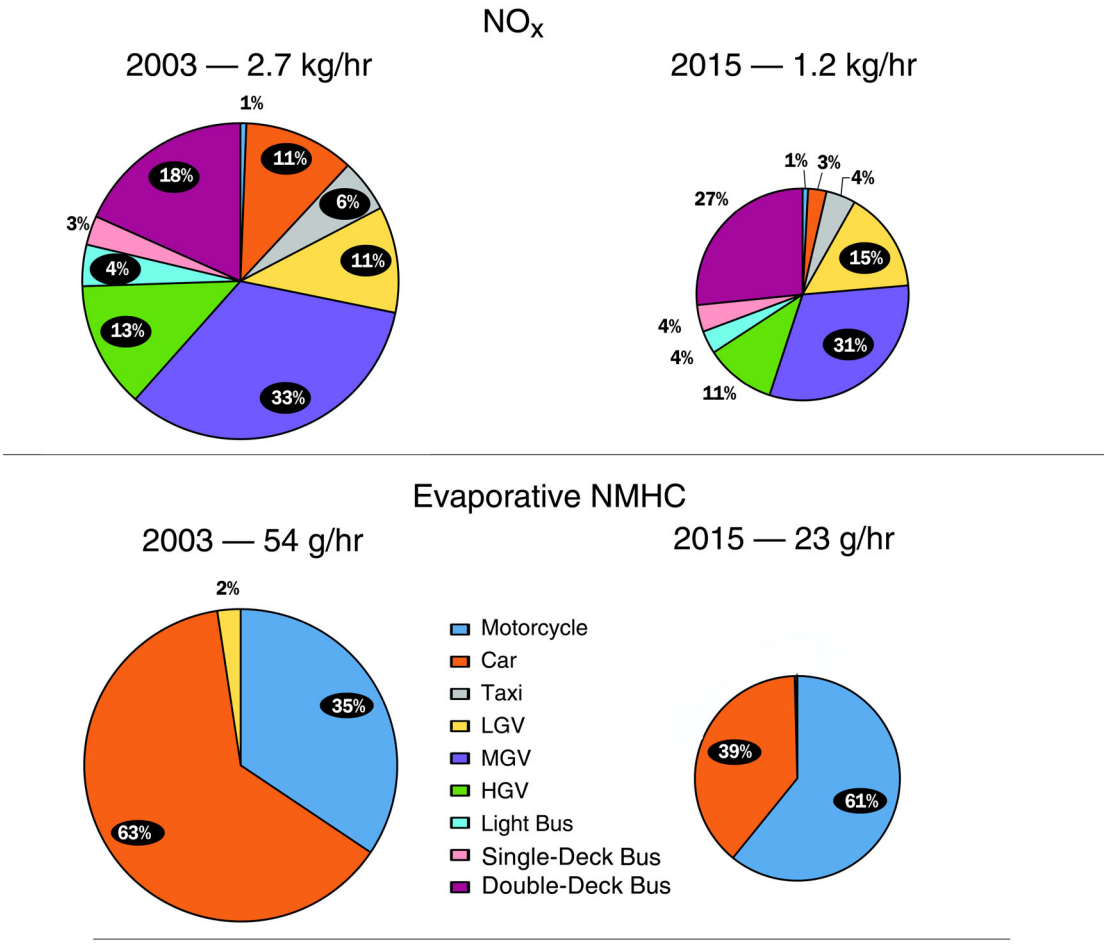

Figure 6. (*Continued*).

differences between Hong Kong and California could not explain the twofold differences between the SMT and the FMT. Appendix Table C.5 shows that in the SMT the DV EF_D for NO_x (2.26 g/veh/km) was within the bounds of the HD EF_Ds for NO_x during the two FMT seasons (3.45 g/veh/km in winter and 1.94 g/veh/km in summer; see Table 1). However, the SMT NDV EF_D for NO_x (0.40 g/veh/km) was higher than the LD EF_D in the FMT (0.24 g/veh/km in winter and 0.09 g/veh/km in summer). Although there are uncertainties in apportioning the NO_x emissions to different SMT fleet components, Appendix Table C.6 also shows that the LPG taxis and public light buses in Hong

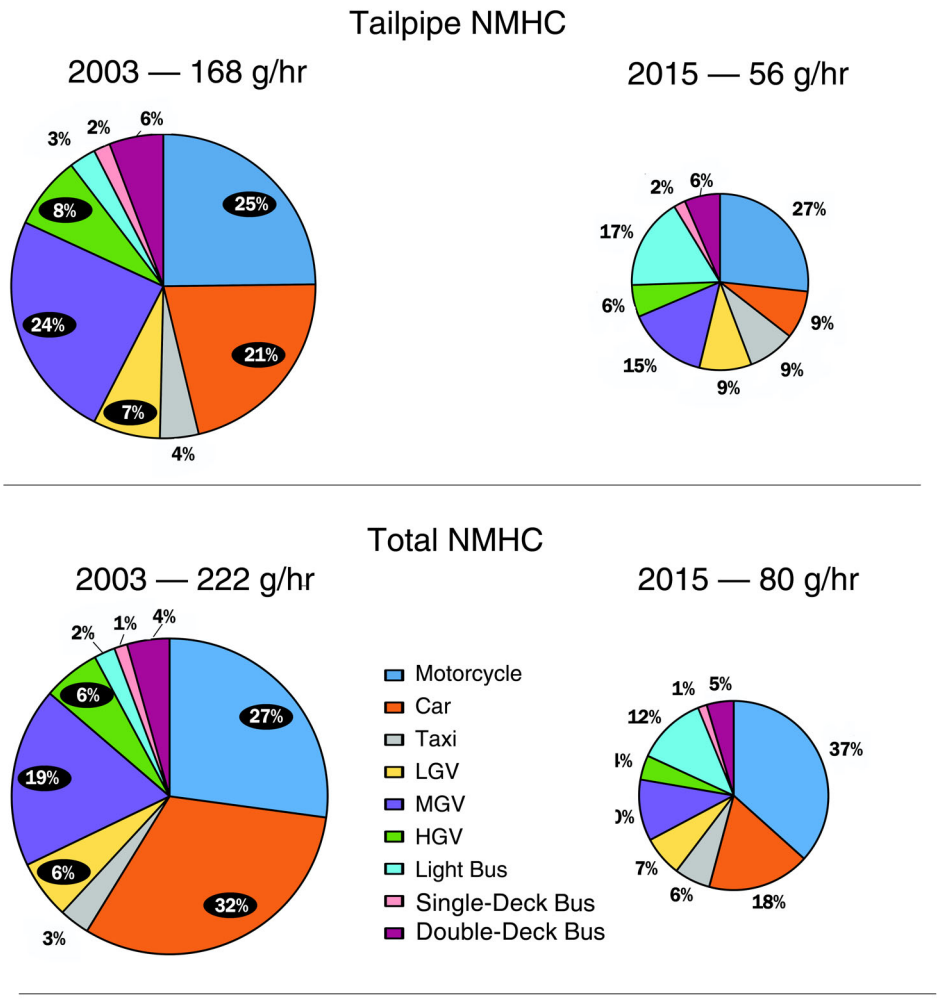

Figure 6. (*Continued*).

Kong have more than sixfold higher NO_x EF_Ds than California cars. Therefore, the higher NDV emissions could be a contributor to the higher fleet-average EF_D for NO_x in the SMT.

Double-deck buses had the highest contribution (26%) to $PM_{2.5}$ emissions in the SMT (Figure 6). These buses are rarely in operation in the United States. Appendix Table C.6 shows that for most vehicle categories the values of EF_Ds for $PM_{2.5}$ in Hong Kong were more than twice those in California, possibly contributing to the higher fleet-average EF_D for $PM_{2.5}$ in the SMT than in the FMT.

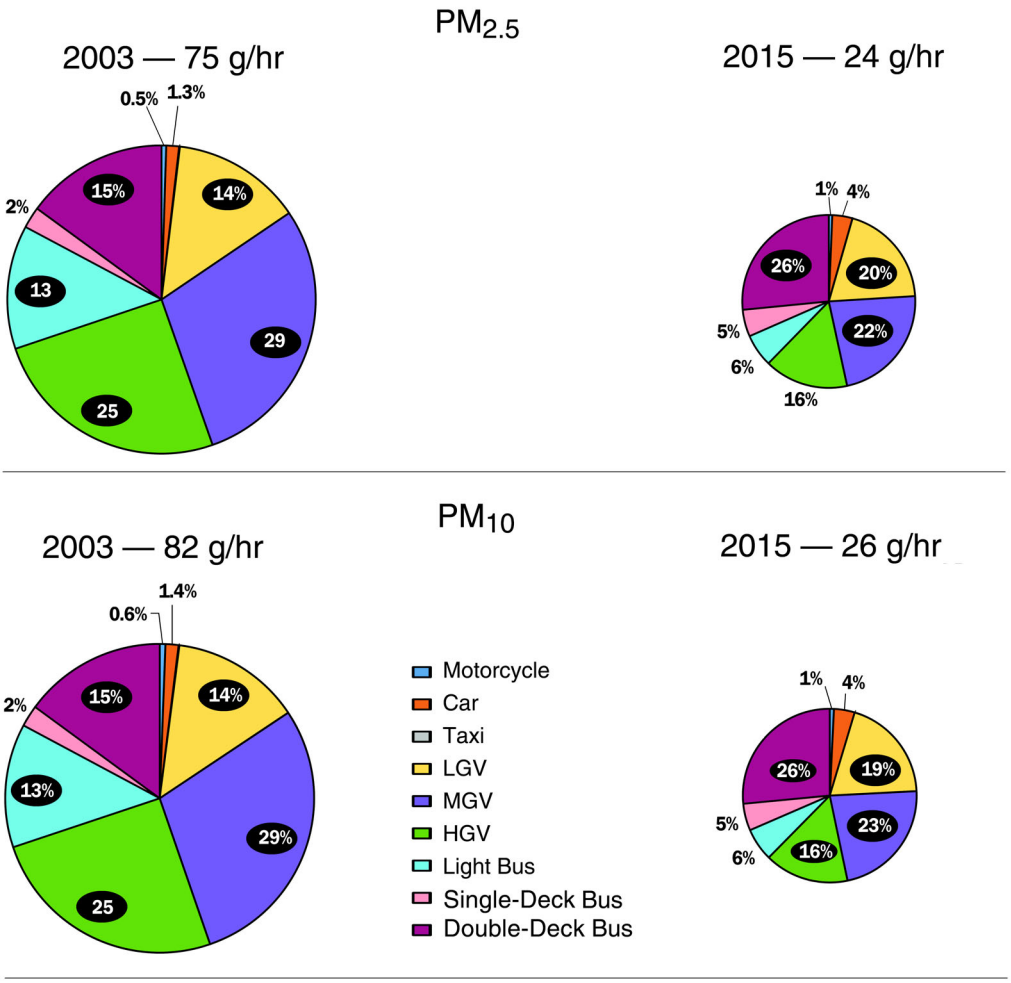

Figure 6. (*Continued*).

COMPARISON OF MEASURED AND MODELED EMISSIONS

SMT Measurement and EMFAC-HK Model Comparison

The SMT measured and EMFAC-HK model estimates of fleet-average EF_Ds for CO_2, CO, NO_x, NMHCs, and $PM_{2.5}$ are compared in Table 3. For the 2003 data, the modeled EF_D for CO_2 differed from the measured value by <5%; the modeled EF_Ds for CO, NO_x, and NMHCs were 1.5, 1.6, and 2.2 times the measured values, respectively; and the modeled EF_D for $PM_{2.5}$ was 61% of the measured value. The modeled EF_Ds agreed better with the 2015 measurements: the modeled EF_D for CO_2 differed from measurements by <4%; the modeled EF_Ds for CO, NO_x, and NMHCs were 73%, 78%, and 135% of the measured values, respectively; and the modeled EF_D for $PM_{2.5}$ differed from the measured value by <3%. Note that the modeled NMHC running evaporative losses were 33% and 40% of running exhaust emissions in 2003 and 2015, respectively. Appendix Figure C.18 (available on the HEI website) compares time series of measured and modeled EF_Ds over the 2015 sampling period and shows that, although the measured values had larger variation, the measured and modeled values agreed reasonably well and followed similar temporal patterns. Table 3 also compares the 2015-to-2003 ratios of measured and modeled EF_D values. The modeled and measured EF_D changes from 2003 to 2015 agreed for CO_2. However, the modeled EF_Ds for CO, NO_x, and NMHCs showed greater decreases than the measured values from 2003 to 2015, mainly because of higher modeled EF_D values in 2003. The measured EF_D for $PM_{2.5}$ had a greater decrease than the EMFAC-HK estimates.

The hourly average vehicle count and modeled EF_Ds for each EMFAC-HK vehicle class are summarized in Appendix Table C.7. EF_Ds were generally higher in 2003 than in 2015, with some exceptions, such as the CO and NMHCs EF_Ds from public light buses. Public light buses were mostly powered by diesel engines in 2003; in 2015, LPG-powered public light buses became dominant (69%) in Hong Kong. LPG vehicles (taxis and public light buses in 2015) emitted substantially higher CO than other vehicle types, in accord with the PMF finding (Appendix Table C.5). The highest $PM_{2.5}$ and PM_{10} EF_Ds resulted from DVs (e.g., heavy goods vehicles [HGVs], nonfranchised buses, and double-deck buses) in both 2003 and 2015. HGVs, nonfranchised buses, and double-deck buses also had the highest EF_Ds for CO_2 and NO_x. Motorcycles and public light buses had the highest EF_Ds for CO and NMHCs in 2015.

Figure 6 shows the breakdown of hourly-average CO_2, CO, NO_x, evaporation/tailpipe/total NMHCs, $PM_{2.5}$, and PM_{10} emission rates over the 2003 and 2015 sampling periods from the manual count of nine traffic classes. The breakdowns of hourly-average emission rates by gasoline, LPG, and diesel fuels are shown in Appendix Figure C.19. The CO_2 emission rates and distribution among vehicle categories were similar between 2003 and 2015 (Figure 6). Private cars and medium goods vehicles [MGVs], because of their large vehicle numbers (~43% and 14%–19% of total fleet, respectively), were the largest contributors

Table 3. Comparison of Measured and Modeled EF_D (Average ± SE), using EMFAC-HK for the SMT Fleet in 2003 and 2015

	EF_D (g/veh/km)				Ratios			
	2003		2015		Modeled/ Measured		2015 / 2003	
Species	Measured	Modeled	Measured	Modeled	2003	2015	Measured	Modeled
CO_2	310 ± 17	323.7 ± 5.0	302 ± 6	313.9 ± 2.5	1.04	1.04	0.97	0.97
CO	1.88 ± 0.11	2.80 ± 0.07	1.80 ± 0.13	1.31 ± 0.01	1.49	0.73	0.95	0.47
NO_x	1.72 ± 0.13	2.80 ± 0.10	1.58 ± 0.14	1.23 ± 0.02	1.63	0.78	0.92	0.44
NMHCs	0.106 ± 0.002	0.233 ± 0.003	0.059 ± 0.002	0.080 ± 0.001	2.20	1.35	0.56	0.34
$PM_{2.5}$	0.131 ± 0.037	0.080 ± 0.003	0.025 ± 0.003	0.024 ± 0.000	0.61	0.97	0.19	0.31

(21%–26%) to CO_2 emissions. Double-deck buses had the highest EF_D for CO_2 and contributed to 17%–19% the total CO_2 emissions. Appendix Figure C.19 (panels A and B) show that DVs were the largest CO_2 contributors (71% in 2003 and 66% in 2015), because of the lower fuel economy (km per liter fuel) of the medium- and heavy-duty diesel vehicles in the tunnel.

The SMT fleet-average CO emission rate decreased by half from 2003 to 2015 (Figure 6), and the contributions among vehicle categories varied. The contributions by private cars decreased from 49% in 2003 to 26% in 2015, because EF_Ds for CO decreased for all vehicles, and the number of cars without a catalytic converter decreased from 4.4% of the fleet in 2003 to 0.4% in 2015 (Appendix Table A.8). On the other hand, because a large fraction of public light buses were converted from diesel to LPG, the light bus contribution to CO emissions increased from 2% in 2003 to 16% in 2015. Motorcycles and taxis were also large CO contributors (15%–24%). Among the three fuels (Appendix Figure C.19 [panels C and D]), the gasoline contribution to CO decreased from 69% in 2003 to 42% in 2015, and the LPG contribution increased from 16% in 2003 to 39% in 2015.

SMT fleet-average NO_x emission rates decreased from 2.7 kg/hr in 2003 to 1.2 kg/hr in 2015. MGVs and double-deck buses were the largest NO_x emitters (Figure 6), accounting for 31%–33% and 18%–27% of total NO_x emissions, respectively. Other diesel-powered vehicles, including LGVs, HGVs, and single-deck buses, contributed 3%–15% of NO_x emissions. DVs were the dominant (>80%) NO_x contributors in both 2003 and 2015 (Appendix Figure C.19 [panels E and F]).

EMFAC-HK assumes NMHC evaporation only occurs for GVs. Therefore, evaporative NMHC emissions were dominated by motorcycles and private cars. Note that although the fraction of motorcycles with a catalytic converter increased from 0% in 2003 to 54% in 2015 (Appendix Table A.8), the evaporative NMHC EF_D for motorcycles without a catalytic converter almost doubled from 2003 to 2015 in EMFAC-HK, likely because of aging. The motorcycle contribution to evaporative NMHC emissions increased from 35% in 2003 to 61% in 2015 (Figure 6). Even though motorcycles were only ~2% of the vehicle fleet, their tailpipe NMHC emission factors were ~2–50 times that of other vehicle categories (Appendix Table C.7). Therefore, motorcycles were the largest contributors to tailpipe NMHC emissions (~25%) in both 2003 and 2015 (Figure 6). NMHC tailpipe emissions from light buses increased from 3% in 2003 to 17% in 2015, because NMHC EF_Ds were higher for LPG than for diesel. The sum of emissions from motorcycles and private cars contributed ~50%–60% of total (evaporative plus tailpipe) NMHC emissions (Figure 6). DVs were the dominant PM emitters, contributing ≥96% of $PM_{2.5}$ and PM_{10} emissions (Appendix Figure C.19 [panels I–L]). MGVs and HGVs were the largest $PM_{2.5}$ contributors in 2003 (29% and 25%, respectively), and double-deck buses and MGVs were the largest $PM_{2.5}$ contributors in 2015 (26% and 22%, respectively) (Figure 6). In EMFAC-HK, LPG-powered taxis were assumed to directly emit negligible amounts of PM, which the PMF analysis suggested may not be true (Appendix Table C.5). The distributions of $PM_{2.5}$ and PM_{10} among vehicle categories were similar, because non-tailpipe emissions, the main contributors to coarse PM, are not included in EMFAC-HK.

As shown in Appendix Figure C.19, compared with the fleet in 2003, the 2015 DV contributions to CO_2, NMHCs, and PM decreased, while their contributions to NO_x increased. LPG vehicle contributions to CO_2, CO, and NMHCs increased. These changes reflect the reduced diesel emissions and increasing number of LPG-powered vehicles in Hong Kong.

FMT Measurement and MOVES Comparison

Sensitivity of EF_Cs to temperature and relative humidity was tested by running MOVES with fixed speed (55 mile/hr, or 89 km/hr) for the entire tunnel grade profile while varying temperature from 20ºF to 90ºF (−7ºC to 32ºC) and relative humidity from 20% to 70%, in order to represent the range of ambient conditions that occurred during the current study. Appendix Table C.8 shows the predicted EF_C changes caused by changes in temperature and relative humidity as well as the observed EF_C variation between winter and summer at the FMT. The observed EF_C variations for LD and HD fleets were determined by comparing the seasonal average of all sampling runs with predominantly LD traffic and >30% HD traffic.

When holding relative humidity constant at 20% and increasing temperature from 20ºF to 90ºF, for passenger cars, MOVES predicted that CO EF_C increased by 39%, $PM_{2.5}$ and EC EF_Cs decreased by 67% and 83%, respectively, and NO_x and NMHC EF_Cs showed minor changes. For long-haul combination trucks, MOVES predicted that EF_Cs for CO, NO_x, NMHCs, $PM_{2.5}$, and EC decreased by 11% to 16%. When holding temperature constant at 90ºF and increasing relative humidity from 20% to 70%, MOVES predicted that CO EF_C for passenger cars increased by 15.3%, and NO_x, evaporative NMHCs, $PM_{2.5}$, and EC EF_Cs decreased by 7.8% to 25.7%. For long-haul combination trucks, MOVES predicted that EF_Cs for all modeled pollutants decreased by 7.2% to 25.4% with constant temperature and relative humidity increasing from

20% to 70%. For the actual fleet compositions and range of temperature and relative humidity during the tunnel study the observed relative differences between winter and summer EF_Cs in FMT agreed well with MOVES for NMHCs, HD CO, and EC. NO_x and $PM_{2.5}$ were qualitatively similar in that both modeled and measured EF_Cs decreased from winter to summer but the relative decreases measured were much larger than predicted by MOVES. LD CO was predicted to decrease by about the same percentage as for HD traffic but there was no significant seasonal difference observed in the measured EF_Cs.

The ratios of EF_C from MOVES to EF_C from measurements are plotted in Figure 7. Error bars are the propagated analytical uncertainty and range of model output for various traffic conditions. MOVES2014a was found to significantly overestimate LD EF_Cs for CO, BTEX, NMHCs, and summer $PM_{2.5}$, with the overestimation being somewhat greater for the summer season. For HD vehicles, total PAHs and aldehydes were overestimated. 1,3-Butadiene was underestimated for all vehicle types. MOVES was most accurate for LD NO_x and HD NMHCs, EC, OC, and $PM_{2.5}$. The small underestimation for LD $PM_{2.5}$ in winter may be a consequence of a contribution to the measured values from resuspended road salt, which is not accounted for by MOVES because it only includes exhaust and particles from brake and tire wear. This component may offset the overestimation of other PM.

Because there were large variations in EFs for individual PAH compounds, the values of total PAHs presented in Figure 7 (panel A) were dominated by a few lower-molecular-weight species, such as naphthalene. Therefore, it is worthwhile to examine the performance of MOVES for each of the 16 PAH compounds included in MOVES. Although the model and measurements quantified gas and particle phases of these semivolatile compounds separately, only the combined gas and particle phases are compared in Figure 7 because of the potential for phase transformations during residence in the tunnel (panel B). The compounds were arranged by increasing molecular weight (and therefore approximately by decreasing volatility), which shows that the overestimation by MOVES was generally greater for PAHs that tend to be present in the particle phase and was also greater for HD vehicle emissions.

It should be noted that the MOVES output was found to be sensitive to the assumed fleet composition. For example, when the default "sourcetypeagedistribution" of the MOVES2014a was used to derive the number of vehicles of each type by model year, the model overpredicted most of the pollutants other than 1,3-butadiene and NO_x (Appendix Figure C.20).

SOURCE PROFILES, MARKERS, AND SOURCE APPORTIONMENT

Profiles of PAHs, Carbonyls, and NMHCs

PAHs were predominantly in the gas phase, with gaseous PAH concentrations being ~15 times higher than those of particulate PAHs in the SMT. Appendix Figure C.21 (available on the HEI website) shows the abundance of individual PAHs normalized to the sum of gaseous and particulate PAHs mass concentrations measured in the SMT. Similar to 2003–2004, acenaphthene was the most abundant gaseous PAH (43.4 ± 6.8%), followed by naphthalene (25.1 ± 7.3%) and acenaphthylene (14.5 ± 3.6%). The sum of two-ring (i.e., naphthalene) and three-ring (i.e., acenaphthylene, acenaphthene, fluorine, phenanthrene, and anthracene) PAHs accounted for ~99% of gaseous PAHs and 92% of total measured PAHs. Pyrene and fluoranthene were the most abundant particulate PAHs, contributing to 1.79 ± 0.57% and 1.31 ± 0.44% of total PAHs. The ratio of indeno[1,2,3-*cd*]pyrene to the sum of indeno[1,2,3-*cd*]pyrene and benzo[*ghi*]perylene was 0.31 ± 0.12 in 2015, similar to the range of ratios (0.29–0.36) measured in 2003. The corresponding ratios were 0.18 for gasoline, 0.37 for diesel, 0.56 for coal combustion, and 0.62 for wood burning (Gogou et al. 1996; Grimmer et al. 1983; Ho et al. 2009a); similar ratios for tunnel measurements and diesel indicate that diesel emissions were important contributors to tunnel PAHs. The ratio of fluoranthene to the sum of fluoranthene and pyrene was 0.42 ± 0.05 in 2015, similar to the range of ratios (0.41–0.45) in the 2003–2004 SMT study and to the value (0.43) reported for automobile emissions (Sicre et al. 1987). Appendix Figure C.22 shows the distribution of individual PAHs in gaseous and particulate phases. More than 85% of the two- and three-ring PAHs were in the gaseous phase, and more than 75% of the four- to six-ring PAHs were in the particulate phase.

The abundance of 16 carbonyl compounds (normalized to the sum of carbonyl mass concentrations) measured in the SMT are plotted in Appendix Figure C.23. Formaldehyde was the most abundant carbonyl, contributing to 63.9 ± 5.3% of total measured carbonyls, followed by acetaldehyde (12.7 ± 2.6%), crotonaldehyde (6.0 ± 2.7%), and acetone (5.4 ± 1.5%). These four carbonyls were also the most abundant carbonyl compounds in the 2003–2004 tunnel measurement campaign (Ho et al. 2007).

Appendix Figure C.24 shows that the alkanes and cycloalkanes were the most abundant NMHCs (59% of the total NMHCs mass concentration) in the SMT, followed by aromatics (23%), alkenes (14%), and alkynes (4%). Appendix Figure C.25 shows the average abundance of NMHC species with abundance >0.5%. Among the

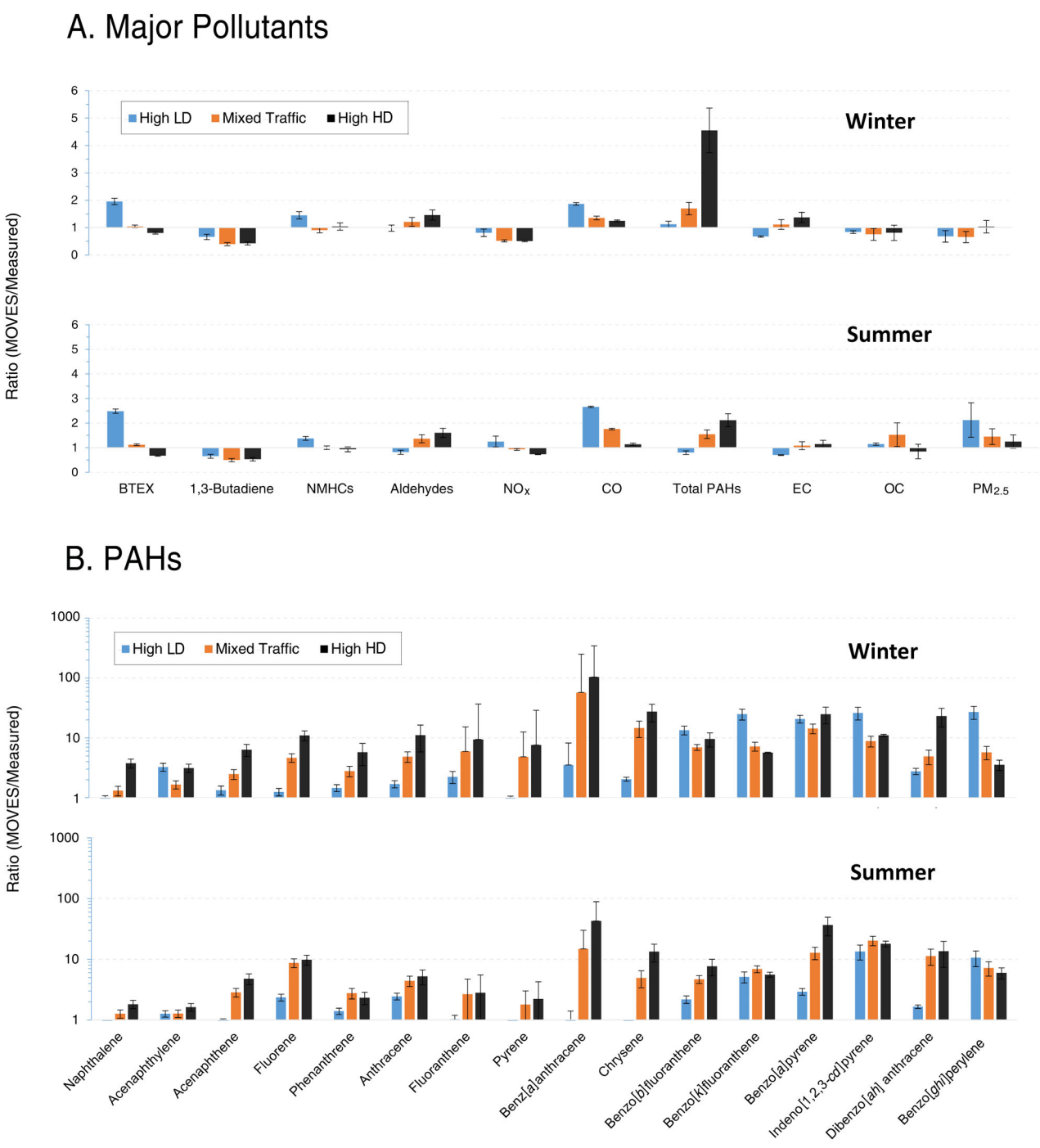

Figure 7. Ratios of EF_C as calculated by MOVES to fleet-average EF_C measured in the FMT in 2015 for (A) major pollutants and (B) PAHs. Results for three fleet compositions are shown: high LD (≥97%), mixed traffic (8–15% HD), and high HD (>30%).

66 quantified NMHCs, the 10 most abundant species were *n*-butane (16.3 ± 4.9%), isobutane (11.9 ± 3.7%), propane (9.9 ± 2.1%), toluene (9.2 ± 3.7%), ethene (7.4 ± 1.9%), *m/p*-xylene (5.5 ± 8.9%), isopentane (4.5 ± 1.1%), ethane (4.0 ± 1.2%), ethyne (4.0 ± 1.0%), and propene (3.2 ± 0.8%). Among these species, *n*-butane, isobutane, and propane are major constituents of LPG; toluene, isopentane, and *m/p*-xylene are markers for gasoline fuel; and ethyne, ethene, and ethane are combustion products that are markers for tailpipe emissions (Guo et al. 2011; Ho et al. 2009b; Tsai et al. 2006; Watson et al. 2001).

The ethyne/ethene molar ratio has been used as an indicator of the efficiencies of engine combustion and catalytic converters (Guo et al. 2011; Hoekman 1992), with lower ratios indicating higher efficiencies. The average ethyne/ethane ratio measured from SMT in 2015 was 0.60 ± 0.14, which is somewhat higher than the 0.53 ± 0.03 ratio in a Hong Kong roadside study (Tsai et al. 2006) and the 0.45 ± 0.07 ratio in the 2003–2004 SMT study (Ho et al. 2009b). The characteristic molar ratio of propane/(*n*- + *i*-butanes) of LPG is 0.38 (Tsai et al. 2006), whereas the measured ratio was 0.36 ± 0.07 in 2015. Similar ratios between LPG vapor and tunnel samples indicate the contributions of evaporative losses from LPG vehicles to tunnel NMHCs. This observation seems to be in contradiction with the assumption in EMFAC-HK that LPG vehicles and DVs do not have evaporative emissions.

Appendix Figure C.26 shows contributions of NMHC groups to total NMHCs measured in the FMT in 2015. Alkanes, alkenes, alkynes, and aromatic compounds contributed most to NMHCs emissions, with cycloalkanes and cycloalkenes contributing ≤5% of the total NMHC emissions. Summer HD emissions of NMHCs were 8% higher than in winter, whereas LD emissions were 14% higher.

Profiles of $PM_{2.5}$ Species

Figure 8 shows the reconstructed $PM_{2.5}$ mass (Chow et al. 2015), assuming major $PM_{2.5}$ constituents of organic matter (calculated as OM = OC × 1.2), EC, SO_4^{2-}, NO_3^-, NH_4^+, geological materials (estimated as 2.2 × [Al] + 2.49 × [Si] + 1.63 × [Ca] + 1.94 × [Ti] + 2.42 × [Fe]), and others (i.e., other measured ions, elements, and unidentified species) for data obtained in 2015 and 2003–2004 (Cheng et al. 2010) in the SMT. EC and OM were the most abundant constituents in both the 2015 and 2003–2004 measurements. The OM abundances were similar (~30%), and the EC fraction decreased from 51% in 2003–2004 to 35% in 2015. The OC/EC ratio was 0.7 ± 0.2 in 2015, which was similar to the OC/EC ratio of 0.5 ± 0.2 in 2003.

The average SMT $PM_{2.5}$ concentration decreased by ~70% (from 229.1 ± 22.1 μg/m^3 in 2003–2004 to 74.2 ± 2.1 μg/m^3 in 2015), indicating that vehicle emission control activities have been effective in reducing $PM_{2.5}$ emissions and have caused PM composition to change. Appendix Figure C.27 compares EF_Ds between 2003–2004

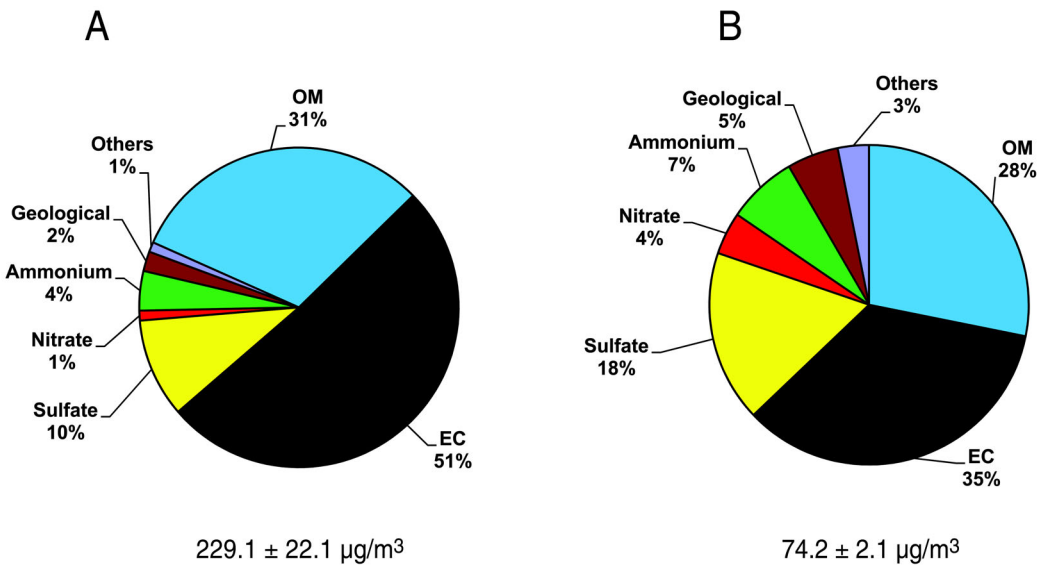

Figure 8. Comparison of reconstructed $PM_{2.5}$ mass for species measured at the SMT in (A) 2003–2004 and (B) 2015. OM = 1.2 × OC. Geological material = (2.2 × Al) + (2.49 × Si) + (1.63 × Ca) + (1.94 × Ti) + (2.42 × Fe). (From Wang et al. 2018. Reprinted by permission of Taylor & Francis Ltd. and the American Association for Aerosol Research.)

and 2015 for $PM_{2.5}$ elements, ions, and carbon. EF_Ds for almost all species showed significant decreases, thus contributing to an overall decrease of $PM_{2.5}$ emissions. The largest concentration decrease of ~80% was found for EC (from 114.1 ± 10.0 μg/m^3 in 2003 to 24.8 ± 0.8 μg/m^3 in 2015). A corresponding reduction of 77% was found in EF_D for EC (from 65.8 ± 18.4 mg/veh/km in 2003 to 15.0 ± 1.2 mg/veh/km in 2015). Similarly, average OM concentrations decreased by ~70% (from 70.2 ± 7.6 μg/m^3 in 2003 to 20.3 ± 0.8 μg/m^3 in 2015), and the corresponding EF_D decreased by 78% (from 42.8 ± 14.0 to 9.3 ± 1.4 mg/veh/km).

The SO_4^{2-} concentrations in the SMT decreased by 48% (from 23.7 ± 9.3 μg/m^3 in 2003 to 12.3 ± 5.2 μg/m^3 in 2015. The SO_4^{2-} in the SMT represents a combination of vehicle emissions and the ambient background. The ambient SO_4^{2-} concentrations also decreased 42%–47% from 2003 to 2015 (HKEPD 2017a), owing to aggressive SO_2 emission controls such as reducing sulfur content in industrial and vehicle fuels, retrofitting power plants with flue gas desulfurization devices, and regulating ship emissions near shore. Appendix Figure C.28 compares SO_4^{2-} concentrations at the SMT inlet and outlet sites with those obtained from two nearby (<5 km) ambient air monitoring sites (Kwai Chuang and Tsuen Wan). The similar tunnel and ambient concentrations suggest that the ambient background concentrations dominated the tunnel SO_4^{2-} concentrations. Because of the significant reductions in EC and OC, the relative SO_4^{2-} abundance in the SMT $PM_{2.5}$ was higher in 2015 (18%) than that in 2003 (10%).

Geological mineral concentrations were similar during the two SMT studies (4.3 ± 0.8 μg/m^3 in 2003 and 4.0 ± 0.4 μg/m^3 in 2015). Because of the decrease in $PM_{2.5}$ concentrations, the relative abundance of geological materials increased from 2% in 2003 to 5% in 2015. Geological materials largely originate from non-tailpipe emissions (e.g., road dust, tire wear, and brake wear). The increased geological mineral fraction confirms the trend that non-tailpipe emissions became relatively more abundant in traffic-related emissions as tailpipe emissions decreased (Amato et al. 2014; Denier van der Gon et al. 2013).

The detailed 2015 SMT average $PM_{2.5}$ profile for ions, carbon, and elements is plotted in Figure 9 (panel A). Besides the high abundance of total carbon (TC), EC, OC, SO_4^{2-}, NH_4^+, and NO_3^-, some trace elements indicative of lubrication oil additives (e.g., Mg, S, Ca, and Zn) and wear (e.g., Al, Fe, and Cu) (Whitacre et al. 2002) were present at >0.05% of $PM_{2.5}$ abundance. The $PM_{2.5}$ source profile for road dust is plotted in Figure 9 (panel B). The dust particles were enriched with OC, EC, and geological elements (e.g., Si, Ca, Fe, and Al). Some abundant elements could also originate from tire wear (e.g., Al, Si, S, Ca, Ti, Fe, Cu, and Zn) and brake wear (e.g., Cu, Zn, Zr, Mo, and Sn) (Denier van der Gon et al. 2013; Gietl et al. 2010; Pant and Harrison 2013).

Average aerosol composition observed in the two traffic bores and the background site at the FMT is shown in Figure 10. Good mass closures were observed at all sites during both seasons. OM constituted 10%–59% of $PM_{2.5}$ mass. EC contribution was markedly higher in the traffic bores than at the background site, constituting, for example, up to 65% of $PM_{2.5}$ mass in Bore 4. There was also a marked increase in the geological component in the traffic bores, where it constituted on average 22% of $PM_{2.5}$ mass. Higher contributions from salt were observed in the traffic bores during the winter campaign from deicing materials. As shown in Appendix Figure C.29, after subtracting the contributions from background air, traffic emissions of $PM_{2.5}$ were dominated by EC and OM, especially in summer. Sodium chloride dominated the ions (Na^+, NH_4^+, SO_4^{2-}, and NO_3^-) in $PM_{2.5}$ in winter. Because of the lower overall tailpipe emissions of LD vehicles, salt contributes to a large fraction of winter-time $PM_{2.5}$ LD emissions. It should be kept in mind, however, that tunnel measurements could overestimate the contribution of salt and dust to $PM_{2.5}$ emissions compared with open-road conditions. Dispersion is restricted in the tunnel such that salt and crustal materials could accumulate there and result in a more "dusty" environment and stronger particulate flux attributable to resuspension.

The measured source profiles in FMT provide detailed chemical speciation for nearly 400 distinct gas- and particle-phase compounds and isomers, with varying levels of significance. To identify chemical species that may be useful as markers to distinguish between emissions from HD and LD vehicles, the regression results were screened for species for which the difference between the EF_Cs for HD and LD fleets was greater than or equal to twice the propagated uncertainty of the extrapolated values. Because gas-phase measurements of semivolatile species are not always available, both particle-only and total (particle plus gas) emission profiles are provided. These potential marker species are shown in Appendix Figure C.30.

SMT NMHCs and $PM_{2.5}$ Source Apportionment

Appendix Figure C.31 compares the SMT gasoline, LPG, and diesel source profiles for $PM_{2.5}$ derived from PMF, all with good mass closure (95–105%). Variability of species abundance in more than 10 replicate model runs is also shown as the uncertainty. The LPG profile has an EC/OC ratio of 0.0, in comparison with 0.36 and 2.9 for the gasoline and diesel profiles, with overall higher *n*-alkane/alkene, PAHs, hopane, and sterane fractions. Indeno[1,2,3-*cd*]pyrene and benzo[*ghi*]perylene, two markers for gasoline exhausts, as

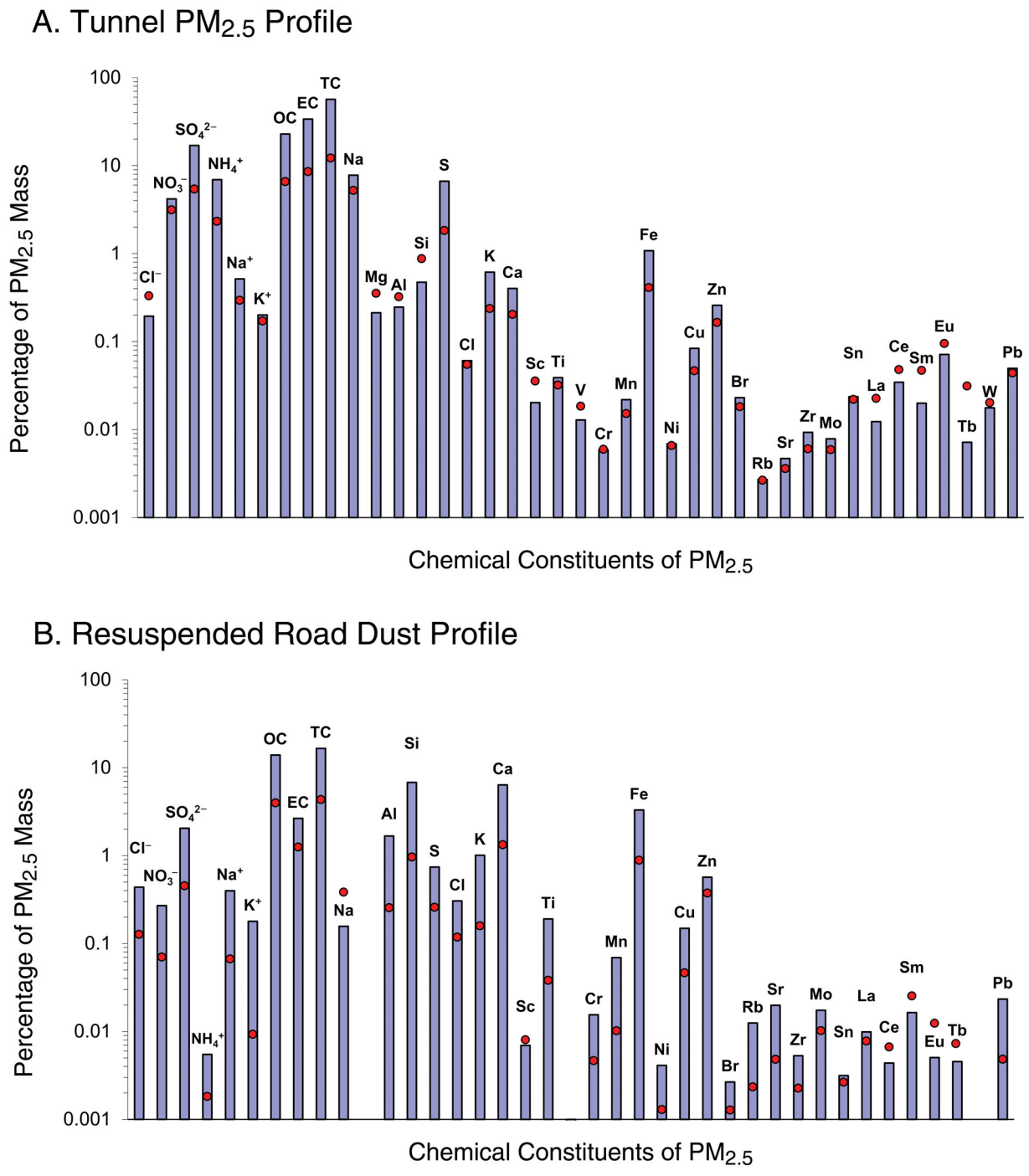

Figure 9. Source profiles for (A) $PM_{2.5}$ in air and (B) resuspended road dust measured in the SMT in 2015. Only species with an abundance >0.005% of $PM_{2.5}$ or larger than the uncertainty are plotted. The height of each bar indicates the average abundance (normalized to $PM_{2.5}$ mass concentration); the *y*-axis values of the dots indicate the larger of the analytical uncertainty or standard deviation.

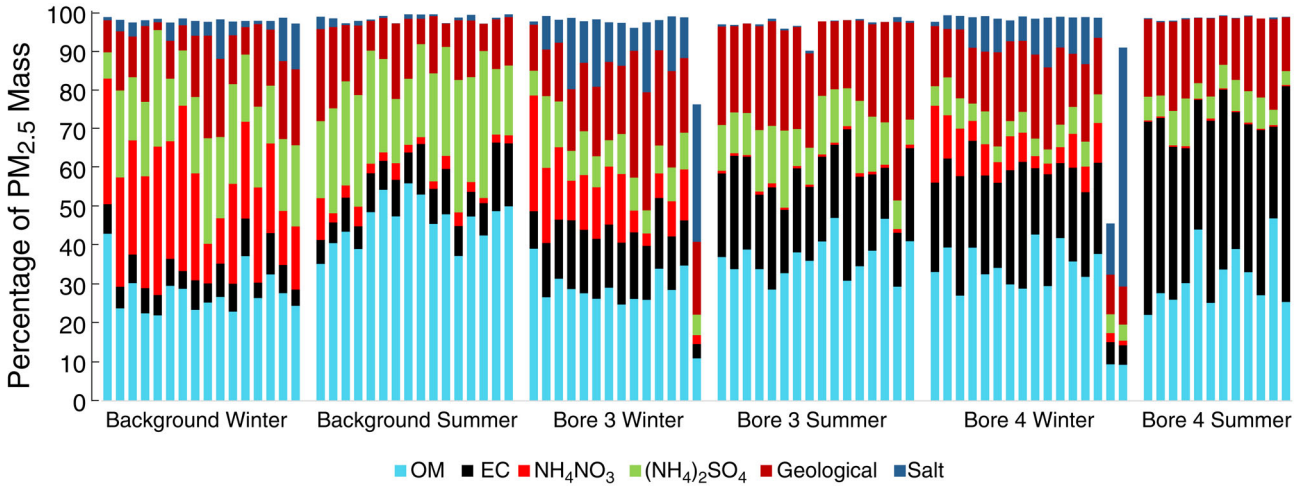

Figure 10. Percentage contribution of the major constituents to $PM_{2.5}$ mass for each sample taken at the two traffic bores and the background site for the FMT in 2015.

suggested by Chow and colleagues (2007b), may not be as useful with traffic that has a substantial LPG component. On the other hand, some heavier PAHs — such as retene, benzo[*ghi*]fluoranthene, and methylfluoranthene — were found to be most enriched in the gasoline profile (Appendix Figure C.31, available on HEI's website).

Based on the 2-hour integrated sampling interval, the EMFAC-HK–predicted $PM_{2.5}$ emissions from DVs and GVs do not track well with the PMF-resolved source contributions (Appendix Figure C.32), especially for the GVs. In the SMT, there were no periods when traffic contained only one type of vehicle, which would have facilitated the validation of the resolved source profiles.

The PMF-derived source contribution estimates indicate the dominance of diesel engine exhaust contributions to SMT $PM_{2.5}$ in 2015, accounting for an average (± standard error) of 51.5 ± 1.8% $PM_{2.5}$ mass, followed by secondary sulfate (19.9 ± 1.0%), gasoline engine exhausts (10.0 ± 0.8%), road dust (7.3 ± 1.3%), secondary nitrate (6.3 ± 0.9%), and LPG exhausts (5.0 ± 0.5%). According to this analysis, diesel exhaust accounts for ~78% of the tailpipe emissions, which is less than the EMFAC-HK estimate of 96% (Appendix Figure C.19 [panel J]).

Because the concentrations of sulfate, nitrate, and dust elements did not differ significantly between inlet and outlet sampling sites, it may be assumed that the $PM_{2.5}$ concentration increases from inlet to outlet sampling locations were attributable to tailpipe emissions with diesel, gasoline, and LPG breakdowns inferred from the PMF results. The EFs for diesel, gasoline, and LPG can then be calculated from their respective emissions and number of vehicles during each 2-hour period (equations 11 and 12). As shown in Appendix Table C.5, the PMF-derived average $PM_{2.5}$ EF_Ds for diesel, gasoline, and LPG were 0.043 ± 0.003 g/vehicle/km, 0.007 ± 0.001 g/vehicle/km, and 0.011 ± 0.001 g/vehicle/km, respectively. However, because of emission distributions among vehicles using the same fuel, the EF_Ds varied widely from sample to sample, with coefficients of variation of 0.61, 1.08, and 1.11 for diesel, gasoline, and LPG, respectively. For the fleet-average EF_D, the coefficient of variation was 0.67.

Appendix Figure C.33 shows the NMHC, CO, NO_x, and SO_2 profiles for GVs, LPG vehicles, and DVs resolved by PMF. The total NMHCs were 4.63, 0.76, and 10.76 times $PM_{2.5}$ mass in the gasoline, diesel, and LPG source profiles, respectively. The most abundant NMHC species in LPG were isobutane (23.2 weight percent [wt%]), *n*-butane (23.0 wt%), and propane (12.0 wt%). Guo and colleagues (2011) showed that these three species were the most abundant species from chassis dynamometer testing of

LPG-fueled taxis at 70 km/hr, with 16.0 wt%, 19.4 wt%, and 37.2 wt% for isobutane, *n*-butane, and propane, respectively. For diesel, the dominant NMHC species were ethene, *n*-butane, and NO_x, results that agree with profiles by Schauer and colleagues (1999). The diesel profile also has the highest *n*-decane abundance among the three fuels (Ho et al. 2009b). The gasoline profile contained the highest levels of aromatics, including toluene (22.8 wt%), *m/p*-xylene (6.6 wt%), and ethylbenzene (4.7 wt%) (Ling and Guo 2014; Schauer et al. 2002).

The EF_Ds from the PMF and EMFAC-HK are compared for the 2015 SMT study in Appendix Figure C.34. The EF_Ds from the PMF generally fell in the range of EMFAC-HK estimates. The largest differences were found for gasoline EF_Ds for $PM_{2.5}$, NMHCs, and NO_x: the PMF EF_Ds for $PM_{2.5}$ and NO_x were 3.7 and 2.7 times higher than those by EMFAC-HK, whereas the PMF NMHCs were only 37% of the EMFAC-HK estimates. The diesel-to-gasoline NO_x EF_D ratio was 29 for EMFAC-HK, which is in better agreement with those reported in the literature (e.g., 20–60 in Appendix Table C.2). The diesel-to-gasoline NO_x ratio was lower (9.0) when estimated by PMF, indicating the NO_x might not be accurately apportioned to LPG, gasoline, and diesel by PMF. As expected, diesel exhaust had the highest $PM_{2.5}$ and NO_x EF_D, and LPG exhaust had the highest NMHC and CO EF_Ds among the three vehicle types (Appendix Table C.5). Appendix Figure C.35 compares the emissions of $PM_{2.5}$, NMHCs, CO, and NO_x by fuel type over the SMT 2-hour sampling periods in 2015 as predicted by EMFAC-HK and PMF. The 2-hour emissions take into account both the EF_Ds and traffic volumes by vehicle type. The total $PM_{2.5}$ and NO_x differed by <10% between EMFAC-HK and PMF, although the distributions among fuel types were somewhat different. The EMFAC-HK assumes that LPG and diesel do not have evaporative losses, which is probably not realistic.

DISCUSSION AND CONCLUSIONS

This study investigated real-word vehicular emissions in two roadway tunnels — the Shing Mun Tunnel in Hong Kong and the Fort McHenry Tunnel in Baltimore, Maryland — that represent fleet compositions in two major geographical regions of the world. The study determined fleet-average and specific vehicle-type emission factors, evaluated the performance of mobile-source emission models, provided updated source profiles for different fleet components, and estimated contributions of non-tailpipe emissions.

A steady decrease in emissions of all measured pollutants during the past 23 years has been observed in the United States, reflecting the effect of emission standards and new technologies that were introduced during this period. Emission reductions were more pronounced for the LD fleet. In comparison with the 1992 FMT study, the current study demonstrated significant reductions in LD emissions for all pollutants. EF_Cs for naphthalene were reduced the most, by 98%; benzene, toluene, ethylbenzene, and xylene (BTEX) by 94%; CO, NMHCs, and NO_x by 87%; and aldehydes by about 71%. Smaller reductions were observed for HD EF_Cs: naphthalene emissions were reduced by 95%, carbonyl emissions decreased by about 75%, BTEX by 60%, and NO_x 58%. A CO comparison was difficult to estimate because of the very large uncertainty in the 1992 data.

In comparison with 2003–2004 EF_Ds, a significant reduction was observed for those of $PM_{2.5}$, SO_2, and total NMHCs for the Hong Kong SMT fleet, indicating the effectiveness of control measures on these pollutants. However, no statistically significant changes were observed for fleet-average EF_Ds of CO, NH_3, NO, NO_2, and NO_x. Source apportionment indicates that the diesel EF_D for NO_x in 2015 was 57% of that in 2003.

Appendix Figure D.4 examines emission inventory and roadside ambient concentration trends in Hong Kong (HKEPD 2016, 2017a,e; HKTD 2016). More details of the annual average ambient concentrations at roadside (i.e., streets with heavy traffic and surrounded by many tall buildings), urban, new town (mainly residential), and rural land use sites are plotted in Appendix Figure D.5. The air quality monitoring station measurements were acquired by either a U.S. EPA federal reference method or a federal equivalent method (HKEPD 2017a). Despite a 19% increase in VKT from 2003 to 2015, both emission inventory and roadside concentrations showed decreasing trends for most criteria pollutants (Appendix Figure D.4). As shown in Table 4, the 2015-to-2003 ratios from emission inventories were 0.57 for CO, 0.43 for NO_x, 0.04 for SO_2, 0.63 for total VOCs, and 0.23 for $PM_{2.5}$. The inventory ratios were similar to the ratios estimated by EMFAC-HK, except that EMFAC-HK showed a larger decrease for VOCs. The 2015-to-2003 ratios of roadside concentrations were 0.62 for CO, 0.51 for NO, 1.04 for NO_2, 0.62 for NO_x, 0.48 for SO_2, and 0.57 for $PM_{2.5}$. Note that the comparisons in Table 4 are qualitative because the tunnel emissions only represent vehicles operating at hot-stabilized conditions at speeds of ~80 km/hr, whereas traffic patterns on city streets are more diverse, including cold and hot starts, stop and go, and transient conditions. Furthermore, the vehicle fleet compositions in the tunnel differed from the

Table 4. Comparison of Various 2015/2003 Ratios for Gases and $PM_{2.5}$ in the SMT

Data Source	Ratio of 2015 to 2003 Levels[a]						
	CO	NO	NO_2	NO_x	SO_2	VOCs	$PM_{2.5}$
Emission rates based on tunnel studies[b]	1.13	1.06	1.32	1.09	0.27	0.61	0.23
Road transport emission inventory	0.57	NA	NA	0.43	0.04	0.63	0.23
Roadside concentration	0.62	0.51	1.04	0.62	0.48	NA	0.57
Emission rates based on EMFAC-HK estimates	0.49	NA	NA	0.45	NA	0.36	0.31

[a] NA = not available.

[b] Emissions were calculated by multiplying 2015/2003 ratios for EF_D (see Tables 1 and 3) with VKT (1.19).

Hong Kong–averaged fleet compositions — the average GVs, LPG vehicles, and DVs were ~45%, 13%, and 42% in the SMT during 2015, and the corresponding average VKT fractions were 42%, 24%, and 34%, respectively, in Hong Kong as a whole (HKEPD 2017c).

Several emission control measures were implemented in Hong Kong between 2003 and 2015, as shown in Appendix Table D.1 (Lau et al. 2015). The substantial decreases in CO, NO_x, VOC, and $PM_{2.5}$ emissions and roadside concentrations from 2012 to 2015 could be attributed to an array of vehicle emission control programs, including the tightening of vehicle emission standards from Euro IV to Euro V in 2012, providing a one-off subsidy for replacing catalytic convertors and oxygen sensors in LPG taxis and light buses, strengthening the emissions control for LPG vehicles and GVs by deploying roadside remote sensing equipment to detect high emitters, and launching an incentive-cum-regulatory scheme to progressively phase out ~82,000 pre-Euro IV diesel commercial vehicles by the end of 2019. By the end of 2015, 47% of the pre-Euro IV diesel commercial vehicles had already been phased out. The sulfur content in diesel and gasoline fuels was reduced to 10 ppmw in 2007 and 2010, respectively (HKEPD 2017d, 2017e).

The control measures were effective in reducing SO_2, and $PM_{2.5}$ emissions and roadside concentrations. Both emissions and roadside concentrations of SO_2, stayed at low levels since 2010 (Appendix Figures D.4 and D.5 [panels E and F]) when both gasoline and diesel sulfur content were reduced to 10 ppmw. The 2015 tunnel emission rate, road transport sector emissions, and roadside concentrations for SO_2, were 27%, 4%, and 48% of the 2003 level, respectively (Table 4). The corresponding 2015-to-2003 ratios for $PM_{2.5}$ were 23%, 23%, and 57%, respectively. EF_Ds for almost all major $PM_{2.5}$ constituents (i.e., ions, OC and EC, and elements) were lower in 2015 than in 2003–2004, contributing to the decrease of EF_D for $PM_{2.5}$. The geological material concentrations in $PM_{2.5}$ remained similar between the two tunnel studies, although their abundance in $PM_{2.5}$ mass increased from 2% in 2003 to 5% in 2015. As tailpipe emissions are being aggressively regulated and reduced, non-tailpipe emissions (e.g., road dust, tire wear, and brake wear) are becoming relatively more important.

For CO, although the emission inventory shows a slight increasing trend from 2003 to 2011 and then a sharp drop from 2012 to 2015 (Appendix Figure D.4), roadside concentrations show a decreasing trend from 2003 to 2015 (Appendix Figure D.5 [panel A]). The ~40% reductions in inventory and roadside concentrations were not observed in the SMT measurements. Appendix Figure D.5 (panel A) shows that urban CO concentrations increased by ~23% whereas new town and rural CO concentrations decreased by 20%–30% in Hong Kong from 2003 to 2015. Whereas NO and NO_x inventory emissions and roadside concentrations decreased by 40%–60%, tunnel-measured NO and NO_x emissions increased by 6%–9%. The reasons why tunnel fleet-average EF_Ds for CO, NO, and NO_x did not decrease as much as emission inventory or roadside ambient concentrations did are not clear. Different driving conditions between SMT and city streets as well as the 3%–8% higher fraction of DVs and GVs in the SMT could be contributing factors. The NO_2/NO_x volume ratios increased in SMT from 2003 and 2015, indicating an

increased NO_2 fraction in primary vehicle exhaust emissions. Appendix Figure D.5 (panel C) shows that NO_2 increased during 2008–2011, an increase that was partially attributed to malfunctioning catalytic converters on LPG vehicles (Lyu et al. 2016). The replacement of LPG catalytic converters in 2013–2014 effectively reduced roadside NO, NO_2, and NO_x concentrations (Appendix Figure D.5 [panels B–D]).

Naphthalene, acenaphthene, and anthracene in the SMT increased by 13%–46% from 2003–2004 to 2015, whereas other gaseous PAHs remained similar or decreased (Appendix Figure C.4 [panel A]). The sum of 17 PAHs increased by 13% in the gas phase and 38% in the particle phase from those in 2003–2004. The sum of 16 carbonyls measured at the SMT in 2015 was 82% higher than that in 2003–2004. The sum of measured NMHCs decreased by 44% from 2003–2004. Yet the emission factors of isobutane and *n*-butane increased from 2003 to 2015 by 32% and 17%, respectively, which could be attributable to the increased number of LPG vehicles.

The relative contributions of non-tailpipe emissions were estimated for both tunnels. In the SMT, NMHC species were enriched for LPG markers (e.g., *n*-butane, isobutane, and propane) and gasoline fuel vapor (e.g., toluene, isopentane, and *m*/*p*-xylene), indicating evaporative losses. EMFAC-HK estimated that the NMHC running evaporative losses were 33% and 40% of running exhaust emissions in 2003 and 2015, respectively. Source apportionment of $PM_{2.5}$ shows that secondary sulfate, secondary nitrate, and road dust contributed to 19.9 ± 1.0%, 6.3 ± 0.9%, and 7.3 ± 1.3% of SMT $PM_{2.5}$ concentrations in 2015, whereas diesel, gasoline, and LPG engine exhaust contributed to 51.5 ± 1.8%, 10.0 ± 0.8%, and 5.0 ± 0.5%, respectively. In the FMT, total NMHC emissions were 13% and 8% higher in winter than in summer for LD and HD vehicles, respectively, increases also likely attributable to evaporative emissions. During winter, a significant contribution of deicing salt to $PM_{2.5}$ emissions was observed in the FMT. Because the overall tailpipe emissions of LD vehicles were lower, salt contributed 33% of winter-time $PM_{2.5}$ LD emissions. It contributed about 9% of winter-time $PM_{2.5}$ HD emissions. The contribution of the salt to $PM_{2.5}$ emissions could be overestimated in comparison with open-road conditions, because salt tends to accumulate in the tunnel because its dispersion is restricted.

Measurements in the two tunnels were used to evaluate performance of two mobile-source emission models. EMFAC-HK was compared with the measurements at the SMT, and MOVES2014a was evaluated using the FMT measurements. EMFAC-HK agreed better with 2015 SMT measurements than with those from 2003. For the 2003 fleet, although modeled and measured CO_2 agreed within 5%, the modeled EF_Ds for CO, NO_x, and NMHCs were 1.5–2.2 times higher than the measured values, and the modeled EF_D for $PM_{2.5}$ was 61% of measurements. For the 2015 fleet, the modeled EF_D and measurements differed <35%.

MOVES2014a was found to significantly overestimate LD EF_Cs for CO, BTEX, NMHCs, and summer $PM_{2.5}$, with the overestimation being somewhat larger for the summer season. For HD vehicles, total PAHs and aldehydes were overestimated. 1,3-Butadiene was underestimated for all vehicle types. MOVES was most accurate for LD NO_x and HD NMHCs, EC, OC and $PM_{2.5}$. The small underestimation for LD $PM_{2.5}$ in winter may be a consequence of measured resuspended road salt that is not accounted for by MOVES, which only includes exhaust and particles from brake and tire wear. This component may offset the overestimation of other particulate matter. Total emissions of 16 PAHs by LD vehicles predicted by MOVES were 0.8 and 1.1 times higher than observations in summer and winter, respectively. Errors were larger for individual PAH compounds. The overestimation by MOVES was generally greater for heavier PAHs, which tend to be present in the particle phase and was also greater for HD vehicle emissions. For example, benz[*a*]anthracene and benzo[*a*]pyrene were overestimated by up to two orders of magnitude for high HD conditions. The reasons for the general overestimation by MOVES are not entirely clear. Vehicle counts available at the FMT do not provide information on vehicle age or fuel type. Differences between the observed fleet and the default vehicle age and fuel type distribution used in MOVES could be a reason for the observed discrepancies.

Tunnel measurements are advantageous for quantifying emission factors from the on-road vehicle fleet under real-world operating conditions at the location of the tunnel. Studying emissions in the same tunnel over time allows evaluation of the emission changes and the effectiveness of controls. The well-defined parameters in tunnel studies allow emission models to be evaluated under these specific conditions. It is recognized that tunnel measurements have several limitations (Franco et al. 2013; HEI Panel on the Health Effects of Traffic-Related Air Pollution 2010): (1) vehicles in both the SMT and the FMT were operating under hot-stabilized conditions; therefore, the results provided emissions during a specific period and under these specific vehicle and road-grade conditions and may not represent real-world urban driving and road conditions; (2) the varying baseline concentrations in the tunnel prevented calculation of emission factors of individual vehicles using the plume capture technique (Dallmann et al. 2013; Wang et al. 2015); and (3) tunnel studies quantify

fresh emissions, which do not represent the dilution, mixing, and aging of emissions on roadways.

IMPLICATIONS OF FINDINGS

Hong Kong on-road vehicle emissions of $PM_{2.5}$, SO_2, and total NMHCs decreased between 2003–2004 and 2015, demonstrating control measure effectiveness and accountability for these pollutants. Low-sulfur fuel regulations and replacing older DVs with newer technologies were effective. NO_x, CO, and non-criteria pollutants such as carbonyls and PAHs in the SMT did not show statistically significant decreases, indicating that expected emission reductions were not attained for approximately steady-state engine operations in the tunnel. The reasons require further investigation. The NO_2/NO_x volume ratios in the SMT increased from 2003–2004 to 2015, indicating an increased NO_2 fraction in primary exhaust emissions.

In the United States, results from the FMT demonstrate that regulations and control technologies introduced in the past decades have resulted in a steady decrease of LD emissions of all measured air pollutants. HD emissions also generally decreased, though to a lesser extent than LD emissions. The slower decrease of HD emissions could be a result of overestimation of HD emissions because higher-polluting LD vehicles are present. This needs to be investigated further.

Non-tailpipe emissions could contribute significantly to the total vehicular emissions. For example, during the winter campaign at the FMT, a significant contribution of road salt to $PM_{2.5}$ was observed. Total NMHC emissions increased by up to 14% at the FMT in summer compared with winter, indicating the magnitude of evaporative emissions. An increase of LPG marker compounds indicative of evaporating emissions was also detected at the SMT. EMFAC-HK showed that NMHC running evaporative losses were ~40% of running exhaust emissions for GVs in the SMT. Road dust contributed 7.3 ± 1.3% of SMT $PM_{2.5}$ concentrations. As tailpipe emissions are progressively reduced in the coming years, the ratio of non-tailpipe emissions to total vehicle emissions may increase further.

EMFAC-HK performed fairly well in comparison with SMT measurements for the 2015 fleet. MOVES2014a, however, generally overestimated pollutant emissions for both LD and HD vehicles. The overestimation by MOVES could be attributable either to inadequate representation of real-world vehicular emissions or to discrepancies between the assumed and actual fleet age and fuel distributions. These factors need to be investigated further.

Methods and results from the current study can be used to (1) improve emission inventories with real-world emission factors; (2) determine source contributions with receptor models using source profiles; (3) further evaluate the effectiveness of emission control measures over time; and (4) determine real-world cost/benefits of control measures.

ACKNOWLEDGMENTS

This study was supported by the HEI Research Agreement Number 4947-RFPA14-1/15-1. The investigators are thankful for operational and technical advice provided by Drs. Maria Costantini, Johanna Boogaard, Allison Patton, and other HEI staff. Mr. David Bush and David Gemmill conducted a careful audit of the field data and the draft final report and offered constructive comments. The HEI Review Committee and external reviewers provided detailed and thoughtful comments. We are grateful to the teams at The Chinese University of Hong Kong, The Hong Kong Polytechnic University, and DRI for field sampling, chemical analyses, traffic counting, and data analysis. We thank the Hong Kong Environmental Protection Department and Hong Kong Transport Department for provision of the data sets and permission for sampling in Shing Mun Tunnel. Drs. Xinmin Wang and Yanli Zhang of the Chinese Academy of Sciences provided assistance in analyzing NMHCs for the SMT study. Technical advice from Drs. Alan Gertler and Barbara Zielinska on study design and data analysis are gratefully acknowledged. Dr. Yan Cheng of Xi'an Jiaotong University provided the 2003–2004 SMT data for reanalysis.

REFERENCES

Amato F, Cassee FR, Denier van der Gon HAC, Gehrig R, Gustafsson M, Hafner W, et al. 2014. Urban air quality: The challenge of traffic non-exhaust emissions. J Hazard Mater 275:31–36.

Bahreini R, Middlebrook AM, de Gouw JA, Warneke C, Trainer M, Brock CA, et al. 2012. Gasoline emissions dominate over diesel in formation of secondary organic aerosol mass. Geophys Res Lett 39:L06805.

Ban-Weiss GA, McLaughlin JP, Harley RA, Kean AJ, Grosjean E, Grosjean D. 2008a. Carbonyl and nitrogen dioxide emissions from gasoline- and diesel-powered motor vehicles. Environ Sci Technol 42:3944–3950.

Ban-Weiss GA, McLaughlin JP, Harley RA, Lunden MM, Kirchstetter TW, Kean AJ, et al. 2008b. Long-term changes

in emissions of nitrogen oxides and particulate matter from on-road gasoline and diesel vehicles. Atmos Environ 42:220–232.

Brimblecombe P, Townsend T, Lau CF, Rakowska A, Chan TL, Močnik G, et al. 2015. Through-tunnel estimates of vehicle fleet emission factors. Atmos Environ 123 Part A:180–189.

Cao JJ, Lee SC, Ho KF, Fung K, Chow JC, Watson JG. 2006. Characterization of roadside fine particulate carbon and its eight fractions in Hong Kong. Aerosol Air Qual Res 6:106–122.

CARB. 2018b. EMFAC2017 Volume I – User's Guide v1.0.2. Sacramento, CA:Mobile Source Analysis Branch, Air Quality Planning & Science Division, California Air Resource Board. Available: *www.arb.ca.gov/msei/downloads/emfac2017-volume-i-users-guide.pdf* [accessed 20 March 2018].

CARB. 2018a. EMFAC2017 Web Database. California Air Resource Board. Available: *www.arb.ca.gov/emfac/2017/* [accessed 20 March 2018].

Carslaw DC, Beevers SD, Tate JE, Westmoreland EJ, Williams ML. 2011. Recent evidence concerning higher NO_x emissions from passenger cars and light duty vehicles. Atmos Environ 45:7053–7063.

Chen L-WA, Watson JG, Chow JC, DuBois DW, Herschberger L. 2010. Chemical mass balance source apportionment for combined $PM_{2.5}$ measurements from U.S. Non-urban and urban long-term networks. Atmos Environ 44:4908–4918.

Chen L-WA, Watson JG, Chow JC, DuBois DW, Herschberger L. 2011. $PM_{2.5}$ source apportionment: Reconciling receptor models for U.S. non-urban and urban long-term networks. J Air Waste Manage Assoc 61:1204–1217.

Chen L-WA, Watson JG, Chow JC, Magliano KL. 2007. Quantifying $PM_{2.5}$ source contributions for the San Joaquin Valley with multivariate receptor models. Environ Sci Technol 41:2818–2826.

Cheng Y, Lee SC, Ho KF, Chow JC, Watson JG, Louie PKK, et al. 2010. Chemically-speciated on-road $PM_{2.5}$ motor vehicle emission factors in Hong Kong. Sci Total Environ 408:1621–1627.

Cheng Y, Lee SC, Ho KF, Louie PKK. 2006. On-road particulate matter ($PM_{2.5}$) and gaseous emissions in the Shing Mun tunnel, Hong Kong. Atmos Environ 40:4235–4245.

Chow JC, Lowenthal DH, Chen LWA, Wang XL, Watson JG. 2015. Mass reconstruction methods for $PM_{2.5}$: A review. Air Qual Atmos Health 8:243–263.

Chow JC, Watson JG. 2013. Chemical analyses of particle filter deposits. In: Aerosols Handbook: Measurement, Dosimetry, and Health Effects, Part 2 (Ruzer L, Harley NH, eds). New York, NY:CRC Press/Taylor & Francis, 179–204.

Chow JC, Watson JG. 2017. Enhanced ion chromatographic speciation of water-soluble $PM_{2.5}$ to improve aerosol source apportionment. Aerosol Sci Eng 1:7–24.

Chow JC, Watson JG, Bowen JL, Frazier CA, Gertler AW, Fung KK, et al. 1993a. A sampling system for reactive species in the western United States. In: Sampling and analysis of airborne pollutants, (Winegar ED, Keith LH, eds). Ann Arbor, MI:Lewis Publishers, 209–228.

Chow JC, Watson JG, Chen L-WA, Chang MCO, Robinson NF, Trimble D, et al. 2007a. The IMPROVE_A temperature protocol for thermal/optical carbon analysis: Maintaining consistency with a long-term database. J Air Waste Manage Assoc 57:1014–1023.

Chow JC, Watson JG, Chen L-WA, Rice J, Frank NH. 2010. Quantification of $PM_{2.5}$ organic carbon sampling artifacts in US networks. Atmos Chem Phys 10:5223–5239.

Chow JC, Watson JG, Houck JE, Pritchett LC, Rogers CF, Frazier CA, et al. 1994. A laboratory resuspension chamber to measure fugitive dust size distributions and chemical compositions. Atmos Environ 28:3463–3481.

Chow JC, Watson JG, Lowenthal DH, Chen L-WA, Zielinska B, Mazzoleni LR, et al. 2007b. Evaluation of organic markers for chemical mass balance source apportionment at the Fresno supersite. Atmos Chem Phys 7:1741–1754.

Chow JC, Watson JG, Pritchett LC, Pierson WR, Frazier CA, Purcell RG. 1993b. The DRI thermal/optical reflectance carbon analysis system: Description, evaluation and applications in U.S. air quality studies. Atmos Environ Part A Gen Top 27:1185–1201.

Chow JC, Watson JG, Robles J, Wang XL, Chen L-WA, Trimble DL, et al. 2011. Quality assurance and quality control for thermal/optical analysis of aerosol samples for organic and elemental carbon. Anal Bioanal Chem 401:3141–3152.

Chow JC, Yu JZ, Watson JG, Ho SSH, Bohannan TL, Hays MD, et al. 2007c. The application of thermal methods for determining chemical composition of carbonaceous aerosols: A review. J Environ Sci Health Part A-Toxic Hazard Subst Environ Eng 42:1521–1541.

Dallmann TR, DeMartini SJ, Kirchstetter TW, Herndon SC, Onasch TB, Wood EC, et al. 2012. On-road measurement of gas and particle phase pollutant emission factors for individual heavy-duty diesel trucks. Environ Sci Technol 46:8511–8518.

Dallmann TR, Kirchstetter TW, DeMartini SJ, Harley RA. 2013. Quantifying on-road emissions from gasoline-powered motor vehicles: Accounting for the presence of medium- and heavy-duty diesel trucks. Environ Sci Technol 47:13873–13881.

Denier van der Gon HAC, Gerlofs-Nijland ME, Gehrig R, Gustafsson M, Janssen N, Harrison RM, et al. 2013. The policy relevance of wear emissions from road transport, now and in the future—An international workshop report and consensus statement. J Air Waste Manage Assoc 63:136–149.

Dreher DB, Harley RA. 1998. A fuel-based inventory for heavy-duty diesel truck emissions. J Air Waste Manage Assoc 48:352–358.

EEA (European Environment Agency). 2016. Greenhouse gas emissions from transport. IND-111-en. Copenhagen, Denmark:European Environment Agency. Available: *www.eea.europa.eu/data-and-maps/indicators/transport-emissions-of-greenhouse-gases/transport-emissions-of-greenhouse-gases-6* [accessed 8 March 2017].

El-Fadel M, Hashisho Z. 2001. Vehicular emissions in roadway tunnels: A critical review. Crit Rev Environ Sci Tech 31:125–174.

Franco V, Kousoulidou M, Muntean M, Ntziachristos L, Hausberger S, Dilara P. 2013. Road vehicle emission factors development: A review. Atmos Environ 70:84–97.

Fraser MP, Cass GR. 1998. Detection of excess ammonia emissions from in-use vehicles and the implications for fine particle control. Environ Sci Technol 32:1053–1057.

Fujita EM, Campbell DE, Zielinska B, Arnott WP, Chow JC. 2011. Concentrations of Air Toxics in Motor Vehicle-Dominated Environments. Research Report 156. Boston, MA:Health Effects Institute. Available: *www.healtheffects.org/publication/concentrations-air-toxics-motor-vehicle-dominated-environments.*

Fujita EM, Campbell DE, Zielinska B, Chow JC, Lindhjem CE, DenBleyker A, et al. 2012. Comparison of the MOVES2010a, MOBILE6.2 and EMFAC2007 mobile source emissions models with on-road traffic tunnel and remote sensing measurements. J Air Waste Manage Assoc 62:1134–1149.

Geller MD, Sardar SB, Phuleria H, Fine PM, Sioutas C. 2005. Measurements of particle number and mass concentrations and size distributions in a tunnel environment. Environ Sci Technol 39:8653–8663.

Gertler AW, Sagebiel JC, Dippel WA, Farina RJ. 1998. Measurements of dioxin and furan emission factors from heavy-duty diesel vehicles. J Air Waste Manage Assoc 48:276–278.

Gertler AW, Gillies JA, Pierson WR, Rogers CF, Sagebiel JC, Abu-Allaban M, et al. 2002. Real-world particulate matter and gaseous emissions from motor vehicles in a highway tunnel. In: Emissions from Diesel and Gasoline Engines Measure in Highway Tunnels. Research Report 107. Boston MA:Health Effects Institute.

Gietl JK, Lawrence R, Thorpe AJ, Harrison RM. 2010. Identification of brake wear particles and derivation of a quantitative tracer for brake dust at a major road. Atmos Environ 44:141–146.

Gogou A, Stratigakis N, Kanakidou M, Stephanou EG. 1996. Organic aerosols in eastern Mediterranean: Components source reconciliation by using molecular markers and atmospheric back trajectories. Org Geochem 25:79–96.

Grieshop AP, Lipsky EM, Pekney NJ, Takahama S, Robinson AL. 2006. Fine particle emission factors from vehicles in a highway tunnel: Effects of fleet composition and season. Atmos Environ 40, Supplement 2:287–298.

Grimmer G, Jacob J, Naujack KW. 1983. Profile of the polycyclic aromatic compounds from crude oils. Fresenius' Zeitschrift für analytische Chemie 314:29–36.

Guo H, Zou SC, Tsai WY, Chan LY, Blake DR. 2011. Emission characteristics of nonmethane hydrocarbons from private cars and taxis at different driving speeds in Hong Kong. Atmos Environ 45:2711–2721.

HEI Panel on the Health Effects of Traffic-Related Air Pollution. 2010. Traffic-Related Air Pollution: A Critical Review of the Literature on Emissions, Exposure, and Health Effects. Special Report 17. Boston MA:Health Effects Institute. Available: *www.healtheffects.org/publication/traffic-related-air-pollution-critical-review-literature-emissions-exposure-and-health* [accessed 5 August 2014].

HEI Special Committee on Emerging Technologies. 2011. The Future of Vehicle Fuels and Technologies: Anticipating Health Benefits and Challenges. Communication 16. Boston MA:Health Effects Institute. Available:

www.healtheffects.org/publication/future-vehicle-fuels-and-technologies-anticipating-health-benefits-and-challenges [accessed 5 August 2014].

HKEMSD. 2017. Hong Kong energy end-use data 2017. Hong Kong:Hong Kong Electrical & Mechanical Services Department (EMSD). Available: *https://www.emsd.gov.hk/filemanager/en/content_762/HKEEUD2017.pdf* [accessed 14 December 2017].

HKEPD. 2016. Air quality in Hong Kong 2015: A report on the results from the air quality monitoring network (AQMN). EPD/TR 1/16. Hong Kong:Air Science Group, Environmental Protection Department, The Government of the Hong Kong Special Administrative Region. Available: *http://www.aqhi.gov.hk/api_history/english/report/files/AQR2015e_final.pdf* [accessed 10 March 2017].

HKEPD. 2017a. Hong Kong air quality monitoring data. Hong Kong:Environmental Protection Department, The Government of the Hong Kong Special Administrative Region. Available: *http://epic.epd.gov.hk/EPICDI/air/station/?lang=en* [accessed on 10 March 2017].

HKEPD. 2017b. EMFAC-HK (version 3.3) user's guide: Calculating emission inventories for vehicles in Hong Kong. Hong Kong Environmental Protection Department. Available: *www.epd.gov.hk/epd/sites/default/files/epd/User%20Guide%20Emfac-HK%20%28Ver%203.1%29.pdf* [accessed on 27 March 2016].

HKEPD. 2017c. EMFAC-HK vehicle emission calculation (version 3.3). Available: *www.epd.gov.hk/epd/english/environmentinhk/air/guide_ref/emfac-hk.html* [accessed 2 May 2017].

HKEPD. 2017d. Cleaning the air at street level. Hong Kong Environmental Protection Department. Available: *www.epd.gov.hk/epd/english/environmentinhk/air/prob_solutions/cleaning_air_atroad.html* [accessed 2 July 2017].

HKEPD. 2017e. Hong Kong air pollutant emission inventory. Hong Kong:Environmental Protection Department, The Government of the Hong Kong Special Administrative Region. Available: *www.epd.gov.hk/epd/english/environmentinhk/air/data/emission_inve.html* [accessed 10 April 2017].

HKPolyU. 2005. Determination of suspended particulate & VOC emission profiles for vehicular sources in Hong Kong. Hong Kong, SAR:Hong Kong Polytechnic University. Available: *www.epd.gov.hk/epd/english/environmentinhk/air/studyrpts/files/1-pt_final_report_20050225d.pdf.*

HKTD. 2016. The annual traffic census 2015. TTSD Publication No. 16CAB1. Hong Kong Transport Department, Traffic and Transport Survey Division. Available: *www.td.gov.hk/filemanager/en/content_4772/annual%20traffic%20census%202015.pdf.*

Ho KF, Ho SSH, Cheng Y, Lee SC, Zhen Yu JZ. 2007. Real-world emission factors of fifteen carbonyl compounds measured in a Hong Kong tunnel. Atmos Environ 41:1747–1758.

Ho KF, Ho SSH, Lee SC, Cheng Y, Chow JC, Watson JG, et al. 2009a. Emissions of gas- and particle-phase polycyclic aromatic hydrocarbons (PAHs) in the Shing Mun tunnel, Hong Kong. Atmos Environ 43:6343–6351.

Ho KF, Lee SC, Ho WK, Blake DR, Cheng Y, Li YS, et al. 2009b. Vehicular emission of volatile organic compounds (VOCs) from a tunnel study in Hong Kong. Atmos Chem Phys 9:7491–7504.

Ho SSH, Yu JZ. 2004. In-injection port thermal desorption and subsequent gas chromatography–mass spectrometric analysis of polycyclic aromatic hydrocarbons and *n*-alkanes in atmospheric aerosol samples. J Chromatogr A 1059:121–129.

Ho SSH, Yu JZ, Chow JC, Zielinska B, Watson JG, Sit EHL, et al. 2008. Evaluation of an in-injection port thermal desorption-gas chromatography/mass spectrometry method for analysis of non-polar organic compounds in ambient aerosol samples. J Chromatogr A 1200:217–227.

Hoekman SK. 1992. Speciated measurements and calculated reactivities of vehicle exhaust emissions from conventional and reformulated gasolines. Environ Sci Technol 26:1206–1216.

Hubert M, Vandervieren E. 2008. An adjusted boxplot for skewed distributions. Comput Stat Data Analy 52:5186–5201.

Huo H, Zhang Q, He K, Yao Z, Wang M. 2012. Vehicle-use intensity in China: Current status and future trend. Energy Policy 43:6–16.

Jiménez-Palacios JL. 1999. Understanding and Quantifying Motor Vehicle Emissions with Vehicle Specific Power and TILDAS Remote Sensing [PhD Dissertation]. Cambridge, MA:Massachusetts Institute of Technology.

Kean AJ, Harley RA, Kendall GR. 2003. Effects of vehicle speed and engine load on motor vehicle emissions. Environ Sci Technol 37:3739–3746.

Kean AJ, Harley RA, Littlejohn D, Kendall GR. 2000a. On-road measurement of ammonia and other motor vehicle exhaust emissions. Environ Sci Technol 34:3535–3539.

Kean AJ, Littlejohn D, Ban-Weiss GA, Harley RA, Kirchstetter TW, Lunden MM. 2009. Trends in on-road vehicle emissions of ammonia. Atmos Environ 43:1565–1570.

Kean AJ, Sawyer RF, Harley RA. 2000b. A fuel-based assessment of off-road diesel engine emissions. J Air Waste Manage Assoc 50:1929–1939.

Kean AJ, Sawyer RF, Harley RA, Kendall GR. 2002. Trends in exhaust emissions from in-use California light-duty vehicles, 1994–2001. Society of Automotive Engineers International.

Kirchstetter TW, Harley RA, Kreisberg NM, Stolzenburg MR, Hering SV. 1999. On-road measurement of fine particle and nitrogen oxide emissions from light- and heavy-duty motor vehicles. Atmos Environ 33:2955–2968.

Kleeman MJ, Schauer JJ, Cass GR. 2000. Size and composition distribution of fine particulate matter emitted from motor vehicles. Environ Sci Technol 34:1132–1142.

Krzyzanowski M, Kuna-Dibbert B, Schneider J. 2005. Health Effects of Transport-related Air Pollution. Copenhagen, Denmark:WHO Regional Office Europe.

Kuykendall JR, Shaw SL, Paustenbach D, Fehling K, Kacew S, Kabay V. 2009. Chemicals present in automobile traffic tunnels and the possible community health hazards: A review of the literature. Inhalation Toxicol 21:747–792.

Landis MS, Lewis CW, Stevens RK, Keeler GJ, Dvonch JT, Tremblay RT. 2007. Ft. McHenry tunnel study: Source profiles and mercury emissions from diesel and gasoline powered vehicles. Atmos Environ 41:8711–8724.

Lau CF, Rakowska A, Townsend T, Brimblecombe P, Chan TL, Yam YS, et al. 2015. Evaluation of diesel fleet emissions and control policies from plume chasing measurements of on-road vehicles. Atmos Environ 122:171–182.

Ling ZH, Guo H. 2014. Contribution of VOC sources to photochemical ozone formation and its control policy implication in Hong Kong. Environ Sci Policy 38:180–191.

Liu T, Wang X, Wang B, Ding X, Deng W, Lü S, et al. 2014. Emission factor of ammonia (NH_3) from on-road vehicles in China: Tunnel tests in urban Guangzhou. Environ Res Lett 9:064027.

Lyu XP, Guo H, Simpson IJ, Meinardi S, Louie PKK, Ling Z, et al. 2016. Effectiveness of replacing catalytic converters in LPG-fueled vehicles in Hong Kong. Atmos Chem Phys 16:6609–6626.

Lyu XP, Zeng LW, Guo H, Simpson IJ, Ling ZH, Wang Y, et al. 2017. Evaluation of the effectiveness of air pollution control measures in Hong Kong. Environ Pollut 220:87–94.

Malm W, Sisler J, Huffman D, Eldred R, Cahill T. 1994. Spatial and seasonal trends in particle concentration and optical extinction in the United States. J Geophys Res 99:1347–1370.

May AA, Nguyen NT, Presto AA, Gordon TD, Lipsky EM, Karve M, et al. 2014. Gas- and particle-phase primary emissions from in-use, on-road gasoline and diesel vehicles. Atmos Environ 88:247–260.

Millstein DE, Harley RA. 2010. Effects of retrofitting emission control systems on in-use heavy diesel vehicles. Environ Sci Technol 44:5042–5048.

Moosmüller H, Mazzoleni C, Barber PW, Kuhns HD, Keislar RE, Watson JG. 2003. On-road measurement of automotive particle emissions by ultraviolet Lidar and transmissometer: Instrument. Environ Sci Technol 37: 4971–4978.

NRC. 2000. Modeling Mobile-source Emissions. Washington, DC:Transportation Research Board, National Research Council, The National Academies Press.

Paatero P. 1997. Least squares formulation of robust non-negative factor analysis. Chemom Intell Lab Syst 37:23–35.

Paatero P. 1999. The multilinear engine — A table-driven, least squares program for solving multilinear problems, including the *n*-way parallel factor analysis model. J Comp Graph Stat 8:854–888.

Pant P, Harrison RM. 2013. Estimation of the contribution of road traffic emissions to particulate matter concentrations from field measurements: A review. Atmos Environ 77:78–97.

Parrish DD. 2006. Critical evaluation of US on-road vehicle emission inventories. Atmos Environ 40:2288–2300.

Perkins JL, Padro-Martinez LT, Durant JL. 2013. Particle number emission factors for an urban highway tunnel. Atmos Environ 74:326–337.

Perrini G, Tomasello M, Librando V, Minniti Z. 2005. Nitrated polycyclic aromatic hydrocarbons in the environment: Formation, occurrences and analysis. Anal Chim 95:567–577.

Pierson WR, Gertler AW, Robinson NF, Sagebiel JC, Zielinska B, Bishop GA, et al. 1996. Real-world automotive emissions — Summary of studies in the Fort McHenry and Tuscarora mountain tunnels. Atmos Environ 30:2233–2256.

Reff A, Eberly SI, Bhave PV. 2007. Receptor modeling of ambient particulate matter data using positive matrix factorization: Review of existing methods. J Air Waste Manage Assoc 57:146–154.

Rogak SN, Green SI, Pott U. 1998. Use of tracer gas for direct calibration of emission-factor measurements in a traffic tunnel. J Air Waste Manage Assoc 48:545–552.

Samy S, Zielinska B, Sagebiel JC, McDonald JD. 2011. Application for a newly developed high-capacity NO_x denuder: Low-NO_x diesel transformation experiments. J Air Waste Manage Assoc 61:319–323.

Sawyer RF, Harley RA, Cadle SH, Norbeck JM, Slott R, Bravo HA. 2000. Mobile sources critical review: 1998 NARSTO assessment. Atmos Environ 34:2161–2181.

Schauer JJ, Kleeman MJ, Cass GR, Simoneit BRT. 1999. Measurement of emissions from air pollution sources. 2. C_1 through C_{30} organic compounds from medium duty diesel trucks. Environ Sci Technol 33:1578–1587.

Schauer JJ, Kleeman MJ, Cass GR, Simoneit BRT. 2002. Measurement of emissions from air pollution sources. 5. C_1-C_{32} organic compounds from gasoline-powered motor vehicles. Environ Sci Technol 36:1169–1180.

Shahir SA, Masjuki HH, Kalam MA, Imran A, Ashraful AM. 2015. Performance and emission assessment of diesel–biodiesel–ethanol/bioethanol blend as a fuel in diesel engines: A review. Renewable Sustainable Energy Rev 48:62–78.

Shindell D, Faluvegi G, Walsh M, Anenberg SC, Van Dingenen R, Muller NZ, et al. 2011. Climate, health, agricultural and economic impacts of tighter vehicle-emission standards. Nature Clim Change 1:59–66.

Sicre MA, Marty JC, Saliot A, Aparicio X, Grimalt J, Albaiges J. 1987. Aliphatic and aromatic hydrocarbons in different sized aerosols over the Mediterranean Sea: Occurrence and origin. Atmos Environ (1967) 21:2247–2259.

Singer BC, Harley RA. 1996. A fuel-based motor vehicle emission inventory. J Air Waste Manage Assoc 46:581–593.

Stout SA, Liu B, Millner GC, Hamlin D, Healey E. 2007. Use of chemical fingerprinting to establish the presence of spilled crude oil in a residential area following Hurricane Katrina, St. Bernard parish, Louisiana. Environ Sci Technol 41:7242–7251.

Tian L, Hossain S, Lin H, Ho K, Lee S, Yu IS. 2011. Increasing trend of primary NO_2 exhaust emission fraction in Hong Kong. Environ Geochem Health 33:623–630.

Tsai WY, Chan LY, Blake DR, Chu KW. 2006. Vehicular fuel composition and atmospheric emissions in south China: Hong Kong, Macau, Guangzhou, and Zhuhai. Atmos Chem Phys 6:3281–3288.

U.S. DOT. 2016. Traffic volume trends: December 2016. Washington D.C.:Office of Highway Policy Information, Federal Highway Administration, U.S. Department of Transportation. Available: *www.fhwa.dot.gov/policyinformation/travel_monitoring/tvt.cfm* [accessed 15 March 2017].

U.S. DOT. 2017. National transportation statistics: 2016. Washington D.C.:Bureau of Transportation Statistics, U.S. Department of Transportation. Available: *www.rita.dot.gov/bts/sites/rita.dot.gov.bts/files/publications/national_transportation_statistics/index.html* [accessed 15 March 2017].

U.S. EPA. 1999a. Compendium method TO-11a: Determination of formaldehyde in ambient air using adsorbent cartridge followed by high performance liquid chromatography (HPLC) [active sampling methodology]. Cincinnati, OH:Center for Environmental Research Information, Office of Research and Development, U.S. Environmental Protection Agency. Available*: www3.epa.gov/ttnamti1/files/ambient/airtox/to-11ar.pdf.*

U.S. EPA. 1999b. Compendium method TO-13a: Determination of polycyclic aromatic hydrocarbons (PAHs) in ambient air using gas chromatography/mass spectrometry (GC/MS). EPA/625/R-96/010b. Cincinnati, OH:Center for Environmental Research Information, Office of Research and Development, U.S. Environmental Protection Agency. Available: *www3.epa.gov/ttnamti1/files/ambient/airtox/to-13arr.pdf.*

U.S. EPA. 1999c. Compendium method TO-15: Determination of volatile organic compounds (VOCs) in air collected in specially-prepared canisters and analyzed by gas chromatography/mass spectrometry (GC/MS). Research Triangle Park, NC:U.S. Environmental Protection Agency. Available: *www3.epa.gov/ttnamti1/files/ambient/airtox/to-15r.pdf.*

U.S. EPA. 2012. Quality assurance guidance document — quality assurance project plan: $PM_{2.5}$ chemical speciation sampling at trends, NCore, supplemental and tribal sites. Research Triangle Park, North Carolina:Ambient Air Monitoring Group, Air Quality Assessment Division, U.S. EPA,

Office of Air Quality Planning and Standards. Available: *www3.epa.gov/ttnamti1/files/ambient/pm25/spec/CSN_QAPP_v120_05-2012.pdf.*

U.S. EPA. 2015. Moves2014a: Latest version of motor vehicle emission simulator (MOVES). Ann Arbor, MI:U.S. Environmental Protection Agency. Available*: www.epa.gov/moves.*

U.S. EPA. 2016. Fast facts — U.S. transportation sector greenhouse gas emissions: 1990–2014. EPA-420-F-13-033a.Office of Transportation and Air Quality, U.S. Environmental Protection Agency Available: *www.epa.gov/greenvehicles/fast-facts-transportation-greenhouse-gas-emissions* [accessed on 8 March 2017].

Wang H, Kawamura K, Ho KF, Lee SC. 2006. Low molecular weight dicarboxylic acids, ketoacids, and dicarbonyls in the fine particles from a roadway tunnel: Possible secondary production from the precursors. Environ Sci Technol 40:6255–6260.

Wang JM, Jeong CH, Zimmerman N, Healy RM, Wang DK, Ke F, et al. 2015. Plume-based analysis of vehicle fleet air pollutant emissions and the contribution from high emitters. Atmos Meas Tech 8:3263–3275.

Wang XL, Chancellor G, Evenstad J, Farnsworth JE, Hase A, Olson GM, et al. 2009. A novel optical instrument for estimating size segregated aerosol mass concentration in real time. Aerosol Sci Technol 43:939–950.

Wang XL, Chow JC, Kohl SD, Percy KE, Legge AH, Watson JG. 2016. Real-world emission factors for Caterpillar 797b heavy haulers during mining operations. Particuology 28:22–30.

Wang XL, Ho KF, Chow JC, Kohl SD, Chan CS, Cui L, et al. 2018. Hong Kong vehicle emission changes from 2003 to 2015 in the Shing Mun tunnel. Aerosol Sci Technol 52:10, 1085–1098; doi:10.1080/02786826.2018.1456650.

Watson JG, Chen L, Chow JC, Doraiswamy P, Lowenthal DH. 2008. Source apportionment: Findings from the US supersites program. J Air Waste Manage Assoc 58:265.

Watson JG, Chow JC, Chen L-WA, Frank NH. 2009. Methods to assess carbonaceous aerosol sampling artifacts for IMPROVE and other long-term networks. J Air Waste Manage Assoc 59:898–911.

Watson JG, Chow JC, Engling G, Chen L-WA, Wang XL. 2016. Source apportionment: Principles and methods. In: Airborne Particulate Matter: Sources, Atmospheric Processes and Health (Harrison RM, ed). London, UK:Royal Society of Chemistry, 72–125.

Watson JG, Chow JC, Frazier CA. 1999. X-ray fluorescence analysis of ambient air samples. In: Elemental Analysis of Airborne Particles, Vol 1 (Landsberger S, Creatchman M, eds). Amsterdam, The Netherlands:Gordon and Breach Science, 67–96.

Watson JG, Chow JC, Fujita EM. 2001. Review of volatile organic compound source apportionment by chemical mass balance. Atmos Environ 35:1567–1584.

Watson JG, Chow JC, Lu Z, Fujita EM, Lowenthal DH, Lawson DR. 1994. Chemical mass balance source apportionment of PM_{10} during the southern California air quality study. Aerosol Sci Technol 21:1–36.

Watson JG, Chow JC, Wang XL, Kohl SD, Chen L-WA, Etyemezian V, et al. 2012. Overview of real-world emission characterization methods. In: Alberta Oil Sands: Energy, Industry, and the Environment. Amsterdam, The Netherlands:Elsevier Press, 145–170.

Watson JG, Tropp RJ, Kohl SD, Wang XL, Chow JC. 2017. Filter processing and gravimetric analysis for suspended particulate matter samples. Aerosol Sci Eng 1:193–205.

Whitacre SD, Tsai H-C, Orban J. 2002. Lubricant basestock and additive effects on diesel engine emissions. U.S. Departament of Energy. Available: *www.afdc.energy.gov/pdfs/32842.pdf* [accessed 27 December 2016].

Wild RJ, Dubé WP, Aikin KC, Eilerman SJ, Neuman JA, Peischl J, et al. 2017. On-road measurements of vehicle NO_2/NO_x emission ratios in Denver, Colorado, USA. Atmos Environ 148:182–189.

Xue J, Li Y, Quiros D, Wang X, Durbin TD, Johnson KC, et al. 2016. Using a new inversion matrix for a fast-sizing spectrometer and a photo-acoustic instrument to determine suspended particulate mass over a transient cycle for light-duty vehicles. Aerosol Sci Technol 50:1227–1238.

Zhang S, Wu Y, Wu X, Li M, Ge Y, Liang B, et al. 2014. Historic and future trends of vehicle emissions in Beijing, 1998–2020: A policy assessment for the most stringent vehicle emission control program in China. Atmos Environ 89:216–229.

Zhang Y, Wang X, Li G, Yang W, Huang Z, Zhang Z, et al. 2015. Emission factors of fine particles, carbonaceous aerosols and traces gases from road vehicles: Recent tests in an urban tunnel in the Pearl River Delta, China. Atmos Environ 122:876–884.

Zhao F, Lai MC, Harrington DL. 1999. Automotive spark-ignited direct-injection gasoline engines. Prog Energy Combust Sci 25:437–562.

Zielinska B, Campbell D, Lawson DR, Ireson RG, Weaver CS, Hesterberg TW, et al. 2008. Detailed characterization and profiles of crankcase and diesel particulate matter exhaust emissions using speciated organics. Environ Sci Technol 42:5661–5666.

Zielinska B, Fujita EM. 1994. Organic gas sampling. In: Environmental Sampling for Trace Analysis, (Markert B, ed). New York, NY:VCH Publishers, 163–184.

Zielinska B, Fung KK. 1994. The composition and concentration of hydrocarbons in the range of C2 to C18 emitted from motor vehicles. Sci Total Environ 146-147:281–288.

Zielinska B, Sagebiel JC. 2001. Collection of In-Use Mobile Source Emissions Samples for Toxicity Testing. Final Report Project # RCI-8-18148-01. Reno, NV:Desert Research Institute.

Zielinska B, Sagebiel J, McDonald JD, Whitney K, Lawson DR. 2004. Emission rates and comparative chemical composition from selected in-use diesel and gasoline-fueled vehicles. J Air Waste Manage Assoc 54:1138–1150.

HEI QUALITY ASSURANCE STATEMENT

The conduct of this study was subjected to independent audits by Mr. David Bush of T&B Systems, Inc. Mr. Bush is an expert in quality assurance for air quality monitoring studies and data management. The audits included an on-site review of study activities for conformance to the study protocol and operating procedures. The audits are briefly summarized below.

July 25–26, 2016

An on-site audit was conducted at the Desert Research Institute (DRI), Reno, Nevada. Mr. David Gemmill of Quality Assurance Consulting, Inc., assisted with the audit. The principal objective of this audit was to evaluate the key elements of the data management process, from collection of the raw data to calculation of the emission factors. The scope of the audit included reviews of the following project components and how they are linked: (1) the data from the measurement instruments; (2) the instrument calibration methodology and frequency; (3) the methods used to validate and/or correct the raw data; and (4) the methods used to calculate the emission factors. The audit identified some data with significant QA issues, which were subsequently removed from the emissions calculations. Some inconsistencies in the calculation of uncertainty estimates were also identified and corrected.

December 2017

A draft version of the final report was reviewed to verify that issues identified during the July 2016 audit had been addressed. The report was reviewed to verify that the data collection/validation process and the analyses' results were accurately presented. The finalized data and emission calculations presented in the report were reviewed and compared against source data, with no significant issues noted. Minor comments focused on recommendations that could provide additional clarifications regarding the conduct of the study and the interpretation of study results.

November 2018

A similar review was conducted on a revised version of the final report. Again, only minor recommendations on further clarifying description of the study were identified.

Written reports of each inspection were provided to the HEI project manager, who transmitted the findings to the Principal Investigators. These quality assurance audits demonstrated that the study was conducted by an experienced team with a high concern for data quality. Study personnel were very responsive to audit recommendations, providing formal responses that adequately addressed all issues. The report appears to be an accurate representation of the study.

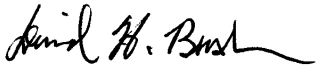

David H. Bush, Quality Assurance Officer

MATERIALS AVAILABLE ON THE HEI WEBSITE

Appendices A, B, C, and D and Additional Materials 1 contain supplemental material not included in the printed report. They are available on the HEI website, *www.healtheffects.org/publications.*

Appendix A. Additional Measurement and Modeling Information

Appendix B. Quality Control and Quality Assurance of Field and Laboratory Data

Appendix C. Additional Results

Appendix D. Additional Discussion

Additional Materials 1: Shing Mun Tunnel and Fort McHenry Tunnel Data Set

ABOUT THE AUTHORS

Xiaoliang Wang, Ph.D., is a research professor in the Division of Atmospheric Sciences at the Desert Research Institute in Reno, Nevada. His research includes pollution source characterization, physical and chemical characterization of aerosols, and aerosol instrument development. He received his Ph.D. from the Department of Mechanical Engineering at the University of Minnesota, Twin Cities in Minneapolis and Saint Paul, Minnesota. Prior to joining DRI, he worked as a senior staff development engineer at TSI Incorporated in Shoreview, Minnesota, for about four years and developed several aerosol instruments, including the DustTrak DRX Aerosol Monitor. He served as the principal investigator for this project. He oversaw all tasks, tracked project progress and expenses, and provided reports to HEI. He led the SMT study and the coordination between the SMT and FMT studies.

Andrey Khlystov, Ph.D., is a research professor in the Division of Atmospheric Sciences at the Desert Research Institute in Reno, Nevada. His expertise is in the development and testing of aerosol instrumentation and sampling techniques, the study of spatial and temporal variability of air pollutants, impact of traffic emissions on near-roadway air quality, and aerosol thermodynamics. He received his Ph.D. in atmospheric sciences from Wageningen University and Research in Wageningen, the Netherlands. He led the FMT study, including the processing and reporting of the data collected at the FMT.

Kin-Fai Ho, Ph.D., is an assistant professor of the Jockey Club School of Public Health and Primary Care at the Chinese University of Hong Kong in Shatin, Hong Kong, China. His research includes aerosol chemistry, particularly the physical and chemical characteristics of gaseous and particulate aerosol from pollution sources and in ambient air. Ho has been involved in several PM monitoring projects in Hong Kong and is familiar with chemical speciation of $PM_{2.5}$ samples. He received his Ph.D. in civil and environmental engineering from the Hong Kong Polytechnic University in Hung Hom, Hong Kong, China. He coordinated the study's field measurement, traffic counting, and chemical analysis in Hong Kong.

Dave Campbell is an associate research scientist in the Division of Atmospheric Sciences at the Desert Research Institute in Reno, Nevada. He has been engaged in data collection, analysis, and receptor modeling for various studies involving characterization pollutants from mobile sources; preparing, collecting, and evaluating source profiles from mobile and stationary sources; and measuring the influence of mobile source contributions on photochemical processes and human exposure. Campbell participated in the FMT field study and data analysis and compared the FMT measurements with the MOVES estimates.

Judith C. Chow, Sc.D., is a research professor in the Division of Atmospheric Sciences at the Desert Research Institute in Reno, Nevada. She has more than 35 years of experience in atmospheric and environmental health research and education. Her research includes developing and applying advanced analytical methods to characterize suspended atmospheric particles for source attribution and to evaluate their effects on visibility, air pollution, ecosystems, and health. She received her Sc.D. in environmental science and physiology from Harvard University in Cambridge, Massachusetts. She served as a technical advisor for the current study, providing assistance in study design, quality assurance and quality control, reporting, and project management.

Steven D. Kohl is an associate research scientist in the Division of Atmospheric Sciences at the Desert Research Institute in Reno, Nevada. He supervises the research and analytical activities for DRI's Environmental Analysis Facility. He performs chemical analysis of aerosol samples by x-ray fluorescence, maintains the field sampling equipment, provides instrument troubleshooting, coordinates sample shipping and receiving, manages field studies, and performs quality assurance audits of field sampling operations. He prepared equipment for the SMT, participated in the SMT field measurement, and oversaw the chemical analysis of the integrated samples.

John G. Watson, Ph.D., is a research professor in the Division of Atmospheric Sciences at the Desert Research Institute in Reno, Nevada. His research has involved non-linear optics, aerosol measurement, real-world source characterization, source apportionment using receptor models, and evaluation of causes of visibility degradation. He developed the U.S. EPA Chemical Mass Balance receptor modeling software and prepared EPA monitoring guidelines for $PM_{2.5}$ and PM_{10} National Ambient Air Quality Standards. He received his Ph.D. in environmental sciences from the Oregon Graduate Institute in Beaverton–Hillsboro, Oregon. He served as a technical advisor for the current study, providing assistance in study design, data analysis, and reporting.

Shun-cheng Frank Lee, Ph.D., is a professor in the Department of Civil and Environmental Engineering at the Hong Kong Polytechnic University in Hung Hom, Hong Kong, China. His research includes characterization of emission sources (including vehicles, ships, and cooking), spatial

and temporal distributions of carbonaceous aerosol in urban areas, air pollution control technology development, and risk assessment. He received his Ph.D. in environmental sciences from University of California, Berkeley. He served as a technical advisor for the current study, providing assistance in SMT measurement and VOC analysis.

Lung-Wen Antony Chen, Ph.D., is an assistant professor in the Department of Environmental and Occupational Health at the University of Nevada, Las Vegas. He is an expert in the field of aerosol measurement and receptor modeling. His research focuses on atmospheric aerosol and co-pollutants from natural and anthropogenic sources, involving development of monitoring and modeling methods for assessing public exposure to the pollutants and associated health risks. He received his Ph.D. in chemical physics from the University of Maryland, College Park. Before joining the University of Nevada, Las Vegas in 2015, he was an associate research professor at the Desert Research Institute in Reno, Nevada. He conducted the study's CMB source apportionment and compared the SMT measurements with the EMFAC-HK estimates.

Minggen Lu, Ph.D., is an associate professor of biostatistics in the School of Community Health Sciences at the University of Nevada, Reno. He has extensive experience in study design, data management, and statistical analysis. His research has involved non-/semi-parametric inference, survival analysis, longitudinal analysis, and survey methodology. He received his Ph.D. in mathematics from Northeastern University in Boston, Massachusetts, and his Ph.D. in biostatistics in 2007 from the University of Iowa in Iowa City. For the current study, he provided statistical assistance in study design, selecting appropriate statistical approaches, and the final data analysis and interpretation.

Steven Sai Hang Ho, Ph.D., is the chief executive officer of the Hong Kong Premium Services and Research Laboratory. He has extensive research experience in environmental sciences and analytical chemistry. He received his Ph.D. in analytical chemistry and environmental science from the Hong Kong University of Science and Technology in Clear Water Bay, Hong Kong, China. He conducted the carbonyl and PAH analyses for the SMT samples.

OTHER PUBLICATIONS RESULTING FROM THIS RESEARCH

Cui L, Wang XL, Ho KF, Gao Y, Liu C, Ho SS, et al. 2018. Decrease of VOC emissions from vehicular emissions in Hong Kong from 2003 to 2015: Results from a tunnel study. Atmos Environ 177:64–74.

Wang XL, Ho KF, Chow JC, Kohl SD, Chan CS, Cui L, et al. 2018. Hong Kong vehicle emission changes from 2003 to 2015 in the Shing Mun tunnel. Aerosol Sci Technol 52:1085–1098. doi:10.1080/02786826.2018.1456650.

Research Report 199, *Real-World Vehicle Emissions Characterization for the Shing Mun Tunnel in Hong Kong and Fort McHenry Tunnel in the United States*, X.L. Wang et al.

INTRODUCTION

Traffic emissions are an important source of urban air pollution, and exposure to traffic-related air pollution has been associated with various adverse health effects. Following the release of HEI Special Report 17*, Traffic-Related Air Pollution: A Critical Review of the Literature on Emissions, Exposure, and Health Effects* (HEI Panel on the Health Effects of Traffic-Related Air Pollution 2010), HEI issued Request for Applications (RFA*) 13-1, *Improving Assessment of Near-Road Exposure to Traffic Related Pollution*. Five studies were funded under this RFA. Subsequently, the HEI Research Committee decided to seek studies in two specific areas not covered by RFA 13-1 where additional work would be useful: better assessing non-tailpipe emissions (such as brake and tire wear and road dust) and taking advantage of tunnels as locations to track changes in emissions associated with new technologies and fuels. HEI issued Request for Preliminary Applications (RFPA) 14-1 in January 2014 to address these two research objectives. Dr. Wang was funded under this RFPA. In response to RFPA 14-1, Dr. Wang and colleagues from the Desert Research Institute (DRI) proposed a 2-year study, "Real-world Vehicle Emission Characterization for the Shing Mun Tunnel in Hong Kong and Ft. McHenry Tunnel in the U.S." The study would evaluate how mobile-source emissions have changed over the last one to two decades through real-world emissions characterization in these two tunnels, comparing and contrasting conditions and fleet composition in Hong Kong and the United States. The Research Committee recommended the proposal by Dr. Wang and colleagues for funding because they thought that Dr. Wang's study of two tunnels with unique characteristics had a strong design and offered a good opportunity to measure emissions from both light-duty and heavy-duty vehicles and to evaluate the effects of regulatory actions and inform regulatory models.

This Critique provides the HEI Review Committee's evaluation of the study. It is intended to aid the sponsors of HEI and the public by highlighting both the strengths and limitations of the study and by placing the Investigators' Report into scientific and regulatory context.

SCIENTIFIC BACKGROUND

Emissions from motor vehicles have evolved substantially over the last few decades because of new fuels, changes in engine designs and operation, and improved emissions control technology to meet various emissions standards targeted at improving air quality and ultimately public health (see Critique Table 1 and Critique Table 2 for an overview of regulations in the Hong Kong and the United States). For example, the introduction of engine exhaust after-treatment devices that reduce emissions of particulate matter (PM) and nitrogen oxides (NO_x, consisting of nitrogen oxide [NO] and nitrogen dioxide [NO_2]) from diesel-powered vehicles has led to substantial reductions in these emissions. However, there have been questions as to whether some of the changes may lead to unintended consequences. For example, the introduction of gasoline direct-injection (GDI) engines — which offer improved fuel efficiency — could lead to higher emissions of ultrafine particles (Health Effects Institute 2017; HEI Special Committee on Emerging Technologies 2011). As diesel fuel and GDI engines currently have substantial market shares, it is important to understand whether they have achieved the expected emission reductions under real-world conditions, an important first step in assessing whether the air quality regulations targeting vehicle emissions have been effective (Health Effects Institute 2010).

An important feature of tunnel studies is that they allow real-world characterization of emissions from a representative cross-section of in-use vehicles driven through the tunnel. They can also capture emissions in different seasons and evaluate different traffic flow situations (Frey 2018). In the past, tunnel studies have provided data on a wide variety of pollutants in relation to (1) vehicle fleet

Dr. Xiaoliang Wang's 2-year study, "Real-World Vehicle Emission Characterization for the Shing Mun Tunnel in Hong Kong and Ft. McHenry Tunnel in the U.S.," began in November 2014. Total expenditures were $661,076. The draft Investigators' Report from Wang and colleagues was received for review in July 2017. A revised report, received in May 2018, was accepted for publication in July 2018. During the review process, the HEI Review Committee and the investigators had the opportunity to exchange comments and to clarify issues in both the Investigators' Report and the Review Committee's Critique.

* A list of abbreviations and other terms appears at the end of this volume.

Critique Table 1. Regulatory Actions to Reduce Vehicle Emissions in Hong Kong, 1992–2018[a]

Name	Implemented	Retrofits and Phase-out
Pre-Euro	1992	2000–2007
Euro I	1995	2007
Euro II	1997	2008–ongoing
Smoky Vehicle Control Programme[b]	1999–2000	Ongoing
Euro III	2001	2008–ongoing
Euro IV	2000–2002 (50 ppmw sulfur ultra-low sulfur diesel) 2006 (emissions standard)	Ongoing
Euro V	2007 (diesel fuel) 2010 (fuels and emissions standard) 2012 (emissions from all vehicles)	Ongoing

[a] Regulatory standards in Hong Kong are based on those developed for Europe and include both emissions limits and fuel standards. Modified from the investigators' report Appendix Table D.1.

[b] Dynamometer smoke test for all light- and heavy-duty vehicles.

Critique Table 2. Regulatory Actions to Reduce Vehicle Emissions in the United States, 1991–2018[a]

Name	Adopted	Phase In	Vehicles Affected	Actions
Tier 1 Standards	1991	1994–1997	New light-duty vehicles	Emission limits for THC, NMHCs, CO, NO_x (different for gasoline and diesel), and PM (diesel only)
Highway Heavy-Duty Engines	1997	2004	New heavy-duty diesel engines in trucks and buses	Reduction in allowable NO_x emissions
Tier 2 Standards	1999	2004–2009	Tier 1 vehicles and new medium-duty passenger vehicles	More stringent emission standards that apply equally to all vehicles affected Limits on the sulfur content of diesel (LSD then ULSD) and gasoline fuels Introduced fleet average standards and certification bins for NO_x
Heavy-Duty Engine and Vehicle Standards and Highway Diesel Fuel Sulfur Control Requirements	2000	2006–2010	On-road heavy-duty diesel engines	DPFs and NO_x exhaust control technology Fuel for highway driving must be ULSD PM, NO_x, and NMHC emission limits and reduced evaporative emissions
Tier 3 Standards	2014	2017–2025	Tier 2 vehicles and new heavy-duty vehicles <14,000 lb	Tighter gasoline sulfur limits; 10% ethanol (E10) gasoline for emission tests Certification bins and fleet average emissions standards for NMOG and NO_x Individual vehicle PM standard

CO = carbon monoxide; DPF = diesel particulate filter; LSD = low-sulfur diesel; NMHCs = nonmethane hydrocarbons; NMOG = nonmethane organic gases; NO_x = nitrogen oxides; PM = particulate matter; THC = total hydrocarbons; ULSD = ultralow sulfur diesel.

[a] Sources for information on the regulatory actions: Tier 1 (DieselNet 2007); Highway Heavy-Duty Engines (U.S. EPA 1997); Tier 2 (DieselNet 2006); Heavy-Duty Engine and Vehicle Standards and Highway Diesel Fuel Sulfur Control Requirements (U.S. EPA 2001); Tier 3 (DieselNet 2016).

composition (e.g., diesel vs. gasoline-fueled vehicles); (2) driving patterns, including speed; (3) meteorological factors, including temperature; and (4) changes in emissions over time due to implementation of new regulations and cleaner technologies (Franco et al. 2013; Frey 2018; Kuykendall et al. 2009). However, it is also well recognized that tunnel studies have limitations, such as a lack of information on detailed characteristics of individual vehicles. Air pollutants emitted in tunnels are also minimally subject to atmospheric and meteorological processes (thus not completely reflective of ambient conditions or human population exposures). In addition, the fleet composition may depend on the location of the tunnel, and driving conditions in tunnels are often relatively constant, without acceleration, deceleration, or cold-start, and thus may not reflect those conditions encountered on urban roads.

However, long-term changes in real-world emissions and other information obtained through repeated tunnel studies can be difficult to obtain in other ways (Franco et al. 2013; Frey 2018). For example, measurement techniques such as dynamometer tests, portable emissions measurement systems, roadside remote sensing of emissions, and chase vehicles can resolve emissions of individual vehicles, but they may not provide results that are representative of the overall on-road fleet. Similarly, the distributions of vehicles used to compile emissions inventories (e.g., databases of registered vehicles) may not be fully representative of the distribution of vehicles on the road. More information on tunnel studies and other methods to measure vehicle emissions can be found in chapter 2 of HEI Special Report 17, *Traffic-Related Air Pollution: A Critical Review of the Literature on Emissions, Exposure, and Health Effects* (HEI Panel on the Health Effects of Traffic-Related Air Pollution 2010) and in the supplemental information of a recent detailed review of trends in on-road transportation emissions (Frey 2018).

HEI previously supported two tunnel studies (Health Effects Institute 2002). Gertler and colleagues studied PM emissions in the Tuscarora Mountain Tunnel on the Pennsylvania Turnpike and evaluated changes over time in particulate and gas-phase emissions by comparing their study results with those of previous studies conducted at the same tunnel (Gertler et al. 2002). In a related project, Grosjean and colleagues characterized carbonyl emissions in the Tuscarora Mountain Tunnel and in the Caldecott Tunnel in California (Grosjean and Grosjean 2002). Both groups of investigators also measured emissions at times when the proportions of gasoline-engine vehicles and diesel-engine vehicles differed in order to characterize emissions from light-duty and heavy-duty vehicles separately. In addition, HEI supported a study that analyzed metal emissions in samples of particulate matter ≤ 2.5 μm and ≤ 10 μm in aerodynamic diameter ($PM_{2.5}$ and PM_{10}, respectively) that were collected in the Kilborn and Howell Tunnels in Milwaukee, Wisconsin (Schauer et al. 2006). These and many other tunnel studies conducted in the United States and elsewhere have yielded important insights. For a review of tunnel studies, see Kuykendall and colleagues (2009), who identified approximately 50 studies conducted at more than 35 different tunnels around the world.

The current study measured emissions from motor vehicles in two tunnels, the Shing Mun Tunnel in Hong Kong and the Fort McHenry Tunnel in Baltimore, Maryland. The tunnels represent two urban locations with very different fleet compositions, emission and fuel standards, and near-road air pollutant concentrations (see Critique Table 3 for key features of the tunnels). In the Hong Kong tunnel, vehicles were classified in nine categories that included passenger cars and light-duty vehicles fueled by a mixture of gasoline and diesel, taxis and light public buses largely fueled by liquefied petroleum gas (LPG), and other heavy-duty vehicles fueled by diesel. In the Baltimore tunnel, vehicles were counted in two categories: light-duty vehicles mostly fueled by gasoline and heavy-duty vehicles mostly fueled by diesel. The Hong Kong tunnel has a single tunnel bore in each direction, whereas the Baltimore tunnel has two bores in each direction with trucks directed to the rightmost bores. Due to the differences in traffic-count methods and the relationships between vehicle class and fuel type, emissions from vehicles in the Hong Kong tunnel are discussed in terms of fuel type, while emissions from vehicles in the Baltimore tunnel are discussed in terms of vehicle class. Both of these tunnels had been intensively studied in the past by investigators from DRI (including some members of the current study team) and elsewhere, prior to recent changes in regulations, technologies, and fleet composition that would be expected to affect pollutant emissions from vehicles.

Emissions in the Hong Kong tunnel were previously characterized in a comprehensive field campaign in August 2003 and January to February 2004. That campaign included measurements of light-duty and heavy-duty differentiated emissions of $PM_{2.5}$ mass, NO, NO_2, and NO_x, and fleet-average emissions of CO (Cheng et al. 2006), chemically speciated $PM_{2.5}$ (Cheng et al. 2010), and organic compounds including carbonyls, volatile organic compounds (VOCs), and polycyclic aromatic hydrocarbons (PAHs) (Ho et al. 2007, 2009a, 2009b; Wang et al. 2006). Measured concentrations of $PM_{2.5}$, NO_x, and CO in the Hong Kong tunnel were found to be higher than concurrently measured concentrations of these pollutants

Critique Table 3. Sampling Conditions and Descriptive Characteristics of the Shing Mun Tunnel and Fort McHenry Tunnel

Parameters	Shing Mun Tunnel	Fort McHenry Tunnel
Location	Hong Kong, China	Baltimore, Maryland, United States
Earlier sampling periods	August 13 to August 31, 2003; January 12 to February 25, 2004	June 18 to June 24, 1992
Current sampling periods[a]	January 19 to March 31, 2015	February 8 to February 15, 2015; July 31 to August 7, 2015
Integrated sample days and hours	Mondays, Tuesdays, and two other days of each week with an intent to sample on all days of the week during morning and evening rush hours (08:00–10:00 LDT and 17:00–19:00 LDT) and midday hours (11:00–13:00 LDT and 14:00–16:00 LDT)[b]	All 7 days of the week during morning (09:00–15:00 LDT) and afternoon (15:00–18:30 LDT); one 5.5-hour midday sample on Sundays; night samples
Description of bores	One bore in each direction, with 2 lanes per bore	Two bores in each direction, with two lanes per bore and trucks directed to the right-most bores
Fleet composition	2003–2004: 9% liquefied petroleum gas, 41% gasoline vehicles, 50% diesel vehicles 2015: 13% liquefied petroleum gas, 45% gasoline vehicles, and 42% diesel vehicles	1992 and 2015: Left bore: <3% heavy-duty (mostly diesel) vehicles and > 97% light-duty (mostly gasoline) vehicles Right bore: 55% to 92% light-duty vehicles and 8% to 45% heavy-duty vehicles
Traffic volume	~53,000 vehicles/day in both 2003–2004 and 2015	~55,000 vehicles/day in both 1992 and 2015
Vehicle running conditions	Hot stabilized, average speed 80 km/hr	Hot stabilized, average speed 89 km/hr
Tunnel length and road surface gradient	1,636 m at +1.054%	2,173.8 m with −1.8% downhill grade and +3.3% uphill grade (ranging −3.76% to +3.76%)
Ventilation	Piston effect by vehicle movement	Air duct beneath the roadway with air supplied by fans in a ventilation building
Measurement sites	Tunnel entrance and exit	Air duct and tunnel exit
Pollutants measured	*Continuous:* CO, CO_2, NO, NO_x, VOCs, $PM_{2.5}$, SO_2, BC, PNC *Integrated*: NH_3, VOCs (C2–C12), carbonyls, PAHs, $PM_{2.5}$, road dust	*Continuous*: CO, CO_2, NO, NO_x, VOCs, $PM_{2.5}$, UFP size distribution *Integrated*: NH_3, VOCs (C2–C12), carbonyls, PAHs, $PM_{2.5}$, road dust, CO, CO_2
Source apportionment method	2003–2004: Fleet-average mixing model 2015: Positive matrix factorization	Fleet-average mixing model

BC = black carbon; DV = diesel vehicles; GV = gasoline vehicles; LDT = local daylight time; LPG = liquefied petroleum gas; PAHs = polycyclic aromatic hydrocarbons; PNC = particle number concentration; UFP = ultrafine particle: VOCs = volatile organic compounds.

[a] Not all pollutants were measured for the entire period. See Investigators' Report Table A.2 for details.

[b] Data acquired during the following tunnel maintenance periods were excluded from analyses: Monday and Wednesday ~0000–0500 LTD in the south bore; Tuesday and Thursday ~0000–0500 LDT in the north bore.

at roadside and at an ambient station (Cheng et al. 2006, 2010). Non-diesel vehicle emissions of $PM_{2.5}$ mass, OC, and EC were lower than diesel vehicle emissions of these pollutants (Cheng et al. 2010). $PM_{2.5}$ emissions from diesel vehicles were about half elemental carbon (EC) and one-fourth organic matter carbon (OC); in comparison, $PM_{2.5}$ emissions from non-diesel (i.e., gasoline and LPG) vehicles were about half OC and 20% EC, with the remaining fraction from sulfate, inorganic species, and unidentified material (Cheng et al. 2010).

Measurements in the Baltimore tunnel in 1992 were used to estimate emissions of CO, NO, NO_x, nonmethane hydrocarbons (NMHCs), and carbonyl compounds (Pierson et al. 1996); PM emissions were not measured in this study. Pierson and colleagues demonstrated that the MOBILE4.1 and MOBILE5 emissions models (predecessors of the U.S. EPA MOtor Vehicle Emission Simulator [MOVES] model used in the current study) generally predicted emissions within 50% of measured emissions, although both models tended toward overprediction. They also reported that evaporative emissions of NMHCs were about 15% of the total NMHCs emitted by light-duty vehicles in the Baltimore tunnel and concluded that the effect of roadway grade on emissions per mile was too large to be ignored (Pierson et al. 1996). Other studies in the Baltimore tunnel collected samples of inorganic and organic compounds for toxicity testing (Zielinska and Sagebiel 2001) and showed that dioxin emissions in the Baltimore tunnel were lower than had previously been reported elsewhere (Gertler et al. 1998). A later study developed inorganic and organic source profiles for gasoline- and diesel-powered vehicles in 1998 (Landis et al. 2007).

The current study built on the previous work in these two tunnels to update the emissions characterizations during calendar year 2015 with a focus on how emissions have changed since the earlier studies were conducted.

SUMMARY OF THE STUDY

SPECIFIC AIMS

Dr. Wang and colleagues evaluated changes in mobile-source emissions over the past one to two decades through characterization of real-world emissions in two tunnels: the Shing Mun Tunnel in Hong Kong and the Fort McHenry Tunnel in Baltimore, Maryland. The specific aims of the study were to:

1. Determine the current fleet-average emission factors for criteria and non-criteria pollutants including: CO, carbon dioxide (CO_2), VOCs, gas- and particle-phase PAHs, carbonyls, ammonia (NH_3), NO_x, ultrafine particles (UFPs), and $PM_{2.5}$ mass and its constituents.
2. Compare current results with data from previous tunnel studies to evaluate the influences of fleet composition, emission controls, and fuel improvements on emission factors and pollutant mixtures.
3. Establish VOC and $PM_{2.5}$ source profiles and compare them with historical and recent profiles to identify markers for different vehicle categories.
4. Estimate the contributions of tailpipe and non-tailpipe emissions to VOC and $PM_{2.5}$.
5. Evaluate performance of the latest versions of mobile-source emission models (i.e., EMission FACtors vehicle emission model used in Hong Kong [EMFAC-HK] for the Hong Kong tunnel and MOVES for the Baltimore tunnel).

STUDY DESIGN AND APPROACH

The investigators conducted their field campaigns in the Hong Kong (winter only) and Baltimore tunnels (summer and winter) in 2015 using monitoring and modeling methods similar to those they had used in earlier studies in the same tunnels (see Scientific Background section and Critique Table 3). First, they measured concentrations of a large suite of more than 300 pollutants at the entrance (or air inlet) and exit of each tunnel. Assuming that the increase in concentrations along the tunnel was from vehicle emissions in the tunnel, they used these measurements to calculate fleet-average pollutant-specific emission factors. Then, they used source apportionment to determine emission factors for specific vehicle classes defined by their fuel (gasoline, diesel, or LPG) in the Hong Kong tunnel and their weight class (light- or heavy-duty) in the Baltimore tunnel. Additionally, they evaluated performance of the mobile-source emission models (EMFAC-HK and MOVES) by comparing modeled emission factors with the emission factors measured in the tunnels.

To assess changes in emissions over time, the investigators compared their results with those from the earlier studies in the same tunnels, and with results in other tunnels in Hong Kong and the United States. Although there were challenges in harmonizing the sampling campaigns and analysis of measurements because of differences in the tunnel configurations, comparing results among the various tunnels allowed the investigators to assess the extent to which the results of the current study are generalizable to other locations.

METHODS

To address aim 1, the investigators measured concentrations of a large number of criteria and non-criteria pollutants at two locations within each tunnel. Critique Table 3 summarizes the pollutants measured and sampling conditions for each tunnel. Measurements in the Hong Kong tunnel were made during only one period in 2015 (January 19 to March 31) because Hong Kong has a tropical climate with similar weather year-round, whereas measurements in the Baltimore tunnel were made in 2015 in the winter (February 8 to February 15) and summer (July 31 to August 7) because Maryland has a temperate climate. The first measurement location was near the tunnel inlet (Hong Kong tunnel) or air supply inlet (Baltimore tunnel), and the second measurement location was near the tunnel exit. For each tunnel and measured pollutant, emission factors (or the amount of a pollutant emitted per vehicle) were calculated as the increase in pollutant concentration from the first to the second measurement location normalized by distance (EF_D), by the carbon content of the fuel burned estimated using the increase in carbon concentrations (measured as CO and CO_2) between the entrance and exit of the tunnel (EF_C), or by the amount of fuel burned starting with EF_D or EF_C and assuming values for fleet-average fuel efficiency and carbon mass fraction (EF_F).

To address aim 2, the investigators compiled measured emission factors from the previous studies in the Hong Kong and Baltimore tunnels as well as for other tunnels in Hong Kong and the United States. The tunnels used for comparison with the Hong Kong tunnel were the Zhujiang Tunnel in Guangzhou, China, and the Aberdeen Tunnel, Lion Rock Tunnel, and Tai Lam Tunnel in Hong Kong. Comparative tunnels for the Baltimore tunnel were the Caldecott Tunnel in California and the Tuscarora Tunnel in Pennsylvania. For both tunnels, the investigators compared (where available) the CO, NH_3, NO, NO_2, NO_x, sulfur dioxide (SO_2), and $PM_{2.5}$ emission factors estimated in aim 1 to emission factors reported in the earlier studies in these tunnels. In the United States, they looked for statistically significant emission factor trends between 1992 and 2015. They also compared results from the two tunnels with each other.

To address aim 3, the investigators used a combination of regression models and source apportionment by positive matrix factorization to disaggregate emission factors for different vehicle classes. For the Hong Kong tunnel, the investigators used positive matrix factorization to find the contributions of motor vehicles (diesel, gasoline, and LPG), road dust, secondary ammonium sulfate ($[NH_4]_2SO_4$), and secondary ammonium nitrate (NH_4NO_3) that best agreed with the measured concentrations of CO, NH_3, NO, NO_2, NO_x, and SO_2 as well as chemical constituents of $PM_{2.5}$ and NMHCs. For the Baltimore tunnel, the investigators assigned emissions to light-duty and heavy-duty vehicles by using a linear regression model that assigned fractions of total emissions based on the fraction of fuel burned (based on traffic counts and fleet-average vehicle efficiency) by vehicles in each category. This separation was possible because they counted vehicles in the two weight categories in two tunnel bores, and heavy-duty vehicles were allowed in only one of the bores. Because the emissions were apportioned using different methods in the two tunnels, the emission factors were discussed in terms of vehicle fuel (diesel, gasoline, or LPG) in the Hong Kong tunnel and in terms of vehicle class (light- or heavy-duty) in the Baltimore tunnel.

To address aim 4, the investigators used Student's *t* tests to compare concentrations and relative contributions of pollutants associated with non-tailpipe emissions in the current study with those in the earlier studies in the same tunnels and various other tunnels in Hong Kong and the United States. They also assessed concentrations of NMHCs as a measure of evaporative emissions. Finally, they measured chemicals associated with crustal material and road salt in $PM_{2.5}$ particles resuspended from the road surface.

To address aim 5, the investigators estimated the emission factors for the pollutants they had measured using the motor-vehicle emissions models used in the regulatory process for Hong Kong (EMFAC-HK version 3.3) and the United States (MOVES version 2014a). They then evaluated how well these models agreed with the emission factors based on the measurements in the current and earlier studies in the Hong Kong and Baltimore tunnels by calculating the ratio of the modeled emission factors to the measured emission factors.

RESULTS

Emission Factor Comparisons

In the Hong Kong tunnel, the investigators reported that between 2003–2004 and 2015, measured fleet-average emission factors decreased for $PM_{2.5}$, SO_2, benzene, and total NMHCs; fleet-average emission factors increased for PAHs, isobutane, and *n*-butane, and they did not substantially change for CO, NH_3, NO, NO_2, NO_x, and carbonyls (Critique Figure 1). The greatest declines in emission factors between 2003–2004 and 2015 in the Hong Kong tunnel were for $PM_{2.5}$, which decreased by about 80% for fleet average and diesel vehicles and was about halved for light-duty vehicles, and SO_2, which dropped about 80% for fleet average (Critique Figure 2). Between 2003–2004 and 2015, total emissions of LPG fuel markers (i.e., isobutane and *n*-butane)

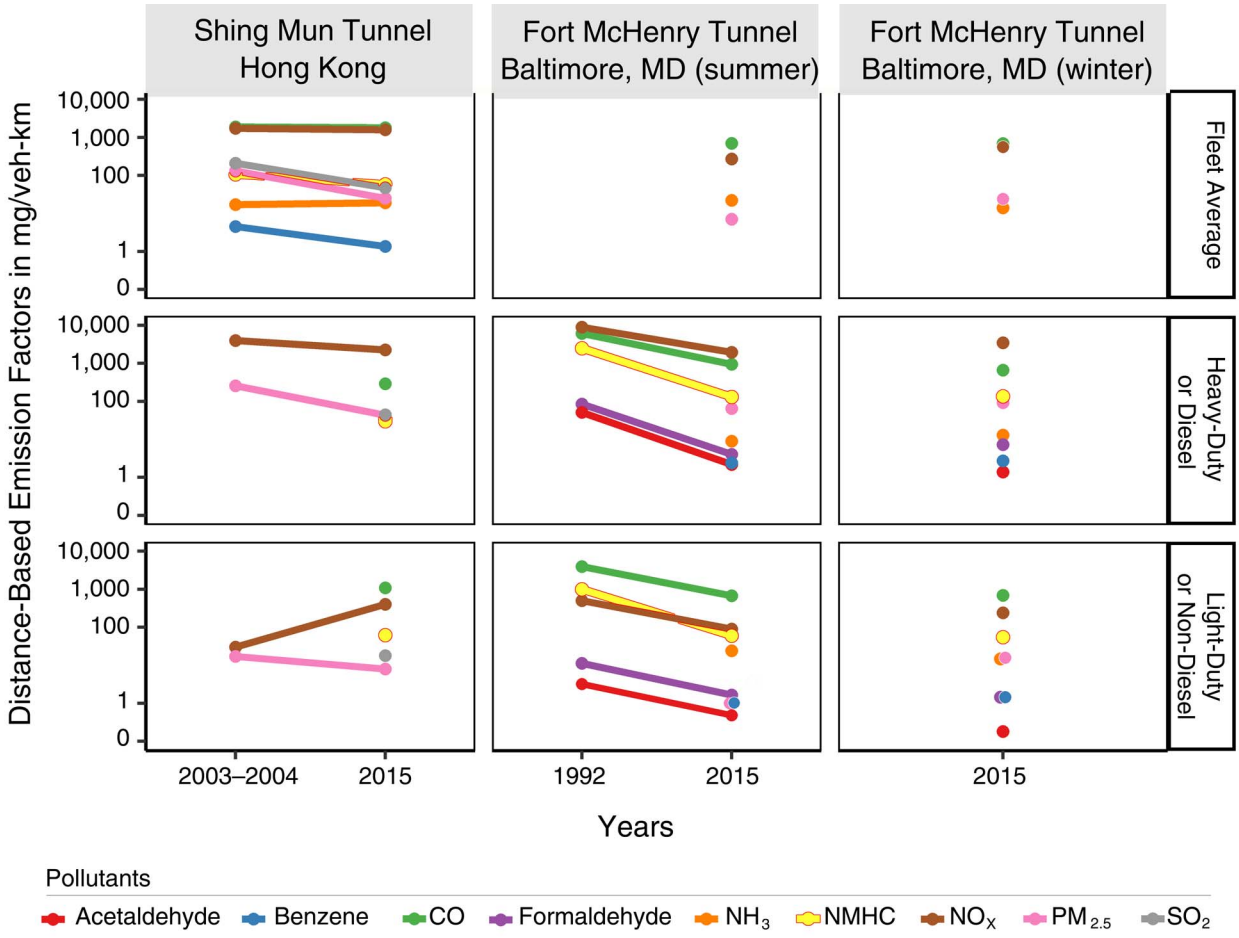

Critique Figure 1. Comparison of emission factors for fleet average, heavy-duty or diesel vehicles, and light-duty or non-diesel vehicles in the current study with earlier studies in the Shing Mun Tunnel in Hong Kong and Fort McHenry Tunnel in Baltimore, Maryland. Lines are meant as a visual aid to link each corresponding pair of measurements and do not imply linear trends over time. Uncertainty estimates are not shown because they would overlap but can be found in the IR Table 1. Not all pollutants were measured in each study.

in the Hong Kong tunnel increased because there was a shift from diesel to LPG vehicles. Emissions of NO_x from non-diesel vehicles also increased, with the shift toward more LPG vehicles on the road. At the same time, the fraction of ambient $PM_{2.5}$ of crustal origin increased because of decreases in tailpipe emissions even though non-tailpipe emissions did not substantially change.

The fleet-average emission factors in the Baltimore tunnel were 78% to 96% lower in 2015 than they were in 1992 for NO_x (expressed as NO_2 equivalents), CO, NMHCs, acetaldehyde, and formaldehyde (Critique Figure 2 and Investigators' Report [IR] Table 1; $PM_{2.5}$ emissions were not measured during the earlier study). In addition, seasonal differences in emission factors were observed in 2015 in the Baltimore tunnel. Summer emission factors for $PM_{2.5}$, NO_x, and NMHCs normalized for distance were lower than those in winter for both light-duty and heavy-duty vehicles (Critique Figure 1).

The investigators usefully compared their results to other tunnel study results across the United States. For light-duty vehicles, fuel-normalized emission factors for CO, NO_x, and $PM_{2.5}$ trended downward between 1992 and 2015 compared with the earlier study in the Baltimore tunnel and other tunnel studies (see IR Figure 5). During the same period, only formaldehyde emissions from heavy-duty vehicles had a statistically significant decrease across tunnel studies in the United States from 1992 to 2015. Although heavy-duty emission factors for $PM_{2.5}$, BTEX (benzene, toluene, ethylbenzene, and xylene), NMHCs, and naphthalene appeared to decrease across the

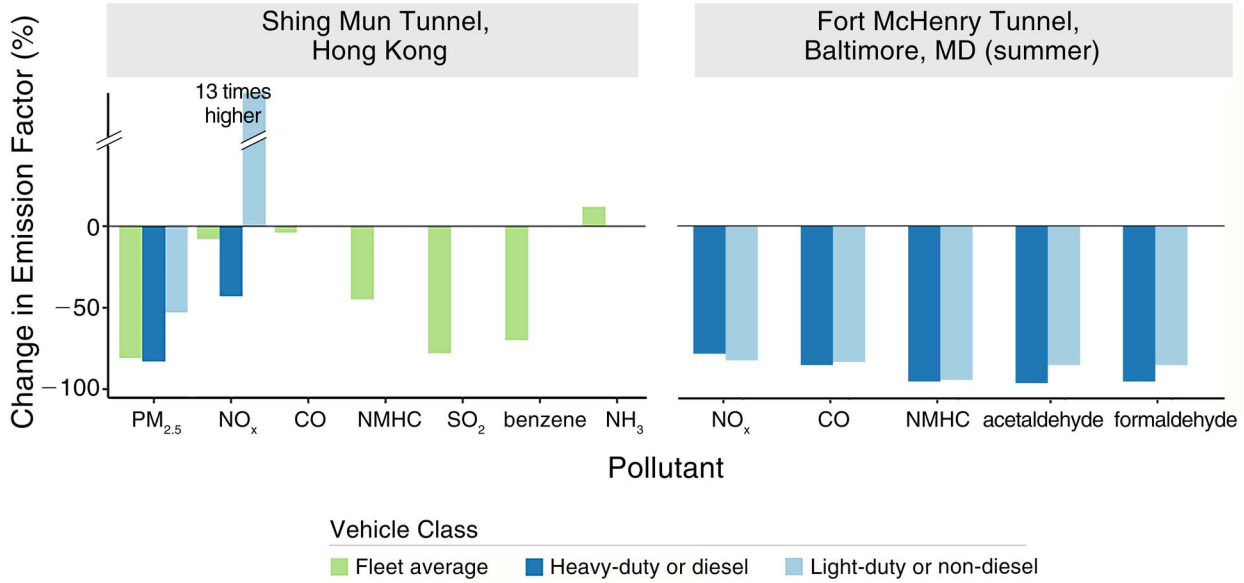

Critique Figure 2. Percent change in emission factors for fleet average, heavy-duty or diesel vehicles, and light-duty or non-diesel vehicles between 2003–2004 and 2015 in the Shing Mun Tunnel in Hong Kong and between 1992 and 2015 in the Fort McHenry Tunnel in Baltimore, Maryland over time. Not all pollutants were measured in each study.

various tunnel studies in the United States, the investigators reported that there was no statistically significant trend in emission factors for these pollutants, in part because so few studies had measured emission factors for these pollutants in tunnels.

In the winter of 2015, fleet-average distance-based emission factors in the Hong Kong tunnel were 2.6 times higher than those in the Baltimore tunnel for CO and 2.8 times higher for NO_x. Emission factors of $PM_{2.5}$ and NH_3 in the two tunnels were about the same.

Source Contributions

In both tunnels, the majority of the $PM_{2.5}$ mass was EC and OC (PM_{10} was not speciated). The investigators reported that the major contributors to $PM_{2.5}$ mass in the Hong Kong tunnel, in order from largest to smallest contribution, were diesel-vehicle exhaust, secondary ammonium sulfate, gasoline-vehicle exhaust, road dust, secondary ammonium nitrate, and LPG-vehicle exhaust. They reported that in 2015 the relative contributions of NO_2 from primary exhaust emissions, emissions from LPG, and geological materials in $PM_{2.5}$ were higher than they had been in 2003–2004.

In the Baltimore tunnel, heavy-duty vehicles had higher emission factors than did light-duty vehicles for $PM_{2.5}$, NO_2, and carbonyl compounds, and light-duty vehicles had higher emission factors for NH_3. De-icing salt was a small but measurable contributor to $PM_{2.5}$ mass in the Baltimore tunnel in winter.

Comparison with Regulatory Models

Emission estimates from the EMFAC-HK model were sometimes higher and sometimes lower but generally within a factor of two of the emission factors estimated from observations in the Hong Kong tunnel tunnels. Emission estimates from the MOVES2014a model were generally higher than (but within a factor of three of) the emission factors estimated from observations in the Baltimore tunnel. For most major pollutants, MOVES2014a overestimated observations by the largest amount in the summer, although PAHs were overestimated by the largest amount under winter conditions with large numbers of heavy-duty vehicles.

HEI REVIEW COMMITTEE EVALUATION

In its independent review of the report, the HEI Review Committee concluded this was a well-designed study resulting in a high-quality emissions data set (see Additional Materials 1 on the HEI website) that will be useful to policymakers and the scientific community. The Committee considered the principal strength of the report to be

the detailed measurements of vehicle emissions in traffic tunnels with analyses that leverage past measurement campaigns to provide a direct assessment of the changes in emissions over time in two different settings. The Committee appreciated that the investigators had synthesized multiple data sources, including comprehensive measurement campaigns, comparative data from the scientific literature, and regulatory models. In addition, the extensive data sets generated can be used in other studies to compare chemical speciation profiles in these and other tunnels over time and among locations.

Below, we discuss the Committee's detailed observations about the contributions and limitations of the study.

AIR POLLUTANT EMISSIONS TRENDS

The Committee agreed with the investigators' conclusions that the emission factors of air pollutants from motor vehicles have (for the most part) steadily decreased in both Hong Kong and the United States (Critique Figure 1 and Critique Figure 2). Some of the most substantial decreases in emission factors have occurred for $PM_{2.5}$ and SO_2 in the Hong Kong tunnel and for both light-duty and heavy-duty vehicle emissions of NO_x and CO in the Baltimore tunnel. The Committee noted that another important result was that the emission factor of NO_x from non-diesel vehicles had increased in the Hong Kong tunnel; this change was likely related to both the increase in the contribution from LPG vehicles and the different methods of separating the fleet-average emissions into diesel and non-diesel vehicles in this and the earlier study. Ammonia sources in urban areas of Asian cities have been a topic of great concern in recent years because ammonia can contribute to secondary particle formation and ammonia in motor vehicle emissions may have been underestimated in the past (Liu et al. 2014); however, there was no trend in ammonia emissions in the Hong Kong tunnel, and the Committee agreed that future work in this area is needed to determine whether traffic is an important source of the overall ammonia levels in ambient air in urban areas in Asia. The Committee also regarded the differences in trends in emission factors of pollutants in the two tunnels — in particular that PAH emission factors had stayed the same or slightly increased in the Hong Kong tunnel and decreased in the Baltimore tunnel — as interesting results that should be further explored.

In evaluating the results, the Committee thought that the comparison of motor vehicle emissions in the two tunnels further improves our understanding about how fleet composition and pollutant emissions have changed over time. Of greatest importance in the comparison between the Hong Kong tunnel and the Baltimore tunnel was the difference in fleet composition: the Hong Kong tunnel fleet was dominated by gasoline- and diesel-fueled vehicles in nearly equal numbers but also had a substantial number of vehicles fueled by LPG, whereas the Baltimore tunnel fleet was dominated by light-duty vehicles mainly fueled by gasoline (Critique Table 3). Both Hong Kong and the United States have seen major changes in emission regulations, engine controls, fuel composition, and emission control technologies between the earlier and current studies (see Critique Table 1 and Critique Table 2), but these changes differed in both nature and scope. In addition, the tunnels differed in whether their ventilation was passive (Hong Kong tunnel) or active (Baltimore tunnel), and there were differences in the pollutants that were measured and the source apportionment methods that were used. On the other hand, the tunnels had similar traffic volumes and speeds, and the engines of vehicles driving through both tunnels were probably hot stabilized (i.e., running at temperatures at which all emission control devices were active).

The Committee appreciated that the investigators went a long way toward unifying the report with respect to the two contrasting tunnels and clarifying the reasons why further unification was not possible. For example, different methods were applied to extract vehicle-class-specific emission factors from the tunnels because the tunnels had different ventilation configurations and the vehicle fleets had different characteristics, which constrained the way that emission factors could be estimated. The Committee noted that the report clearly explains discrepancies in how the measurements were made and in the conditions of the tunnels themselves, and that it was helpful that the investigators reported results for both tunnels in the same units of emission factors per km (EF_D) and per kg-carbon (EF_C) even though they were more confident in their estimation of EF_D in the Hong Kong tunnel and of EF_C in the Baltimore tunnel.

SYNTHESIS OF MULTIPLE DATA SOURCES

The Committee considered the authors' synthesis of multiple emission and air-quality data sources — including emissions models, near-road and ambient air quality measurements, and efforts to determine the source profiles in the tunnels — to be a major strength of the current study because the various approaches complemented each other.

The Committee concluded that the comparison of measurements in multiple tunnels made over many years showed that the differences in emission factors observed in the current study and in earlier studies in the same tunnels were generally consistent with observations in other

tunnels in Hong Kong and the United States (IR Figure 5 and IR Appendix Tables C.2 to C.4, available on the HEI website). In some cases (e.g., emission factors for $PM_{2.5}$ from diesel vehicles), the Committee noted that the expected trends across several studies in various tunnels in the United States were not statistically significant. They proposed that these differences may have occurred because the measurements in different studies were conducted by different teams with different measurement techniques, and the conditions in the tunnels likely varied. However, comparisons of measurements in the same tunnels at different times showed the expected decreases in emission factors. This result increased the Committee's confidence in the general applicability of the results and highlighted differences that may represent both uncertainty in the measurements of the emission factors and spatial variability in emissions.

The Committee also noted that the comparisons of measured emission factors with modeled estimates provided a valuable check on the performance of two widely used emissions models in real-world conditions. In the future, the measured emission factors can inform evaluation and development of models used for air quality management and planning. In particular, the Committee liked that the investigators showed consistency among the changes in emissions in Hong Kong based on tunnel studies, a road transport emission inventory, roadside concentrations, and emission rates based on the EMFAC-HK model estimates. However, the Committee thought that it was important to further explore the reasons for why the MOVES emission model generally overestimated emission factors relative to tunnel observations. Variations in real-world engine operation and contributions of cold-start emissions were posited by the investigators as possible explanations for this difference. It is also possible that the age distribution of vehicles used in the MOVES simulation may be outdated because it used default county-level registered vehicles and vehicle-miles traveled from the 2011 National Emissions Inventory rather than on-road age distributions and vehicle activity in 2015, and the fleet emissions have rapidly declined since 2011. Based on the slope of the emissions trend curves across multiple tunnel studies in the United States (see IR Figure 5), the Committee noted that a substantial fraction of the downward trend in emissions had occurred in the 4 years between 2011 and 2015. Bias could also be introduced if the vehicle populations driving through the tunnels were not representative of the vehicle populations over the broader geographical area near the tunnels that form the basis of the EMFAC-HK and MOVES model simulations.

Nevertheless, trends of decreasing emission factors were generally in agreement across all data sources explored. Therefore, the Committee agreed with the investigators that there was high confidence in the determination that motor vehicle emission factors of most pollutants have substantially decreased between the earlier studies and the current study. The synthesis across data sources also highlighted data gaps where questions remain. In particular, the reasons for discrepancies between emissions models and emission factors obtained from observations should be further explored. The data generated for the current study may also be useful to validate and improve emissions models in the future.

DETERMINATION OF SOURCE PROFILES

Regarding the source apportionment in the Hong Kong tunnel, the Committee agreed with the investigators that emissions of $PM_{2.5}$, SO_2, and total NMHCs from gasoline and diesel vehicles had decreased between 2003–2004 and 2015. They also agreed that NMHC markers of LPG fuel had increased between 2003–2004 and 2015, reflecting the greater use of LPG for transportation. At the same time, emissions of non-tailpipe geological materials in the Hong Kong tunnel had not changed, although the relative contribution of non-tailpipe emissions had increased due to decreasing vehicle exhaust emissions. However, the Committee would have appreciated stronger acknowledgment that there is significant uncertainty in the attribution of emissions to specific sources and that the identified air pollutant source categories could all reflect a mixture of emissions from different vehicle types. For example, the investigators saw *n*-butane as one of the more prominent NHMCs in LPG exhaust, but *n*-butane is also a prominent compound in gasoline and diesel vehicle emissions. Overall, the Committee considered that the detailed chemical speciation of this study may inform the establishment of vehicle source profiles representing emissions from current on-road vehicle fleets, even with substantial uncertainty remaining in the attribution of emissions to specific components of the vehicle fleet.

Across multiple tunnels in the United States, light-duty vehicle emission factors for NO_x, CO, $PM_{2.5}$, and formaldehyde, but not NMHCs, appear to have declined; however, those trends were not statistically significant for heavy-duty vehicles emission factors for NO_x, $PM_{2.5}$, NMHCs, and other regulated pollutants (IR Figure 5). The Committee and the investigators agreed that this difference should be further explored because these different trends for light-duty and heavy-duty emission factors may be a result of uncertainty in the apportionment of emissions because of high-emitting light-duty vehicles (IR Appendix

D, available on the HEI website). However, the Committee reasoned that possible explanations may be that differences in measured impact factors in different tunnels were related to different measurement techniques, compliance, or inspection and maintenance programs.

Because different source apportionment methods were applied in the two tunnels, direct comparisons are difficult to make. The Committee agreed that regression models should not be used to attribute emissions to specific vehicle types in the Hong Kong tunnel. However, it may have been useful to apply the positive matrix factorization method to both tunnels in order to see whether the light-duty and heavy-duty vehicle sources used in the regression models emerged as important sources in the Baltimore tunnel using this alternative method. Even with this limitation, the Committee concluded that the investigators generally were successful at unifying the two campaigns.

ROBUSTNESS OF THE RESULTS

This study was well conducted and produced a large amount of high-quality data. However, the Committee thought that certain aspects of the results were less robust than others and the investigators could have been more nuanced in their discussion of how different levels of robustness may have affected the determination of emission estimates and trends using different approaches. For example, it was unclear how uncertainties in the CO and CO_2 measurements may have propagated through the calculations to affect all of the emission factor estimates expressed both on a per-carbon and on a per-kg-fuel basis.

The Committee also noted that differences between the measurement-based source profiles and modeled source profiles using EMFAC-HK and MOVES could be related to uncertainty in the source apportionment results, the emissions model estimates, or both. Further, attribution of compounds associated with evaporative losses to diesel and LPG by positive matrix factorization could be incorrect, as opposed to (or in addition to) EMFAC-HK being incorrect in its assumed evaporative losses. Similarly, for a more robust comparison between the current and earlier results, it would be important to assess whether the level of uncertainty in measurement techniques had changed since the earlier studies in the same tunnels. However, while these areas of uncertainty need to be considered because they affect the level of confidence in the exact values of the emission factors, the Committee concluded that the measurements, modeling results, and their interpretation in this study were sound.

Another area where uncertainty had the potential to affect the results was in the positive matrix factorization analysis in the Hong Kong tunnel. The Committee thought that replacing missing data with mean values could have distorted the results and that it would have been better to run the analysis with the subset of 61 samples that had NMHC measurements in order to determine fuel-specific emission profiles containing both $PM_{2.5}$ and NMHC species. In response to this concern, the investigators repeated the positive matrix factorization model using uncertainties for the filled-in values of 10 to 100 times the average values. Because the results did not change for different assumed values for uncertainty, the investigators suggested that they had confirmed that the model outcomes depended only on actual measurements. However, the Committee was not completely satisfied with the sensitivity analysis, as there were a large number of samples with missing NMHC data. Therefore, the Committee recommended that the positive matrix factorization results for NMHCs should be viewed with caution.

Overall, however, the Committee found that even with the identified uncertainties in the measurements and analyses the major conclusions of the study were reasonable and useful. It appreciated the many details and descriptions of complex data sets in the report and expected that more in-depth evaluation of these large data sets would be worthwhile; the data may also be useful in updates to emissions models used in the regulatory process. Therefore, the Committee was pleased that the investigators decided to make all their data publicly available.

SUMMARY AND CONCLUSIONS

Wang and colleagues successfully collected a comprehensive set of emissions measurements in two traffic tunnels that have been studied before and used those data to estimate emission factors for full fleets and specific vehicle classes. Then they compared the current measurements with earlier measurements in the same tunnels and with modeled earlier and current emission factors. Major contributions of the current study were the assessment of emission trends over time, comparisons of measured and modeled emission estimates, and synthesization of results from these multiple data sources.

An important finding of the study is that the concentrations of most of the pollutants measured in the two tunnels were markedly lower in 2015 than they were in earlier studies in the same tunnels because emission factors had decreased while the number of vehicles traveling through the tunnels remained similar. In the Hong Kong tunnel, emissions of $PM_{2.5}$, SO_2, and most other pollutants decreased, although the increased proportion of LPG-fueled vehicles resulted in increased emissions of LPG markers (hydrocarbons) and NO_x. In the Baltimore tunnel, fleet-average emissions of NO_x, CO, NMHCs, acetaldehyde, and formaldehyde were all substantially lower (78% to 96%) in 2015 than in 1992. Much of this difference was

related to reductions in emissions from light-duty vehicles, although determination of the relative effectiveness of the regulations for light-duty versus heavy-duty vehicles needs further investigation.

Dr. Wang and colleagues increased the confidence in their findings by making comparisons with other data sources, although uncertainty about the magnitude of the emissions remains. The uncertainties highlighted in this study may inform future improvements in emissions models. For example, given that MOVES overestimated the real-world emissions in the Baltimore tunnel, it will be important to understand the reasons for that overestimation in order to develop accurate emissions inventories. In addition, the measurements will be useful to evaluate trends in vehicle emissions in the future. Though slightly different sets of pollutants were measured and different methods for source apportionment were used for each tunnel, the investigators were able to apportion the major pollutants (including CO, NO_x, $PM_{2.5}$, and NMHCs) to specific components of the vehicle fleets. Despite the different tunnel configurations and fleet characteristics in the two tunnels, the results in both tunnels were generally consistent, or any differences could be explained by well-understood properties of the vehicle fleets.

Quantifying the contribution of vehicle emissions to ambient concentrations of major pollutants including $PM_{2.5}$ (and its major constituents), NO_x, and NMHCs is a topic of interest for policy makers; therefore, having vehicle source profiles that represent emissions from the current fleet is important. The data collected in the current study are available online and are useful in tracking past as well as future changes in motor vehicle emissions and updating emissions models used in the regulatory process. As populations grow, urbanization continues, and the density of vehicle traffic in major cities increases, large numbers of people continue to be exposed to traffic-related emissions that affect population health even as emissions from individual vehicles go down, underscoring the role of studies such as this to quantify emissions from motor vehicles.

ACKNOWLEDGMENTS

The Review Committee thanks the ad hoc reviewers, particularly Andrew Grieshop of North Carolina State University, for their help in evaluating the scientific merit of the Investigators' Report. The Committee is also grateful to Maria Costantini and Hanna Boogaard for their oversight of the study, to Allison Patton for her assistance in preparing its Critique, to Mary Brennan for her editing of this Report and its Critique, and to Fred Howe, Hope Green, Hilary Selby Polk, and Ruth Shaw for their roles in preparing this Research Report for publication.

REFERENCES

Cheng Y, Lee SC, Ho KF, Louie PKK. 2006. On-road particulate matter ($PM_{2.5}$) and gaseous emissions in the Shing Mun Tunnel, Hong Kong. Atmos Environ 40(23):4235–4245; doi:10.1016/j.atmosenv.2006.04.002.

Cheng Y, Lee SC, Ho KF, Chow JC, Watson JG, Louie PK, et al. 2010. Chemically-speciated on-road PM(2.5) motor vehicle emission factors in Hong Kong. Sci Total Environ 408(7):1621–1627; doi:10.1016/j.scitotenv.2009.11.061.

DieselNet. 2006. United States: Cars and Light-Duty Trucks: Tier 2. Available: *www.diese lnet.com/standards/us/ld_t2.php* [accessed November 29, 2018].

DieselNet. 2007. United States: Cars and Light-Duty Trucks: Tier 1. Available: */www.dieselnet.com/standards/us/ld_t1.php* [accessed November 29, 2018].

DieselNet. 2016. United States: Cars and Light-Duty Trucks: Tier 3. Available: *www.dieselnet.com/standards/us/ld_t3.php* [accessed November 29, 2018].

Franco V, Kousoulidou M, Muntean M, Ntziachristos L, Hausberger S, Dilara P. 2013. Road vehicle emission factors development: A review. Atmos Environ 70:84–97; doi:10.1016/j.atmosenv.2013.01.006.

Frey HC. 2018. Trends in onroad transportation energy and emissions. J Air Waste Manag Assoc 68(6):514–563; doi:10.1080/10962247.2018.1454357.

Gertler A, Gillies J, Pierson W, Rogers C, Sagebiel J, Abu-Allaban M, et al. 2002. Real-world particulate matter and gaseous emissions from motor vehicles in a highway tunnel. In: Emissions from Diesel and Gasoline Engines Measured in Highway Tunnels. Research Report 107. Boston, MA:Health Effects Institute.

Gertler AW, Sagebiel JC, Dippel WA, Farina RJ. 1998. Measurements of dioxin and furan emission factors from heavy-duty diesel vehicles. J Air Waste Manag Assoc 48(3):276–278; doi:10.1080/10473289.1998.10463677.

Grosjean D, Grosjean E. 2002. Airborne carbonyls from motor vehicle emissions in two highway tunnels. In: Emissions from Diesel and Gasoline Engines Measured in Highway Tunnels. Research Report 107. Boston, MA:Health Effects Institute.

Health Effects Institute. 2002. Emissions from Diesel and Gasoline Engines Measured in Highway Tunnels. Research Report 107. Boston, MA:Health Effects Institute.

Health Effects Institute. 2010. Proceedings of an HEI Workshop on Further Research to Assess the Health Impacts of

Actions Taken to Improve Air Quality. Communication 15. Boston, MA:Health Effects Institute.

Health Effects Institute. 2017. HEI Workshop on Fuel Composition and PM - December 8, 2016. Executive Summary. Boston MA:Health Effects Institute.

HEI Panel on the Health Effects of Traffic-Related Air Pollution. 2010. Traffic-Related Air Pollution: A Critical Review of the Literature on Emissions, Exposure, and Health Effects. HEI Special Report 17. Boston, MA:Health Effects Institute,.

HEI Special Committee on Emerging Technologies. 2011. The Future of Vehicle Fuels and Technologies: Anticipating Health Benefits and Challenges. Communication 16. Boston, MA:Health Effects Institute.

Ho KF, Ho SSH, Cheng Y, Lee SC, Yu JZ. 2007. Real-world emission factors of fifteen carbonyl compounds measured in a Hong Kong tunnel. Atmos Environ 41:1747–1758; doi:10.1016/j.atmosenv.2006.10.027.

Ho KF, Ho SSH, Lee SC, Cheng Y, Chow JC, Watson JG, et al. 2009a. Emissions of gas- and particle-phase polycyclic aromatic hydrocarbons (PAHs) in the Shing Mun Tunnel, Hong Kong. Atmos Environ 43:6343–6351; doi:10.1016/j.atmosenv.2009.09.025.

Ho KF, Lee SC, Ho WK, Blake DR, Cheng Y, Li YS, et al. 2009b. Vehicular emission of volatile organic compounds (VOCs) from a tunnel study in Hong Kong. Atmos Chem Phys 9:7491–7504; doi:10.5194/acp-9-7491-2009.

Kuykendall JR, Shaw SL, Paustenbach D, Fehling K, Kacew S, Kabay V. 2009. Chemicals present in automobile traffic tunnels and the possible community health hazards: A review of the literature. Inhal Toxicol 21(9):747–792; doi:10.1080/08958370802524357.

Landis MS, Lewis CW, Stevens RK, Keeler GJ, Dvonch JT, Tremblay RT. 2007. Ft. McHenry tunnel study: Source profiles and mercury emissions from diesel and gasoline powered vehicles. Atmos Environ 41(38):8711–8724; doi:10.1016/j.atmosenv.2007.07.028.

Liu T, Wang X, Wang B, Ding X, Deng W, Lü S, et al. 2014. Emission factor of ammonia (NH3) from on-road vehicles in China: Tunnel tests in urban Guangzhou. Environ Res Lett 9:064027; doi:10.1088/1748-9326/9/6/064027.

Pierson WR, Gertler AW, Robinson NF, Sagebiel JC, Zielinska B, Bishop GA, et al. 1996. Real-world automotive emissions—Summary of studies in the Fort McHenry and Tuscarora mountain tunnels. Atmos Environ 30(12):2233–2256; *https://doi.org/10.1016/1352-2310(95)00276-6.*

Schauer J, Lough G, Shafer M, Christensen W, Arndt M, DeMinter J, et al. 2006. Characterization of Metals Emitted from Motor Vehicles. Research Report 133. Boston, MA:Health Effects Institute.

U.S. Environmental Protection Agency. 1997. Control of Emissions of Air Pollution from Highway Heavy-Duty Engines. Final Rule. 40 CFR Parts 9 and 86. Fed Reg 62(203):54694–54730. Available: *www.gpo.gov/fdsys/pkg/FR-1997-10-21/pdf/97-27494.pdf.*

U.S. Environmental Protection Agency. 2001. Control of Air Pollution from New Motor Vehicles: Heavy-Duty Engine and Vehicle Standards and Highway Diesel Fuel Sulfur Control Requirements. Final Rule. 40 CFR Parts 69, 80, and 86. Fed Reg 66(12):5002–5193. Available: *www.govinfo.gov/content/pkg/FR-2001-01-18/pdf/01-2.pdf.*

Wang H, Kawamura K, Ho KF, Lee SC. 2006. Low molecular weight dicarboxylic acids, ketoacids, and dicarbonyls in the fine particles from a roadway tunnel: Possible secondary production from the precursors. Environ Sci Technol 40(20):6255–6260; doi:10.1021/es060732c.

Zielinska B, Sagebiel J. 2001. Collection of in-use mobile source emissions samples for toxicity testing. Final Report Project # RCI-8-18148-01. Reno, NV:Desert Research Institute.

ABBREVIATIONS AND OTHER TERMS

ABBREVIATIONS AND OTHER TERMS

Al	aluminum
Ba	barium
BC	black carbon
Br	bromine
BTEX	benzene, toluene, ethylbenzene, and xylene
C	carbon or concentration
Ca	calcium
CH_4	methane
CMB	chemical mass balance receptor models
Cl^-	chloride ion
CO	carbon monoxide
CO_2	carbon dioxide
CSN	Chemical Speciation Network (U.S. EPA)
Cu	copper
DNPH	2,4-dinitrophenylhydrazine
DRI	Desert Research Institute
DV	diesel vehicle
E85	85% ethanol/15% gasoline fuel blend
EAF	Environmental Analysis Facility (DRI)
EEA	European Environment Agency
EC	elemental carbon
ECR	elemental carbon by reflectance
EF	emission factor
EF_C	fuel carbon-based emission factor (in g/kg-C)
EF_D	distance-based emission factor (in g/km/veh)
EF_F	fuel-based emission factor (in g/kg fuel burned)
EMFAC-HK	EMission FACtors vehicle emission model used in Hong Kong
EPA	(U.S.) Environmental Protection Agency
Fe	iron
FE	fuel economy (in km/kg fuel)
FMT	Fort McHenry Tunnel
GC/MS	gas chromatography/mass spectrometry
GV	gasoline vehicle
H	hydrogen
HD	heavy-duty
HGV	heavy goods vehicle
HKEPD	Hong Kong Environmental Protection Department
IMPROVE A	Interagency Monitoring of Protected Visual Environments Alternative
K^+	potassium ion
LD	light-duty
LDT	local daylight time
LGV	light goods vehicle
LGV3	light goods vehicles ($\leq$2.5t)
LGV4	light goods vehicles (2.5–3.5t)
LGV6	light goods vehicles (3.5–5.5t)
LPG	liquefied petroleum gas
MC	motorcycle
MD	medium duty
Mg	magnesium
MGV	medium-goods vehicle
MOVES	MOtor Vehicle Emission Simulator (U.S. EPA)
Na^+	sodium ion
NDV	non-diesel vehicles (including gasoline and LPG-fueled vehicles)
NFB	nonfranchised bus
NH_3	ammonia
NH_4^+	ammonium ion
$NH_4\ NO_3$	secondary ammonium nitrate
$(NH_4)_2SO_4$	secondary ammonium sulfate
Ni	nickel
NMHCs	nonmethane hydrocarbons
NO	nitric oxide
NO_2	nitrogen dioxide
NO_3^-	nitrate ion

(Continued)

ABBREVIATIONS AND OTHER TERMS

NO_x	nitrogen oxides
O_3	ozone
OBD-II	Onboard Diagnostics–Version 2
OC	organic carbon
OCR	organic carbon by reflectance
OM	organic matter
PAHs	polycyclic aromatic hydrocarbons
PC	private car
PID	photoionization detector
PM	particulate matter
$PM_{2.5}$	particulate matter ≤2.5 μm in aerodynamic diameter
PM_{10}	particulate matter ≤10 μm in aerodynamic diameter
PMF	positive matrix factorization
ppmw	parts per million by weight
PV	private light bus
r	correlation coefficient
RFA	request for applications
RFPA	request for preliminary applications
S	sulfur
Sb	antimony
SCE	source contribution estimate
Si	silicon
SMPS	scanning mobility particle sizer
SMT	Shing Mun Tunnel
SO_2	sulfur dioxide
SO_4^{2-}	sulfate ion
SVOCs	semi-volatile organic compounds
TC	total carbon, sum of organic and elemental carbon
Ti	titanium
U.S. EPA	United States Environmental Protection Agency
UFP	ultrafine particle
ULSD	ultra-low sulfur diesel
V	vanadium
VKT	vehicle-kilometers traveled
VMT	vehicle-miles traveled
VOCs	volatile organic compounds

RELATED HEI PUBLICATIONS: MOBILE SOURCE EMISSIONS

Number	Title	Principal Investigator	Date
Research Reports			
196	Developing Multipollutant Exposure Indicators of Traffic Pollution: The Dorm Room Inhalation to Vehicle Emissions (DRIVE) Study	J.A.Sarnat	2018
194	A Dynamic Three-Dimensional Air Pollution Exposure Model for Hong Kong	B. Barratt	2018
184	Advanced Collaborative Emissions Study (ACES): Lifetime Cancer and Non-Cancer Assessment in Rats Exposed to New-Technology Diesel Exhaust		2015
	Part 1. Assessment of Carcinogenicity and Biologic Responses in Rats After Lifetime Inhalation of New-Technology Diesel Exhaust in the ACES Bioassay	J.D. McDonald	
	Part 2. Assessment of Micronucleus Formation in Rats After Chronic Exposure to New-Technology Diesel Exhaust in the ACES Bioassay	J.C. Bemis	
	Part 3. Assessment of Genotoxicity and Oxidative Damage in Rats After Chronic Exposure to New-Technology Diesel Exhaust in the ACES Bioassay	L.M. Hallberg	
	Part 4. Assessment of Plasma Markers and Cardiovascular Responses in Rats After Chronic Exposure to New-Technology Diesel Exhaust in the ACES Bioassay	D.J. Conklin and M. Kong	
180	Characterizing Ultrafine Particles and Other Air Pollutants In and Around School Buses	Y. Zhu and Q. Zhang	2014
173	Selective Detection and Characterization of Nanoparticles from Motor Vehicles	M.V. Johnston	2013
172	Potential Air Toxics Hot Spots in Truck Terminals and Cabs	T.J. Smith	2012
165	Allergic Inflammation in the Human Lower Respiratory Tract Affected by Exposure to Diesel Exhaust	M. A. Riedl	2012
163	The London Low Emission Zone Baseline Study	F. Kelly	2011
158	Air Toxics Exposure from Vehicle Emissions at a U.S. Border Crossing: Buffalo Peace Bridge Study	J.D. Spengler	2011
156	Concentrations of Air Toxics in Motor Vehicle–Dominated Environments	E.M. Fujita	2011
155	The Impact of the Congestion Charging Scheme on Air Quality in London	F. Kelly	2011
	Part 1. Emissions Modeling and Analysis of Air Pollution Measurements		
	Part 2. Analysis of the Oxidative Potential of Particulate Matter		
153	Improved Source Apportionment and Speciation of Low-Volume Particulate Matter Samples	J.J. Schauer	2010
149	Development and Application of a Sensitive Method to Determine Concentrations of Acrolein and Other Carbonyls in Ambient Air	T.M. Cahill	2010
147	Atmospheric Transformation of Diesel Emissions	B. Zielinska	2010

(Continued)

Copies of these reports can be obtained from HEI; PDFs are available for free downloading at www.healtheffects.org/publications.

RELATED HEI PUBLICATIONS: MOBILE SOURCE EMISSIONS

Number	Title	Principal Investigator	Date
145	Effects of Concentrated Ambient Particles and Diesel Engine Exhaust on Allergic Airway Disease in Brown Norway Rats	J.R. Harkema	2009
139	Effects of Long-Term Exposure to Traffic-Related Air Pollution on Respiratory and Cardiovascular Mortality in the Netherlands: The NLCS-AIR Study	B. Brunekreef	2009
138	Health Effects of Real-World Exposure to Diesel Exhaust in Persons with Asthma	J. Zhang	2009
133	Characterization of Metals Emitted from Motor Vehicles	J. J. Schauer	2006
107	Emissions from Diesel and Gasoline Engines Measured in Highway Tunnels		2002
	Real-World Particulate Matter and Gaseous Emissions from Motor Vehicles in a Highway Tunnel	A. W. Gertler	
	Airborne Carbonyls from Motor Vehicle Emissions in Two Highway Tunnels	D. Grosjean and E. Grosjean	
Special Reports			
19	Diesel Emissions and Lung Cancer: An Evaluation of Recent Epidemiological Evidence for Quantitative Risk Assessment	HEI Diesel Epidemiology Panel	2015
17	Traffic-Related Air Pollution: A Critical Review of the Literature on Emissions, Exposure, and Health Effects	HEI Panel on the Health Effects of Traffic-Related Air Pollution	2010
16	Mobile-Source Air Toxics: A Critical Review of the Literature on Exposure and Health Effects	HEI Air Toxics Review Panel	2007
	Diesel Exhaust: A Critical Analysis of Emissions, Exposure and Health Effects	HEI Diesel Working Group	1995
Workshop			
	Workshop on Effects of Fuel Composition on PM; Executive Summary	HEI	2016
HEI Communications			
17	Advanced Collaborative Emissions Study (ACES) Phase 3A: Characterization of U.S. 2007-Compliant Diesel Engine and Exposure System Operation	J.L. Mauderly and J.D. McDonald	2012
16	The Future of Vehicle Fuels and Technologies: Anticipating Health Benefits and Challenges	HEI Special Committee on Emerging Technologies	2011
10	Improving Estimates of Diesel and Other Emissions for Epidemiologic Studies	HEI	2003

Copies of these reports can be obtained from HEI; PDFs are available for free downloading at www.healtheffects.org/publications.

HEI BOARD, COMMITTEES, and STAFF

Board of Directors

Richard F. Celeste, Chair *President Emeritus, Colorado College*

Sherwood Boehlert *Of Counsel, Accord Group; Former Chair, U.S. House of Representatives Science Committee*

Enriqueta Bond *President Emerita, Burroughs Wellcome Fund*

Jo Ivey Boufford *President, New York Academy of Medicine*

Homer Boushey *Emeritus Professor of Medicine, University of California, San Francisco*

Michael T. Clegg *Professor of Biological Sciences, University of California, Irvine*

Jared L. Cohon *President Emeritus and Professor, Civil and Environmental Engineering and Engineering and Public Policy, Carnegie Mellon University*

Stephen Corman *President, Corman Enterprises*

Alan I. Leshner *CEO Emeritus, American Association for the Advancement of Science*

Henry Schacht *Managing Director, Warburg Pincus; Former Chairman and Chief Executive Officer, Lucent Technologies*

Research Committee

David Savitz, Chair *Professor of Epidemiology, School of Public Health, and Professor of Obstetrics and Gynecology, Alpert Medical School, Brown University*

Jeffrey R. Brook *Senior Research Scientist, Air Quality Research Division, Environment Canada, and Assistant Professor, University of Toronto, Canada*

Francesca Dominici *Professor of Biostatistics and Senior Associate Dean for Research, Harvard T.H. Chan School of Public Health*

David E. Foster *Phil and Jean Myers Professor Emeritus, Department of Mechanical Engineering, Engine Research Center,* University of Wisconsin, Madison

Amy H. Herring *Sara & Charles Ayres Professor of Statistical Science, Duke University, Durham, North Carolina*

Barbara Hoffmann *Professor of Environmental Epidemiology, Institute of Occupational, Social, and Environmental Medicine, University of Düsseldorf, Germany*

Allen L. Robinson *Raymond J. Lane Distinguished Professor and Head, Department of Mechanical Engineering, and Professor, Department of Engineering and Public Policy, Carnegie Mellon University*

Ivan Rusyn *Professor, Department of Veterinary Integrative Biosciences, Texas A&M University*

Review Committee

James A. Merchant, Chair *Professor and Founding Dean Emeritus, College of Public Health, University of Iowa*

Kiros Berhane *Professor of Biostatistics and Director of Graduate Programs in Biostatistics and Epidemiology, Department of Preventive Medicine, Keck School of Medicine, University of Southern California*

Frank Kelly *Professor of Environmental Health and Director of the Environmental Research Group, King's College London*

Jana B. Milford *Professor, Department of Mechanical Engineering and Environmental Engineering Program, University of Colorado, Boulder*

Jennifer L. Peel *Professor of Epidemiology, Colorado School of Public Health and Department of Environmental and Radiological Health Sciences, Colorado State University*

Roger D. Peng *Professor of Biostatistics, Johns Hopkins Bloomberg School of Public Health*

HEI BOARD, COMMITTEES, and STAFF

Officers and Staff

Daniel S. Greenbaum *President*
Robert M. O'Keefe *Vice President*
Rashid Shaikh *Director of Science*
Jacqueline C. Rutledge *Director of Finance and Administration*
Emily Alden *Corporate Secretary*

Hanna Boogaard *Consulting Senior Scientist*
Aaron J. Cohen *Consulting Principal Scientist*
Philip J. DeMarco *Compliance Manager*
Hope Green *Editorial Project Manager*
Kathryn Liziewski *Research Assistant*
Kethural Manokaran *Research Assistant*
Lissa McBurney *Science Administrative Assistant*
Pallavi Pant *Staff Scientist*
Allison P. Patton *Staff Scientist*
Hilary Selby Polk *Managing Editor*
Lindy Raso *Executive Assistant*
Anna S. Rosofsky *Staff Scientist*
Robert A. Shavers *Operations Manager*
Annemoon M.M. van Erp *Managing Scientist*
Eleanne van Vliet *Staff Scientist*
Donna J. Vorhees *Director of Energy Research*
Katherine Walker *Principal Scientist*

HEALTH
EFFECTS
INSTITUTE

75 Federal Street, Suite 1400
Boston, MA 02110, USA
+1-617-488-2300
www.healtheffects.org

RESEARCH
REPORT

Number 199
March 2019